Synthesis and Evaluation of Novel Monocarboxylate Transporter 1 Inhibitors as Potential Anticancer Agents

A THESIS

SUBMITTED TO THE FACULTY OF

UNIVERSITY OF MINNESOTA

BY

Michael J. Williams

IN PARTIAL FULFILLMENT OF THE REQUIREMENTS

FOR THE DEGREE OF

MASTER OF SCIENCE

Advisor:

Venkatram R Mereddy

April 2017

ACKNOWLEDGEMENTS

"I would like to express my appreciation and sincere gratitude to Dr. Venkatram R. Mereddy, my thesis advisor, for his valuable advice, continuous support and expert guidance towards personal and professional aspects. I am also thankful for his endless support that helped me in advancing on the path to achieving my goals in life.

Furthermore, I would like to express my deepest gratitude to my committee members Dr. Joseph Johnson and Dr. Viktor Zhdankin for their constant support.

I would also like to thank the Department of Chemistry and Biochemistry for its financial support over the years. My thanks go to the faculty in the Department of Chemistry and Biochemistry for the knowledge they have taught me during this time. I thank all the members of my group for their incessant support given me for the past three years. I thank my family, friends, and daughter for their support during my education.

ABSTRACT

Cancer cells pursue aggressive glycolysis for ATP generation and rapid cell proliferation. Disruption of glycolysis leads to tumor growth inhibition and hence glycolytic inhibitors can be developed as anticancer agents. Monocarboxylate transporters 1 and 4 are involved in the efflux and influx of glycolytic end products lactate and pyruvate in cancer cells and inhibition of these transporters is a novel way to arrest the tumor growth. In the present work, several Ŭ,ß-unsaturated imidazolidine diones have been synthesized as potential MCT1 inhibitors that can cross the blood brain barrier. Unfortunately, none of the compounds exhibit any MCT1 inhibition properties even at high concentrations. In another project, Ŭ-cyanoacyloxyamides from Ŭ-cyanocinnamic acid and 4-hydroxy-Ŭ-cyanocinnamic acid (CHC) have been synthesized via three component Passerini reaction. The preliminary biological studies indicate that several of Passerini based prodrugs exhibit moderate to good MCT1 inhibition properties at low µM concentration. Importantly, some of these prodrugs exhibit 100-200 times more potency than the parent CHC molecule. Future studies should involve more biological studies to identify a lead candidate compound for further development.

TABLE OF CONTENTS

I	Acknowledgments	**i**
II	Abstract	**ii**
III	Table of Contents	**iii**
IV	List of Schemes	**iv**
V	List of Figures	**v**
VI	List of Tables	**vi**
VII	List of Abbreviations	**vii**
VIII	CHAPTER 1: Introduction	**1**
IX	CHAPTER 2: Exploration of Ꞵ,ɓ-Unsaturated Hydantoins As Potential MCT1 Inhibitors For Glioblastoma Multiforme Treatment	**23**
X	CHAPTER 3: Cyanocinnamic Acid Prodrugs via Passerini Reaction: Synthesis and Biological Evaluation as MCT1 Inhibitors	**32**
XI	CHAPTER 4: Experimental and Spectral Characterization	**40**
XII	References	**75**
XIII	Appendix	**78**

LIST OF SCHEMES

Scheme	Title of the scheme	Page number
Scheme 1a	Synthesis of MCT1 inhibitor pyrimidine-2,4(3H)-dione	**8**
Scheme 1b	Synthesis of indole based pyrimidine-2,4(1H,3H)dione	**9**
Scheme 1c:	Synthesis of thiophenylpyrimidine derivatives	**10**
Scheme 1d	Synthesis of pyrimidinedione derivatives	**11**
Scheme 1e	Synthesis of pteridinetrione derivatives	**12**
Scheme 1f	Synthesis of *N,N*-dialkyl cyanocinnamic acid derivatives	**14**
Scheme 1g	Synthesis of 3-methoxy-4-*N,N*-dialkyl cyanocinnamic acid derivatives	**16**
Scheme 1h	Synthesis of *N,N*-dialkyl carboxy coumarin derivatives	**19**
Scheme 2a	General synthesis of Ŭ,ƀ-unsaturated imidazolidine diones	**25**
Scheme 2b	Synthesis of Ŭ,ƀ-unsaturated imidazolidine dione derivatives	**26**
Scheme 2c	Synthesis of monocarboxy hydantoin derivative	**28**
Scheme 3a:	General scheme of Passerini reaction	**32**
Scheme 3b	Synthesis of Ŭ-cyanocinnamic acid and Ŭ-cyanoacyloxyamide prodrugs	**33**
Scheme 3c	Synthesis of CHC based Ŭ-cyanoacyloxyamides	**35**
Scheme 3d	Synthesis of pyruvate based Ŭ-cyanoacyloxyamides	**38**

LIST OF FIGURES

Figure	Description of the figure	Page number
Figure 1a	Some of the important hallmarks of cancer cells for rapid proliferation and invasion	1
Figure 1b	Warburg effect in cancer cells	**6**
Figure 1c:	AstraZenecaôs lead MCT1 inhibitors **1-3**	**7**
Figure 1d:	Structure of CHC **28**	**12**
Figure 1e:	MCT1 IC_{50} values of *N,N*-dialkyl cyanocinnamic acid derivatives	**15**
Figure 1f:	MCT1 IC_{50} of 3-methoxy-4-*N,N*-dialkyl cyanocinnamic acid derivatives	**16**
Figure 1g:	Tumor growth inhibition of **35f** in WiDr cancer xenograft model	**18**
Figure 1h:	MCT1 IC_{50} values of *N,N*-dialkyl carboxy coumarin derivatives	**20**
Figure 1i:	Tumor growth inhibition of **39b** in GL261-luc2 cancer syngraft model	**20**
Figure 2a:	Structures of hydontoin and hydontoin based drugs	**24**
Figure 2b:	Cyanocinnamic acid and Ŭ,ɓ-unsaturated imidazolidine dione	**25**
Figure 2c:	Western blot of MCT1 expression in RBE4 cell line	**27**

LIST OF TABLES

Table	Description of the table	Page number
Table 2a	MCT1 Inhibition Studies in Hydantoin Derivatives	**28**
Table 3a:	MCT1 IC_{50}^{*} values of Ŭ-cyanoacyloxyamide prodrugs	**34**
Table 3b:	MCT1 IC_{50}^{*} values of CHC based Ŭ-cyanoacyloxyamide derivatives	**36**

LIST OF ABBREVIATIONS

Oxidative Phosphorylation (OxPhos)

Vascular Endothelial Growth Factor (VEGF)

Adenosine triphosphate (ATP)

Nicotinamide Adenine Dinucleotide Phosphate (NAD(P)H)

Monocarboxylate Transporters (MCTs)

Lithium Diisopropylamide (LDA)

TBDMS

TFA

EDC and HOBt

Estrogen Receptor Positive Breast Cancer (MCF7)

Glioblastoma Multiforme (GBM)

Rat Brain Endothelium Cell Line (RBE4)

Blood Brain Barrier (BBB)

CHAPTER 1: INTRODUCTION

Normal cells are strictly controlled by various chemical, physical, and electrochemical gradient signals. These signals sustain controlled cellular growth and basal level tasks required for healthy tissue function. Any deviations or malformations of normal cells are eliminated by apoptotic signaling or the immune system intervention. Conversion of normal cells to a cancerous state is a process that requires overcoming regular cellular control systems. These adaptations and characteristics are termed ñhallmarks of cancerò, and are based on careful observation in subtle differences between regular cells and cancer cells (**Figure 1a**).[1-3]

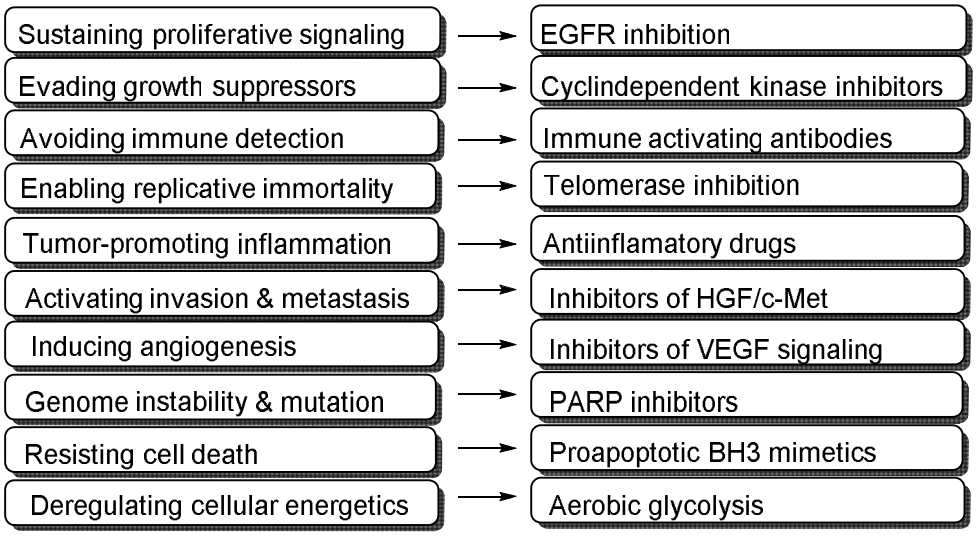

Figure 1a: Some of the important hallmarks of cancer cells for rapid proliferation and invasion

Cancer cells propagate rapidly and thus require a constant release of proliferative factors while evading growth suppressor signals from the surrounding environment.[3,4] This rapid replication is susceptible to apoptosis unless cellular immortality is achieved. This acquired immortality will help resist cellular death when the rate of replication

reaches a maximum threshold.[2] Cellular immortality also helps maintain genetic instability which is important for the development of malignant characteristics that are advantageous to a rapidly proliferating cancerous mass (**Figure 1a**).

Normal cells utilize mitogenic growth signals to enter a proliferative state, whereas cancer cells no longer require these signals to maintain rapid proliferation. Once the cancer cell attains self-sustainable proliferative signaling, these cells tend to divide rapidly and hence, requires a great amount of energy and structural precursors for the synthesis of proteins, RNA, and DNA. Oxidative phosphorylation (OxPhos) is an innate characteristic within normal cells and malignant cells, but OxPhos has a maximum rate of ATP production which limits the rate of proliferation.[5,6] To overcome energy deficiency and maintain rapid proliferation, cancer cells overexpress glycolytic enzymes.[6-10] This increase in the protein expression is a very quick process with respect to mitochondrial synthesis, and is enough to compensate for energy deficiency.[2,3,10,11] This deregulation of cellular energetics is inefficient on a molecular scale and results in an accumulation of ketone bodies. However, this is advantageous as the cell has access to many precursors required for structural synthesis of proteins and other organelles.

Another issue of rapid proliferation is overcoming space and nutrient restrictions. Cancer cells overcome spatial issues by activating invasive and metastatic signals, and promoting inflammation in the surrounding tissue. Competition for nutrients is another problem of rapid growth of cancer which can be overcome by the stimulation of growth factors such as vascular endothelial growth factor (VEGF) that promote angiogenesis. These growth factors enable the cancer cells to propagate their vasculature deep into the

tumor to further facilitate its proliferation via distribution of nutrients and oxygen (**Figure 1a**).[2,6]

Although cancerous/non-cancerous cells attain sustainable proliferative signaling, overcome spatial and nutrient requirements, any other aberration in cellular expression will be recognized by the immune system and the cell undergo apoptosis. This constant tissue surveillance is a very efficient system at recognizing malignancies and eradicating them entirely.[12-15] Usually, >80% of potential malignancies are eliminated via the immune system and itôs surveillance.[1,2] Therefore, the final obstacle that a cancer cell must overcome is the immune response. Once cancer cell overcomes immune response, it is able to proliferate uncontrollably by disabling components of immune system cells, and recruiting immunosuppressive inflammatory cells resulting in unchecked exponential increase in tumor mass and lead to ultimate organ failure (**Figure 1a**).[12,15]

These ñHallmarksò of cancer are important to understand the strategies employed in tumors which could be easy targets for cancer therapeutics. These strategies are tumor specific, and allow for selective elimination of the tumor cells. Selective elimination is the ultimate goal of any therapy as it alleviates any harmful side effects due to non-selective elimination of the healthy cells.

Glycolysis:

One universally employed strategy for energy production in cancerous and non-cancerous cells under hypoxic conditions is the upregulation of glycolysis.[3,6-8,16-18] Glycolysis is not dependent on oxygen for the production of ATP and is normally experienced when exercising.[10,16,19] As the cell undergoes oxidative stress, energy

deregulation induces hypoxic conditions to generate more ATP.[7,16] This oxidative stress leads to an oxygen gradient by activating hypoxia inducing factor HIF1-Ŭ, and thereby enhancing the stress-induced glycolysis. Glycolysis is a 10-step process that is involved in the conversion of glucose into the OxPhos precursor pyruvate. This process is dependent on the expression of several glycolytic proteins and can be upregulated in times of energy demand and under hypoxic conditions. Glycolysis produces two moles of ATP for one mole of glucose whereas 36 moles of ATP is produced in OxPhos. OxPhos is a process sequestered in the mitochondria and is closely coupled with glycolysis via pyruvate. Pyruvate is transported into the mitochondria and enters the Kreb cycle. This cycle is a very atom efficient process resulting in the formation of energy rich NAD(P)H which carry electrons to the electron transport chain and generates ATP. It utilizes a proton gradient driven by electrons carried from the Kreb cycle.

Although glycolysis is an energy inefficient process, the quick demands of the energy requirements prefers excessive glycolysis over OxPhos. Extracellular glucose is able to easily transport across the cell membrane where hexokinase phosphorylates glucose to glucose 6-phosphate and traps the glucose in the cell. In step four of glycolysis, two molecules of D-glyceraldehyde 3-phosphate are generated. Both molecules produce one unit of ATP at steps seven and ten and the net result of glycolysis is two moles of ATP.[7] The final product of this process is pyruvate which readily converts into lactate via lactate dehydrogenase.[16,17,20,21] These ketone bodies can be taken at any step within the glycolytic pathway and utilized in structural synthesis, amino acid generation and cell wall stabilization.[6,16] This is a reversible process and dependent on the concentration of pyruvate and lactate. Overall, glycolysis is an excellent source of ATP

under extreme stress and/or hypoxic conditions and hence, favored by cancer cells for energy production.

Tumor Metabolism:

The difference between a normal cell and a cancerous cell is that cancer cells evade apoptotic factors, maintain genetic instability, and proliferate rapidly.[2,7] One of the main requirements for the rapid proliferation and propagation of cancer cells is to meet their high energy demands via glycolysis. OxPhos produces adequate energy to maintain basal level cellular activity, but OxPhos must be augmented in order to support high energy requirements of cancer cells. Cancer cells adapt other pathways to meet these energetic needs, one of which is the upregulation of glycolysis. This process creates less energy but is a quick means for ATP generation. The upregulation of glycolysis in cancer cells results in the increase of intracellular lactate and leads to a rapid decrease in cytosolic pH. Under normal conditions, this decrease in the pH puts the cell at greater risk for apoptosis induced by acidic conditions.[22-23] In order to maintain intracellular homeostasis, cancer cells upregulate transport proteins called monocarboxylate transporters (MCTs).[24-26]

Monocarboxylate transporters (MCTs):

MCTs are proton-linked membrane proteins that are responsible for the transport of metabolites such as lactate and pyruvate which play an important role in carbohydrate, fat and amino acid metabolism.[24-26] Although MCT family consists of isoforms 1-14, literature reports show that only MCTs 1-4 are involved in the transport of lactate and

other ketone bodies. The overexpression of MCT1/4 has been linked to increase glycolytic activity and poor patient outcome.[6,12,16,18,24] The upregulation of MCT1/4 is a very specific characteristic of late stage malignant tumors, and is an excellent target for small molecule inhibitors.

Higher glycolytic activity is observed in tumor hypoxic regions resulting in the increase of extracellular lactate concentration. At risk of a rapid decrease of extracellular pH in cancer cells, a symbiotic relationship develops between aerobic and hypoxic cells. The extracellular transport of lactate from the glycolytic dependent hypoxic cells is facilitated by MCT1 and this lactate is quickly taken up by the adjacent aerobic cancer cells via MCT4. This lactate is then utilized to produce ATP via OxPhos in mitochondria. This energy symbiosis between aerobic and hypoxic cells is termed the ñWarburg effectò (**Figure 1b**).[4,27,28] Inhibition of transporter protein MCT1 in cancer cells leads to lactic acid acidosis in hypoxic cells and limits the lactate consumed by neighboring oxygen rich cells and subsequently reduces the energy availability for cancer cells. Hence, targeting MCT1 is alluring for it is cancer specific, and represents a potential target for the development of cancer therapeutics.

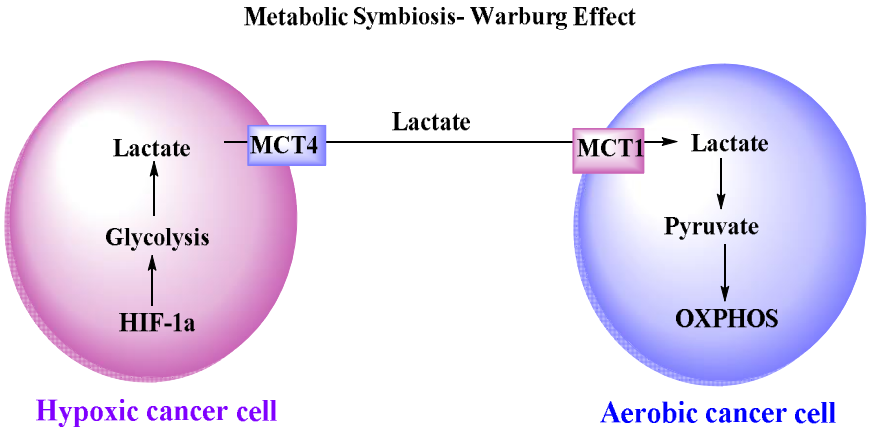

Figure 1b: Warburg effect in cancer cells.

Owing to the importance of tumor glycolysis in cancers, various MCT1 inhibitors have been synthesized in the past few years. Synthesis, biological activity and background literature of some of these inhibitors have been discussed below. AstraZeneca initially developed three series of pyrimidine and pyridazinone based molecules **1-3** (**Figure 1c**). These molecules were evaluated for MCT1 binding affinity and the K_i values for **1-3** was found to be 0.33, 0.1 and 0.28 nM, respectively.[29]

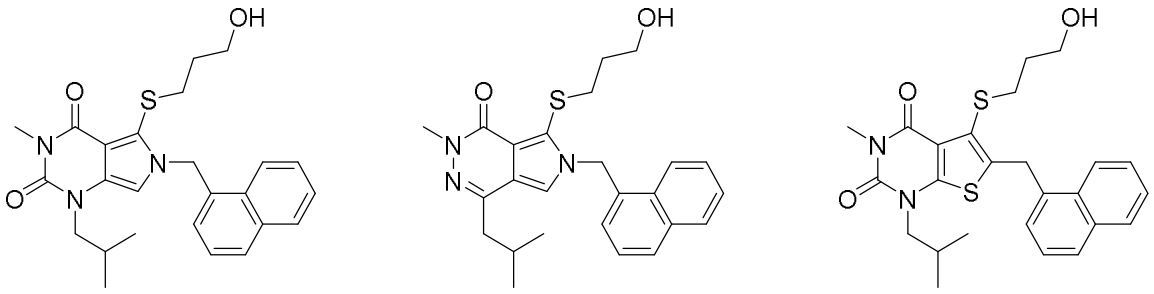

Figure 1c: AstraZenecaôs lead MCT1 inhibitors **1-3**

The synthesis of these pyrimidine based MCT1 inhibitors involved several steps, reagents and synthetic routes, some of which are described below.

Carbamate **4** was alkylated with isobutyl amine and subsequently cyclized to obtain **5**. It was methylated using dimethylsulfate to form **6** and the nitrile group was reduced to aldehyde **7** using a solution of Raney nickel in formic acid. Methyl group in **7** was then brominated and treated with 1-naphthalenylmethylamine to obtain imine which was cyclized *in situ* to obtain pyrrolopyrimidine dione **8**. Dione **8** was treated with a strong base LDA and sulfonothioate **9** to obtain the final product pyrimidine dione **1** (**Scheme 1a**).[30]

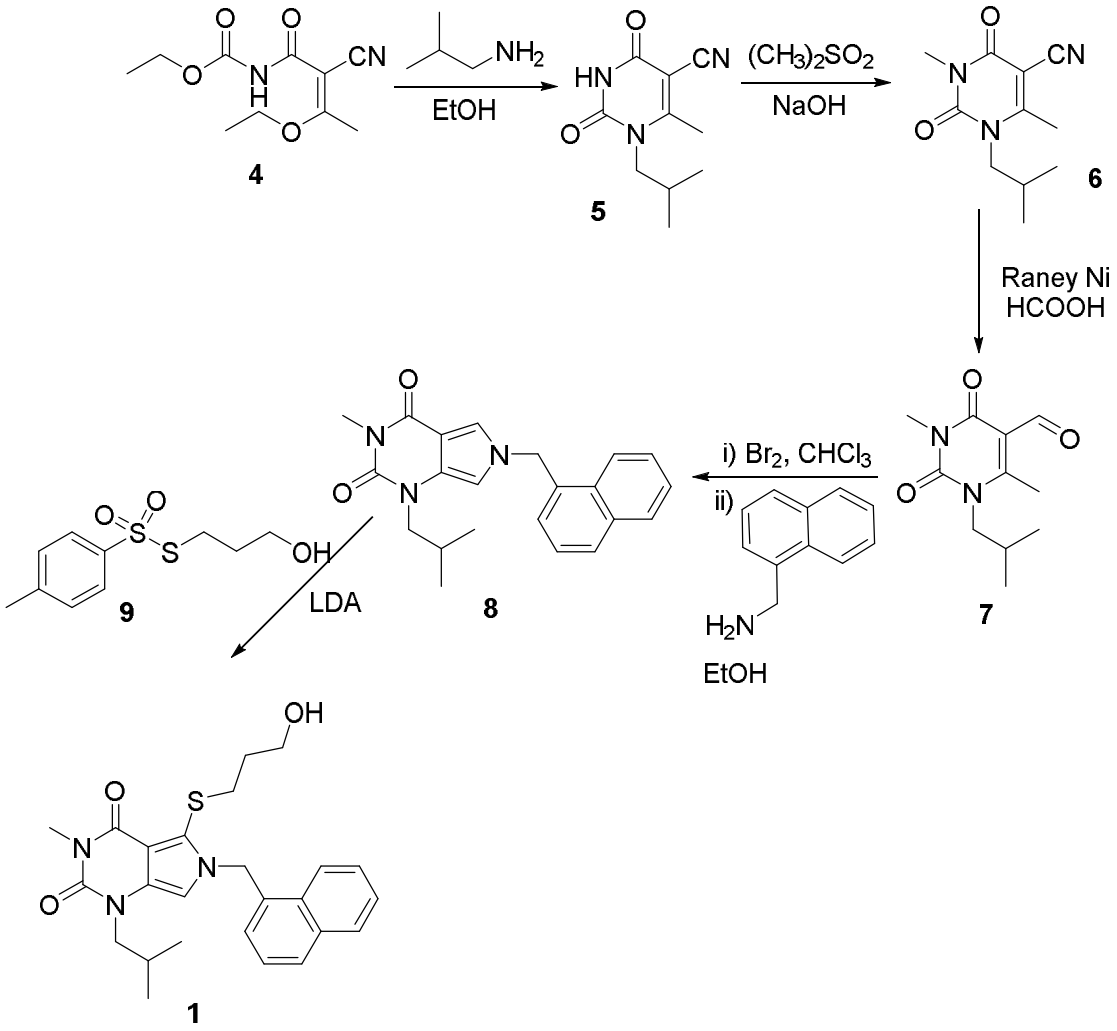

Scheme 1a: Synthesis of MCT1 inhibitor pyrimidine-2,4(3H)-dione **1**

AstraZeneca also came up with few other MCT1 inhibitors **12, 17-19** that involved multiple steps and chiral centers. Methyl carboxylate **10** was C-alkylated with indole in presence of $NaHCO_3$ to obtain methindolyl derivative **11**. This product **11** was further hydrolyzed to acid and coupled with (R)-3-hydroxypyrrolidine using EDC and HOBt to obtain final product **12** (**Scheme 1b**). The product **12** was evaluated for its MCT1 binding capability and its K_i value was found to be 0.79nM, which was relatively low compared to other 5-substituted thioether derivatives **1-3**.[29]

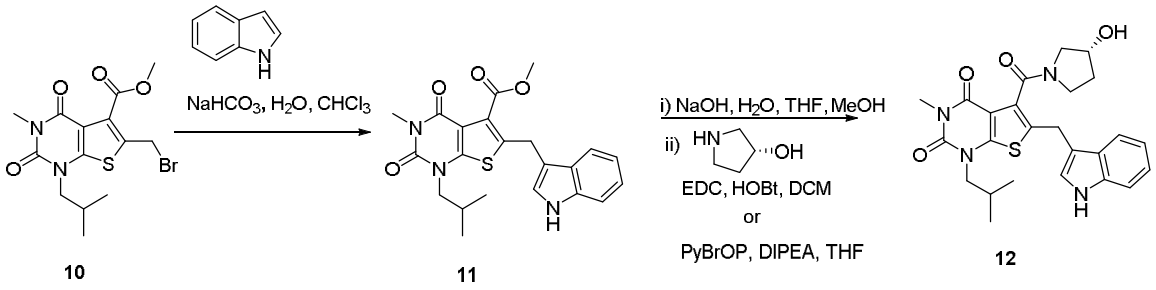

Scheme 1b: Synthesis of indole based pyrimidine-2,4(1H,3H)-dione

3,6-dimethylpyrimidine-2,4(1H,3H)-dione **13** was alkylated with isopropyliodide in presence of potassium carbonate to yield the product **14**. Thiophene group was introduced by treating product **14** with NaSH and further cyclized with ethyl 3-bromopyruvate and $TiCl_4$ to obtain thiophene ester, which was hydrolyzed to get the acid **15**. The corresponding acid was treated with various functionalized aldehydes in presence of LDA and TFA, triethylsilane to obtain **16**. The acid is further converted to obtain corresponding MCT1 inhibitors **17-19** by treating with various amines (**Scheme 1c**).[31]

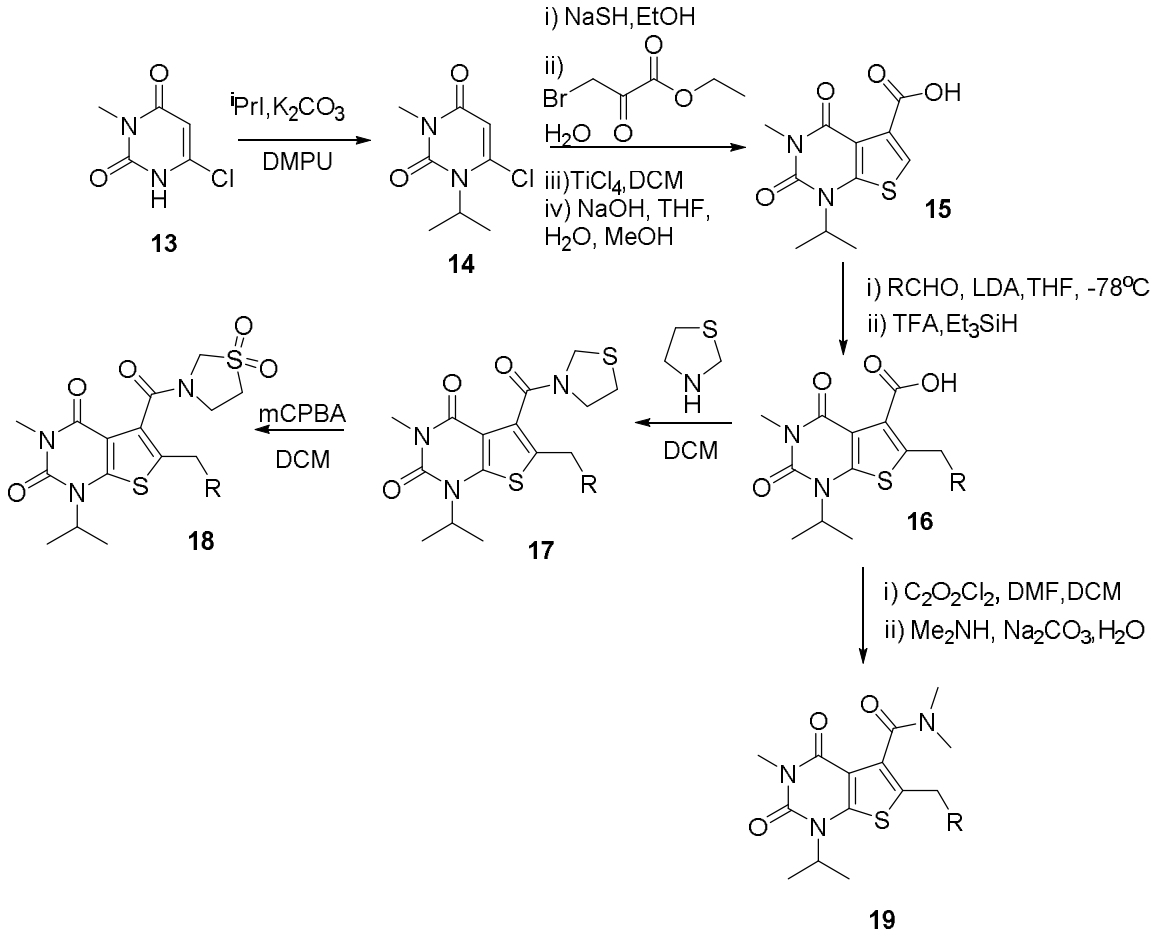

Scheme 1c: Synthesis of thiophenylpyrimidine derivatives

Another lead MCT1 inhibitor reported by AstraZeneca was compound **23**.The preparation of **23** involved coupling of acid **20** with (R)-3-hydroxypyrrolidine in presence of EDC and HOBt to form amide **21**. The hydroxy group was protected with TBDMS and treated with LDA and 6-fluoroquinoline-4-carbaldehyde to get alcohol **22**. This alcohol **22** was deoxygenated and deprotected to obtain the final product **23** (**Scheme 1d**).[31]

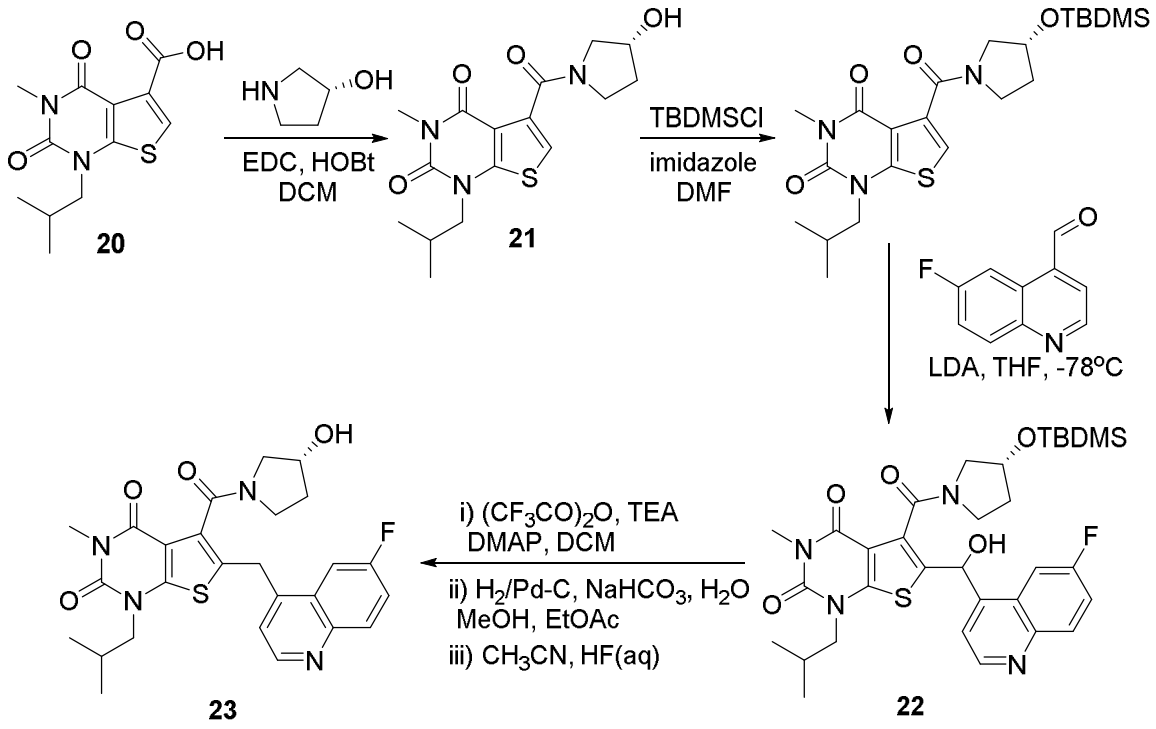

Scheme 1d: Synthesis of pyrimidinedione derivatives

Roush *et al.* also reported several pyrimidinone derivatives as MCT1 inhibitors. Dione **24** was alkylated with isobutyl iodide and subjected to nitration to get nitrate **25**. Furthermore, the product **25** was coupled with naphthylalanine methyl ester and subsequently cyclized by reduction followed by DDQ oxidation to obtain the product **26**. The alcohol **26** was protected with triflyl group upon treatment with triflic anhydride and further treated with pent-4-yn-1-ol in presence of $Pd(PPh_3)_4$ and the product was subjected to reduction catalyzed by Lindlarôs catalyst to get the final product pteridinetrione **27** (**Scheme 1e**). This compound **27** was evaluated for MCT1 inhibitory activity and it was found to be 112 nM.[32]

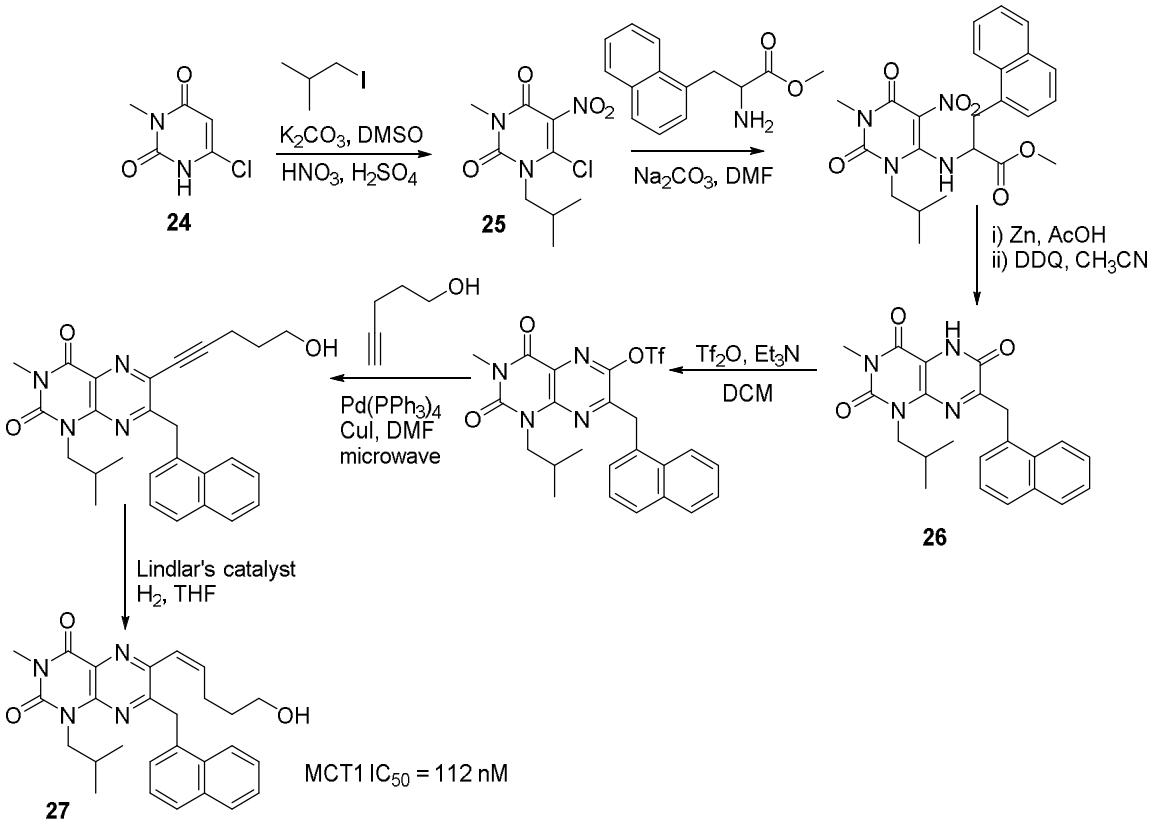

Scheme 1e: Synthesis of pteridinetrione derivatives

4-hydroxy-Ŭ-cyanocinnamic acid (CHC) **28** is a known MCT1 inhibitor and is frequently employed as an MCT1 inhibitor for various biochemical studies (**Figure 1d**).[10,33] Literature reports show that **28** inhibits tumor growth in various cancer xenograft/syngraft models.

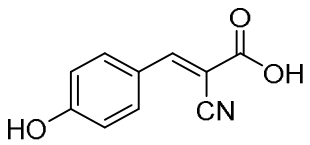

28

CHC

Figure 1d: Structure of CHC **28**

The lack of higher potency of **28** impedes its development as an anticancer drug candidate for clinical usage. Surprisingly, literature search indicated that structure activity relationship (SAR) studies of **28** were never carried out to improve its MCT inhibition potency, cytotoxicity, and pharmacokinetic properties. In this regard, recently, Mereddyôs group carried out a detailed SAR study on **28**, and identified several potent MCT1 inhibitors (**Schemes 1f-h**). Based on **28**, various derivatives were synthesized with *N,N*-dialkyl substitution at 4-position. The synthesis involved *N,N*-dialkylation of aniline **29** in presence of alkyl bromide and subsequent Vilsmeier Haack formylation using $POCl_3$ to obtain aldehyde **30**. The aldehyde was subjected to Knoevenagel condensation with cyanoacetic acid using a mild base piperidine to get the final cyanoacetic acid **31** (**Scheme 1f**).[34]

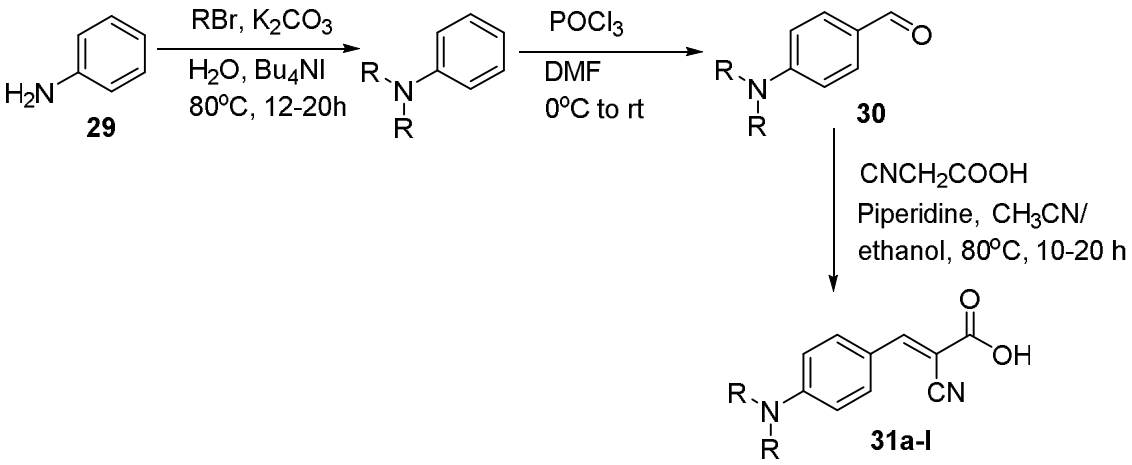

Scheme 1f: Synthesis of *N,N*-dialkyl cyanocinnamic acid derivatives

The derivatives **31a-l** were evaluated for MCT1 inhibition and these molecules were found to be very potent with MCT1 IC_{50} values in the range of 10-400nM (**Figure 1e**).[34]

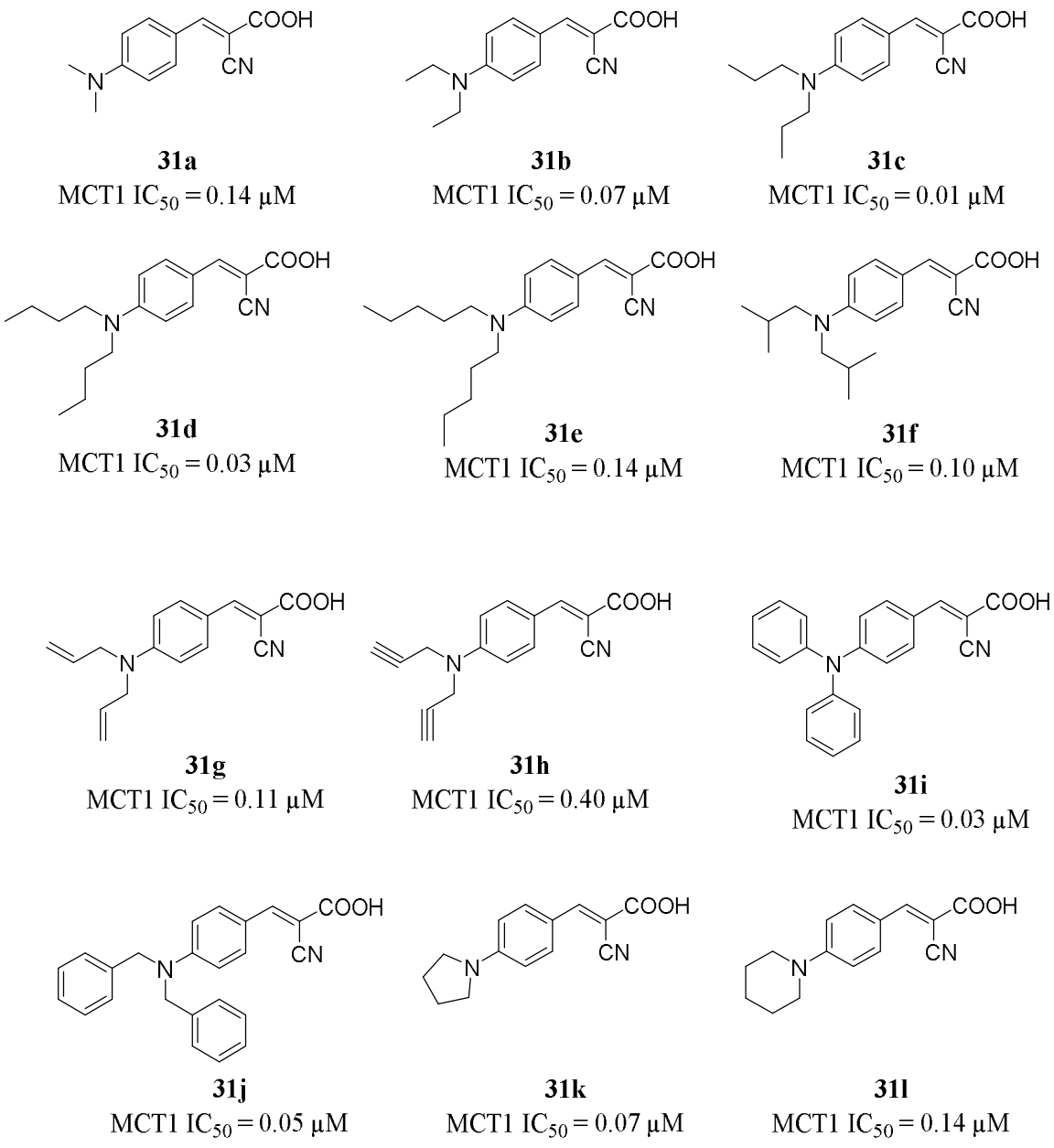

Figure 1e: MCT1 IC_{50} values of *N,N*-dialkyl cyanocinnamic acid derivatives

Based on the results obtained for *N,N*-dialkyl cyanocinnamic acid derivatives, Mereddyôs lab further functionalized these derivatives by introducing methoxy group at 3-position. m-Anisidine **32** was alkylated to form 3-methoxy-4-*N,N*-dialkylaniline **33**, which was formylated using Vilsmeier Haack conditions to obtain aldehyde **34**, which

was further condensed with cyanoacetic acid via Knoevenagel condensation to form the final product **35** (**Scheme 1g**). To increase the solubility, some of these acids were converted to corresponding sodium salts **36** by treating with $NaHCO_3$.[34]

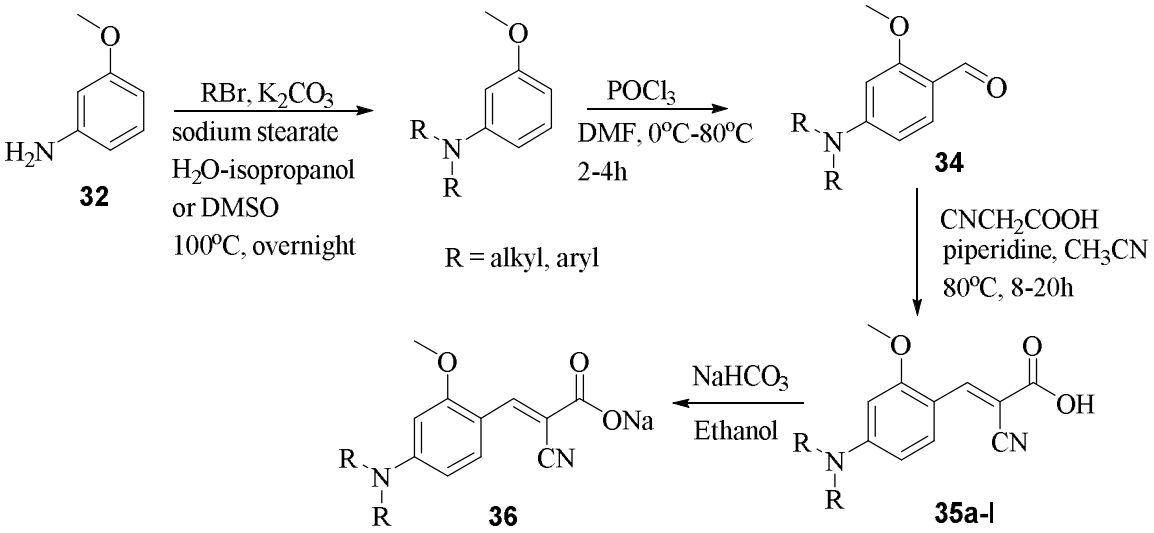

Scheme 1g: Synthesis of 3-methoxy-4-*N,N*-dialkyl cyanocinnamic acid derivatives

All these derivatives **35a-i** were also evaluated for MCT1 inhibition activity and these compounds were found to be even more potent than previous generation derivatives **31a-l**. The MCT1 IC_{50} values of these compounds **35a-i** were in the range of 8-48nM (**Figure 1f**).[34]

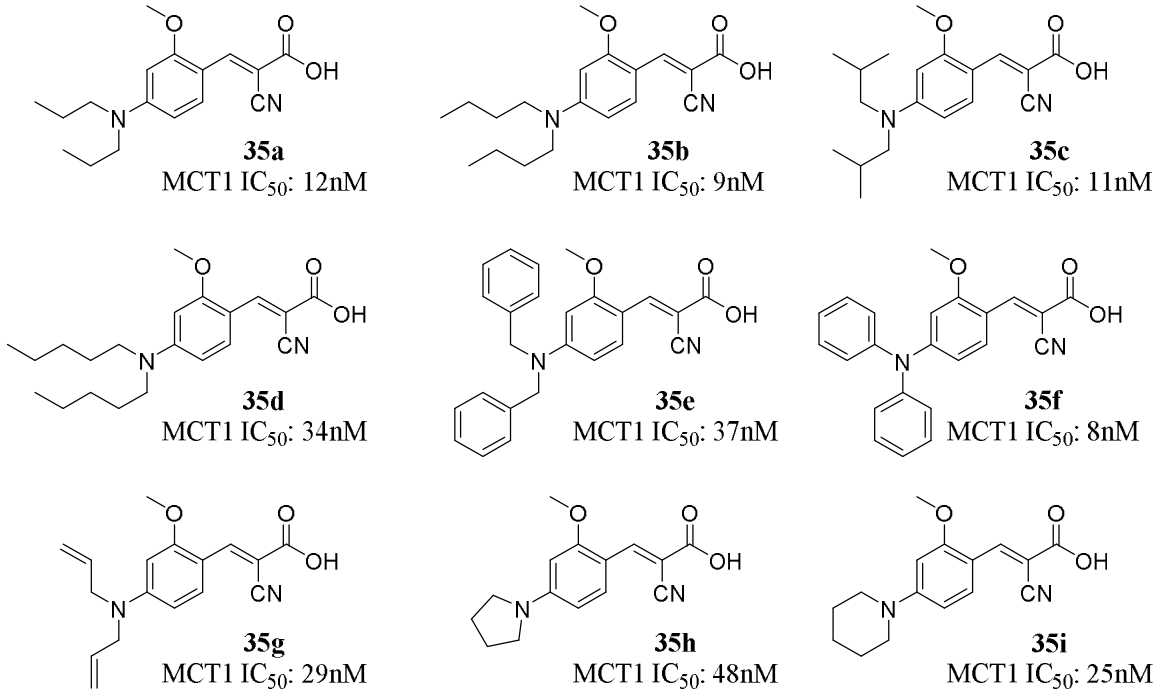

Figure 1f: MCT1 IC_{50} of 3-methoxy-4-*N,N*-dialkyl cyanocinnamic acid derivatives

Compound **35f** was designated as a lead molecule and further tested for its anticancer efficacy in MCT1 expressing colorectal adenocarcinoma (WiDr) tumor xenograft model using female BALB/c nude mice. **35f** (50mg/kg, oral gavage, twice daily dosage) exhibited significant tumor growth inhibition of 45% compared to the control group (**Figure 1g**). In a similar study in WiDr xenograft model, the treatment was started on day-6 of tumor inoculation and the compound **35f** exhibited 56% tumor growth inhibition (**Figure 1g**).[34]

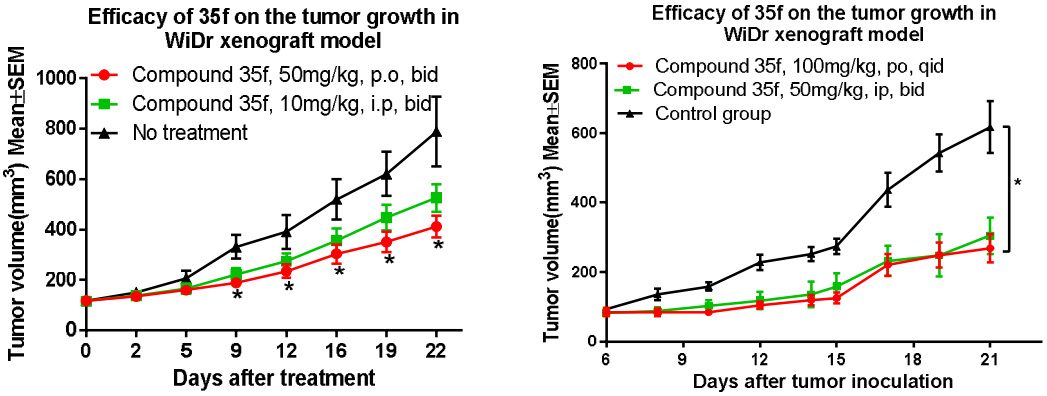

Figure 1g: Tumor growth inhibition of **35f** in WiDr cancer xenograft model

Although lead derivative **35f** showed promising results in *in vivo* tumor growth studies, **35f** had poor oral bioavailability and exhibited toxicity at higher concentrations. In this regard, Mereddyôs lab developed coumarin based MCT1 inhibitors to increase oral bioavailability and decrease *in vivo* toxicity. Coumarins were synthesized using 3-aminophenol **37** as a starting material. Amine **37** was alkylated using alkyl bromide and formylated under Vilsmeier Haack conditions to obtain the aldehyde **38**. It was then condensed with diethyl malonate in presence of piperidine, then refluxed in NaOH and treated with dilute HCl to obtain the final product **39** (**Scheme 1h**).[35]

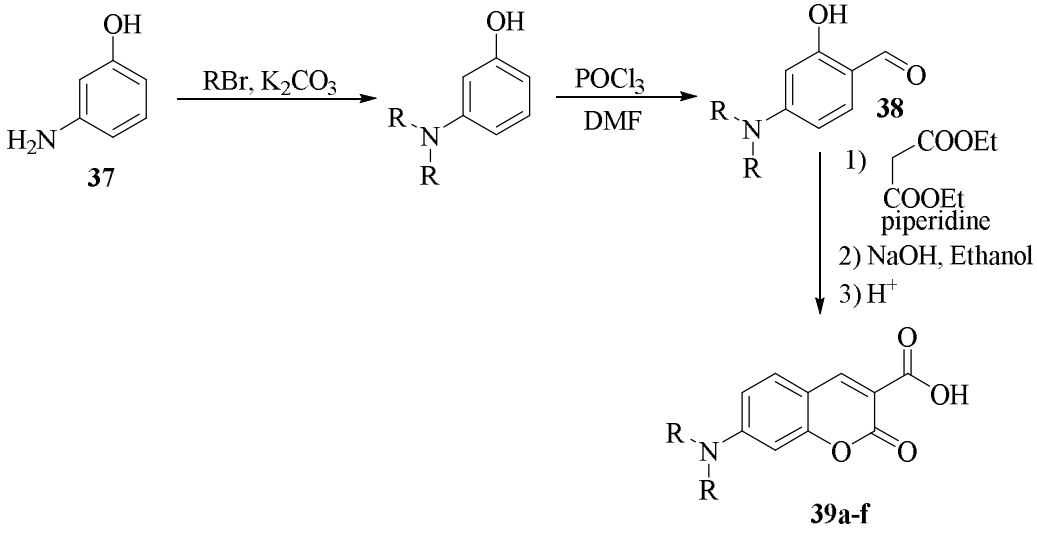

Scheme 1h: Synthesis of *N,N*-dialkyl carboxy coumarin derivatives

Compounds **39a-f** were also evaluated for their MCT1 inhibition properties and were found to be in the range of 90-450nM (**Figure 1h**).[35]

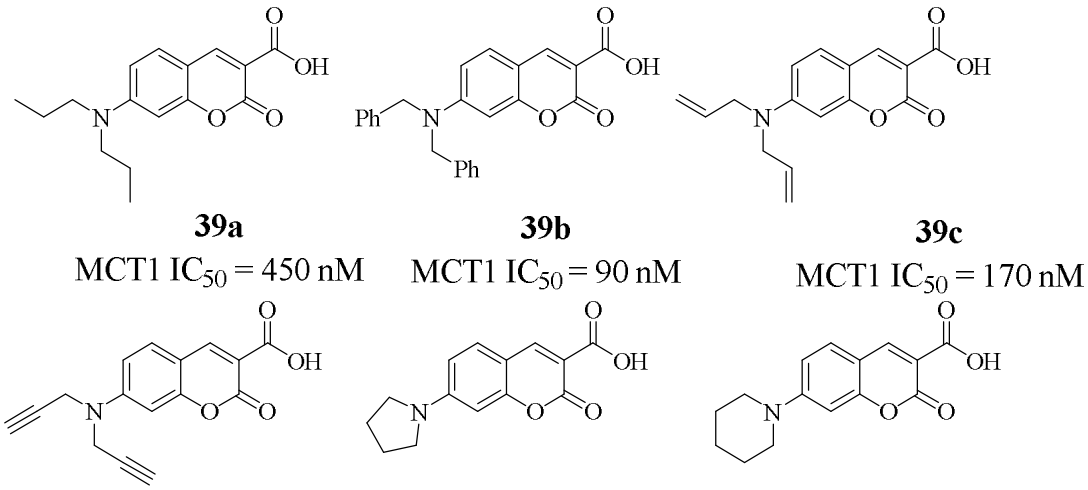

Figure 1h: MCT1 IC_{50} values of *N,N*-dialkyl carboxy coumarin derivatives

Based on the encouraging results, compound **39b** was evaluated for anticancer efficacy in MCT1 expressing GL261-luc2 tumor syngraft model. Compound **39b** exhibited significant tumor growth inhibition of 77% compared to control group (**Figure 1i**).[35]

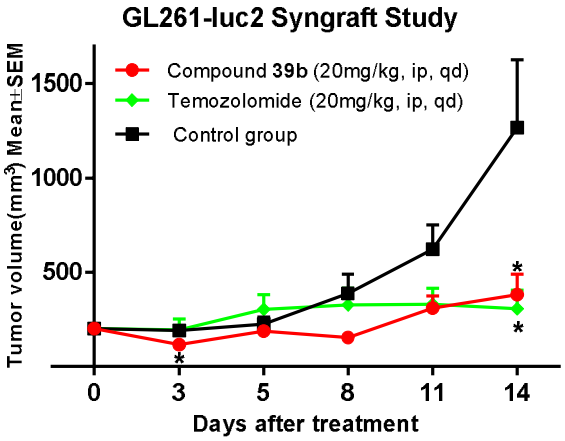

Figure 1i: Tumor growth inhibition of **39b** in GL261-luc2 cancer syngraft model

While these studies were going on, Sonveaux *et al.* reported *N,N*-dialkyl substituted carboxy coumarin derivatives as potent MCT1 inhibitors. The synthetic scheme involved palladium catalyzed amination of 3-bromophenol **40** and subsequent Vilsmeier Haack formylation to obtain aldehyde **41** and condensation with meldrum acid to form aminocarboxy coumarin **42** (**Scheme 1i**). Taking **42** as a lead candidate compound, they carried out numerous tumor growth inhibition studies in MCT1 expressing mouse xenograft models. These studies indicated an efficient tumor growth inhibition in cervical cancer (SiHa), estrogen receptor positive breast cancer (MCF7) and colorectal adenocarcinoma (HCT116) models, respectively.[36,37]

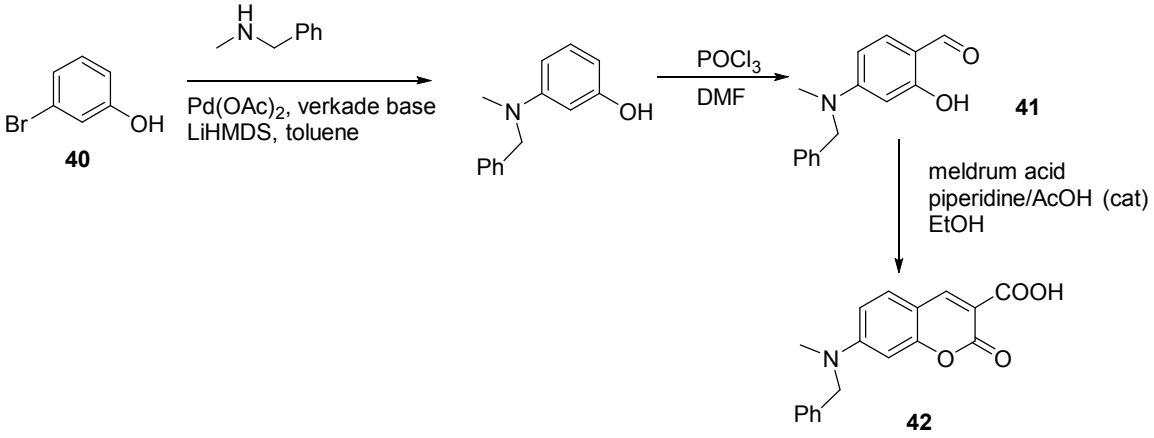

Scheme 1i: Synthesis of aminocarboxy coumarin derivatives

As described above, glycolysis is one of the important hallmarks of many solid tumors and disrupting the glycolysis can lead to tumor growth suppression. As also described above, MCT1 appears to be a highly valid therapeutic target to develop novel anticancer agents that can act as single agents or in combination with various other cytotoxic agents for better therapeutic outcome in cancer treatment.

CHAPTER 2: EXPLORATION OF α,β-UNSATURATED HYDANTOINS AS POTENTIAL MCT1 INHIBITORS FOR GLIOBLASTOMA MULTIFORME TREATMENT

Present Work: Results and Discussion

Glioblastoma multiforme (GBM) is a highly aggressive brain malignancy.[38,39] Apart from surgical resection and radiation therapy, GBM patients are also treated with chemotherapy. However, the chemotherapeutic options are extremely limited, with only two drugs, temozolomide (TMZ, a small molecule DNA alkylator) and bevacizumab (an anti-angiogenic monoclonal antibody), being currently prescribed for this virulent form of cancer. Clinical usage of highly expensive bevacizumab is controversial as it does not extend the overall survival of patients and it only improves some quality of life through reduction of edema. In spite of these treatment protocols, the 5-year survival rate of GBM patients is dismally low (~5%) with a median survival of ~12 months. Novel chemotherapeutics that are selectively toxic to cancer cells, preferably that work on chemoresistant cells, and that extend the overall survivability of GBM patients are an unmet medical need.

Brain tumors including glioblastoma express MCT1 and in fact CHC **28** was utilized for an efficient tumor growth inhibition in glioblastoma rat models.[33] Since **28** doesnôt cross blood brain barrier (BBB), it was administered intracranially directly to the tumor bed via osmotic pump. Intracranial delivery directly into the tumor is impractical in a clinical setting and hence development of MCT1 inhibitors that can cross BBB is highly critical.

As indicated in schemes **1g** and **1h** in introduction, two of the lead candidate compounds **35f** and **39b** that are based on **28** exhibited significant tumor growth inhibition in various mice xenograft and syngraft models. However, these derivatives are based on monocarboxylic acids, and due to their ionization, they do not cross the blood brain barrier (BBB) efficiently. Hence, these candidate compounds cannot be used for brain tumor or glioblastoma multiforme treatment.

Hydantoin **2a** is a urea based imido imidazolidine compound and derivatives of hydantoin are found in several medicinally important compounds. Hydantoin based pharmaceutical compounds readily cross BBB to be used for brain related diseases. For example, hydantoin containing anticonvulsants include phenytoin and fosphenytoin. Some other hydantoin containing pharmaceuticals are muscle relaxant dantrolene and antiarrhythmic agent ropitoin (**Figure 2a**).

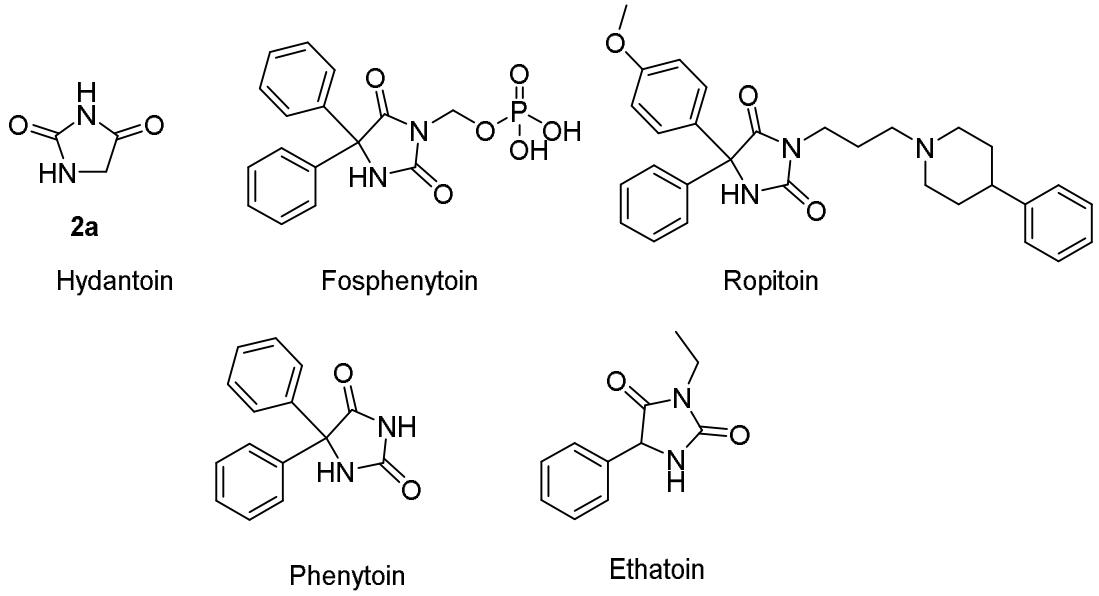

Figure 2a: Structures of hydontoin and hydontoin based drugs

Hydantoin **2a** contains an active hydrogen atom that can be abstracted readily in the presence of amines or hydroxy containing bases, and they can be readily condensed

with aldehydes in a Knoevenagel type fashion to provide Ŭ,ß-unsaturated imidazolidine diones (**Scheme 2a**).

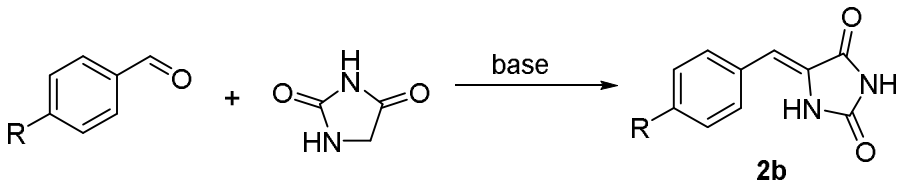

Scheme 2a: General synthesis of Ŭ,ß-unsaturated imidazolidine diones

28 and first generation *N,N*-dialkyl CHC derivatives contain a double bond with two electron withdrawing groups such as cyano, carboxylic acid, or ester. We hypothesized that the hydantoin group in **2b** could also exhibit MCT inhibition properties without an ionizable carboxylic acid group (**Figure 2b**). We envisioned that the condensed product **2b** would have optimal physicochemical properties to cross the BBB for potential brain tumor treatment. In this regard we have synthesized several hydrontoin derivatives from various substituted benzaldehydes.

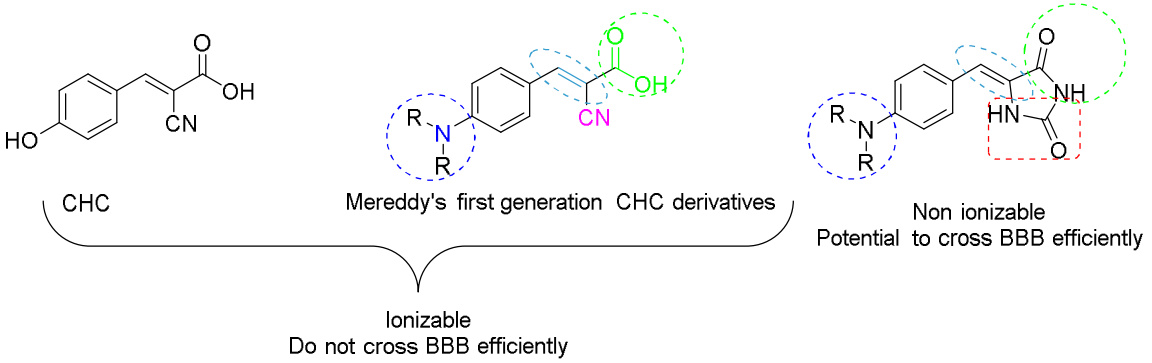

Figure 2b: Cyanocinnamic acid and Ŭ,ß-unsaturated imidazolidine dione

Initially, we reacted benzaldehyde with commercially available hydantoin **2a** in the presence of acetic acid and ammonium acetate to obtain (Z)-5-

benzylideneimidazolidine-2,4-dione **2c**. The reaction was sluggish at room temperature and refluxing in ammonium acetate and acetic acid, the product **2c** was obtained in 65% yield upon simple filtration and recrystallization in ethyl acetate (**Scheme 2b**). We employed ammonium acetate as a base since this particular base provided better yields in Knovenagel condensation of hydantoins with aldehydes.

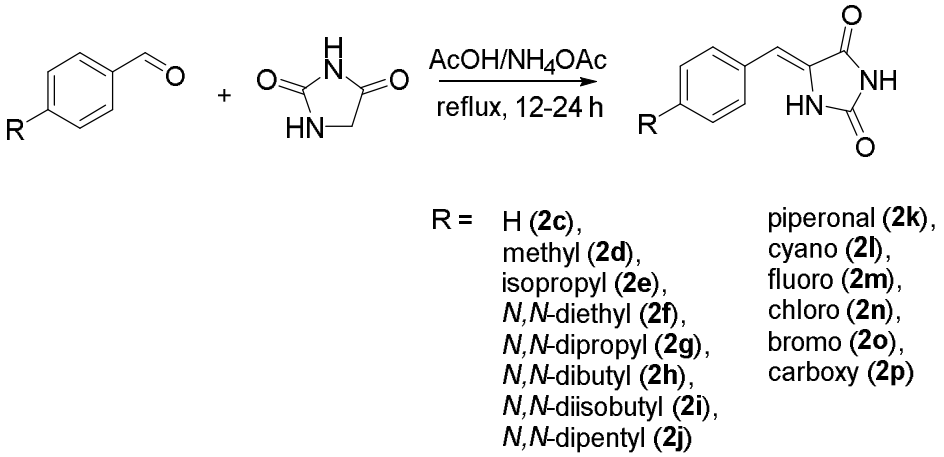

Scheme 2b: Synthesis of α,β-unsaturated imidazolidine dione derivatives

Apart from benzaldehyde, we have also employed tolualdehyde and 4-isopropyl benzaldehyde. These two aldehydes readily coupled with **2a** to give benzylideneimidazolidine diones **2d** and **2e** in good yields (69 and 72%). Since *N,N*-dialkyl substitution on CHC template provided excellent MCT1 inhibition properties we initially chose 4-*N,N*-diethyl, 4-*N,N*-dipropyl, 4-*N,N*-dibutyl, 4-*N,N*-diisobutyl, and 4-*N,N*-dipentyl benzaldehydes to condense them with **2a**. All these aldehydes upon treatment with hydantoin in the presence of ammonium acetate in refluxing acetic acid gave the corresponding imidazoldine diones **2f-2j** in 65-75% yields. The analytically pure samples were readily obtained with simple recrystallization in ethyl acetate. As a part of the examples of electron donating substituents, we have also included bicyclic piperonal

to obtain the corresponding imidazolidine dione **2k** in excellent yield. In the electron withdrawing category, we have selected 4-fluoro, 4-chloro, and 4-bromo benzaldehydes. These aldehydes smoothly condensed with **2a** under standard conditions in the presence of ammonium acetate and we were able to obtain the corresponding imidazoldine diones **2l-2n** in 64-78% yields. All the synthesized compounds **2b-2n** were thoroughly characterized by ^{1}H NMR, ^{13}C NMR, and C, H, N elemental analysis.

After synthesizing the representative Ǆ,ǅ-unsaturated hydantoin derivatives **2b-2n**, we evaluated them for their MCT1 inhibition properties. We have chosen rat brain endothelial (RBE4) cell line for the MCT1 inhibition study. This cell line primarily expresses MCT1 as confirmed by western blot analysis (**Figure 2c**).

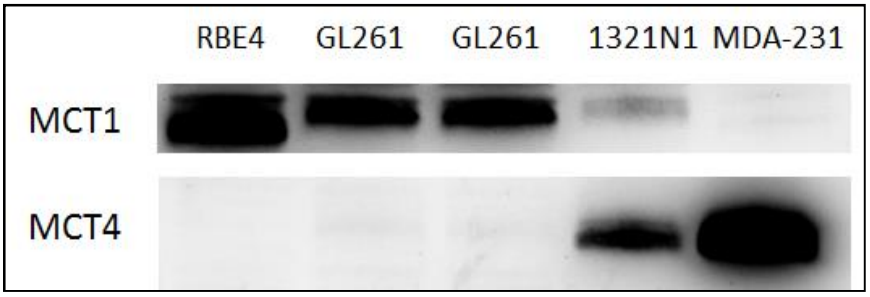

Figure 2c: Western blot of MCT1 expression in RBE4 cell line

For MCT1 inhibition, we have employed [^{14}C]-lactate uptake study as reported by Mereddyǀs group previously. Briefly, RBE4 cells were seeded into 24 well plate and exposed to candidate compounds in the presence of [^{14}C]-lactate for 20 minutes. The cells were washed, lysed and the radioactivity of these cell lysates was measured using Beckman scintillation counter. Initially, we tested the compounds at higher concentrations of 50 and 100 ε M. Unfortunately, none of the compounds exhibited any MCT1 inhibition even at these high concentrations (**Table 2a**). Disappointed by lack of

potency even at high concentrations, we chose 4-carboxy benzaldehyde for condensation with **2a** (Scheme **2c**). The rationale for choosing this compound is the presence of the monocarboxylic acid after hydantoin condensation. Unfortunately, this monocarboxy hydantoin derivative **2o** also did not exhibit any MCT1 inhibition properties. Disappointed by the lack of any MCT1 inhibition property, we did not pursue this project any further.

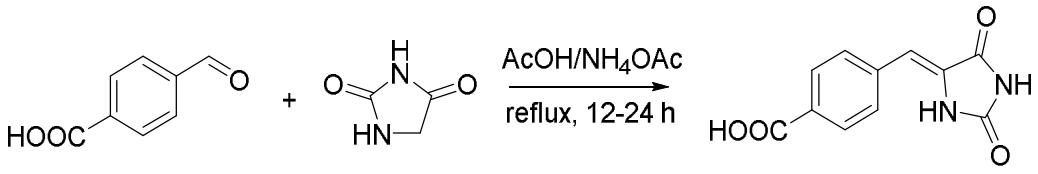

Scheme 2c: Synthesis of monocarboxy hydantoin derivative

Table 2a: MCT1 Inhibition Studies in Hydantoin Derivatives

Sl. No.	Compound	MCT1 IC_{50}
2c	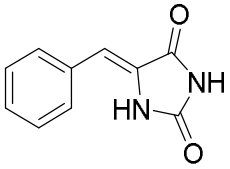	> 100 µM
2d	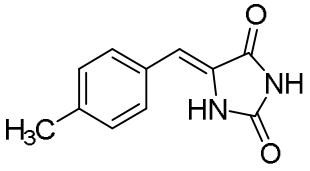	> 100 µM
2e	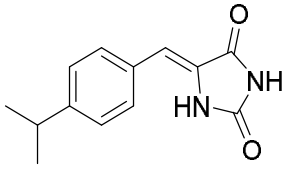	> 100 µM

2f	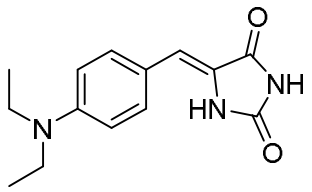	> 100 µM
2g	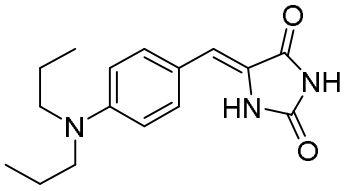	> 100 µM
2h	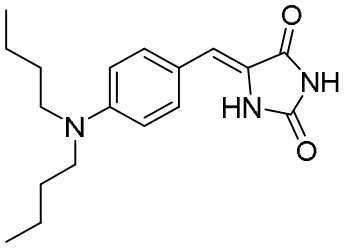	> 100 µM
2i	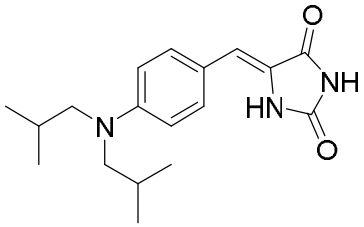	> 100 µM
2j	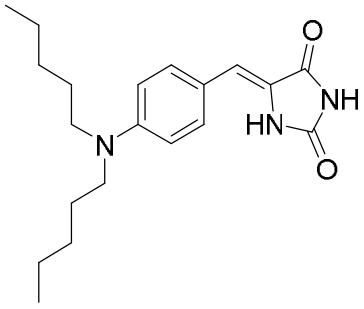	> 100 µM
2k	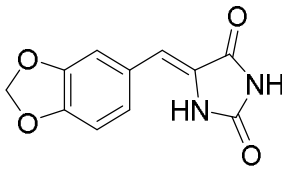	> 100 µM

2l	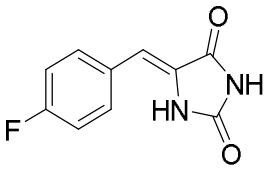	> 100 µM
2m	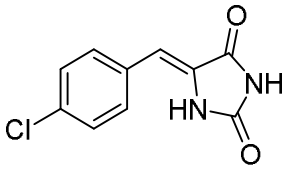	> 100 µM
2n	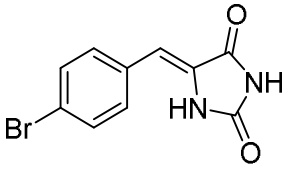	> 100 µM
2o	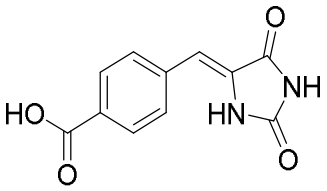	> 100 µM

Conclusion:

In conclusion we have synthesized several Ŭ,ɓ-unsaturated imidazolidine diones **2c-2o** via condensation of various electron donating and electron withdrawing benzaldehydes with hydantoin **2a** in the presence of ammonium acetate in refluxing acetic acid. We evaluated the condensed products for their MCT1 inhibition properties via [^{14}C]-uptake using RBE4 cell line. Unfortunately, none of the compounds exhibited any MCT1 inhibition properties even at high concentrations. These imidazolidine dione compounds have excellent pharmaceutical properties to cross the BBB for potential brain tumor treatment. We abandoned this project due to the lack of MCT1 inhibition properties.

CHAPTER 3: CYANOCINNAMIC ACID PRODRUGS VIA PASSERINI REACTION: SYNTHESIS AND BIOLOGICAL EVALUATION AS MCT1 INHIBITORS

Current Work: Results and Discussion

Since hydantoin based Ű,ß-unsaturated imidazolidine diones **2c-2p** did not show any MCT1 inhibition property, we thought to preserve the cyanocinnamate moiety, and synthetize hydrophobic prodrugs that have the potential to cross the BBB. In this regard, we employed the Passerini three-component coupling reaction that involves coupling of a carboxylic acid with an aldehyde in the presence of an isocyanide (**Scheme 3a**). This coupling reaction has been extensively studied and utilized for preparing various synthetic intermediates and pharmaceutical derivatives.

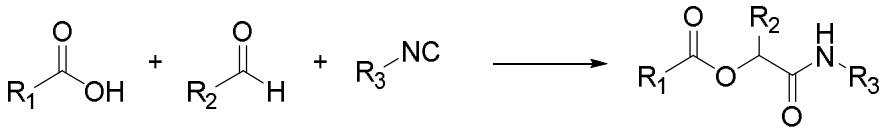

Scheme 3a: General scheme of Passerini reaction

As a representative example we have chosen Ű-cyanocinnamic acid **3a** for Passerini coupling reaction with various aldehydes and t-butyl isocyanide. **3a** was readily synthesized via Knovenagel condensation of benzaldehyde with cyanoacetic acid in the presence of NaOH (**Scheme 3b**). Keeping **3a** as a representative example, we synthesized various Passerini reaction derived hydroxamide prodrugs (**Scheme 3b**).

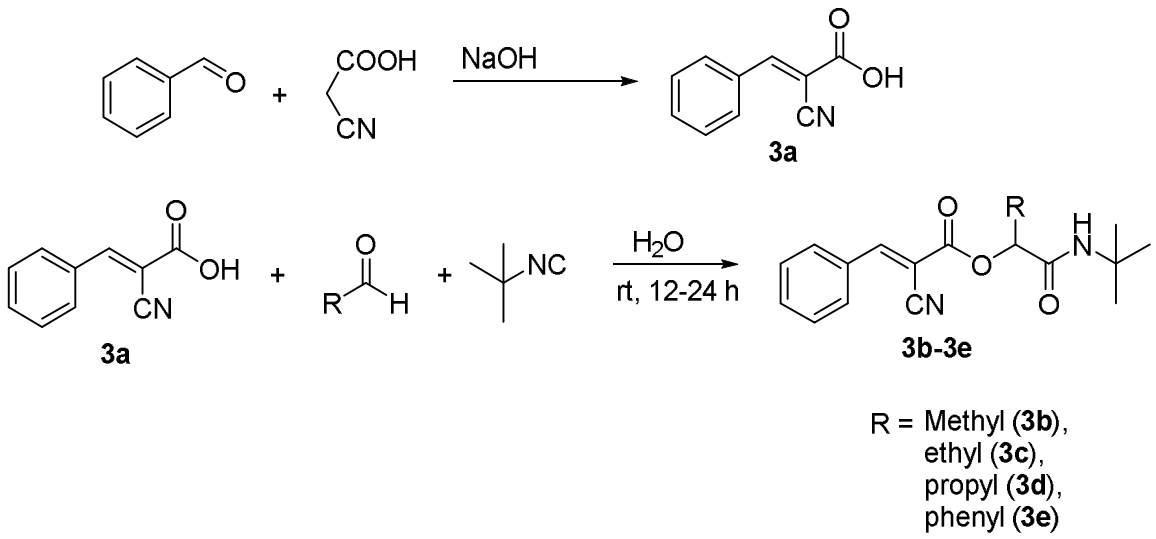

Scheme 3b: Synthesis of Ŭ-cyanocinnamic acid and Ŭ-cyanoacyloxyamide prodrugs.

We have utilized t-butyl isocyanide as a representative example in the isocyanide category. Initially, keeping cyanocinnamic acid **2a** and t-butyl isocyanide as constants, we carried out Passerini reaction with various aldehydes in water.[40-42] Although Passerini reaction can be carried out in a number of different solvents, we have chosen to use water because of the cleanliness of the reaction and the crude products that could be readily isolated by simple filtration. Aliphatic aldehyde examples included acetaldehyde, propionaldehyde and butyraldehyde. We were able to obtain the corresponding Passerini products via simple suction filtration through Buchner funnel. The crude products were recrystallized in ethyl acetate to obtain analytically pure samples **3b-3d** in 44-59% yields. We have chosen benzaldehyde as an aromatic example and the corresponding Passerini product **3e** was obtained in 48% yield. All these compounds were characterized using ^{1}H NMR, ^{13}C NMR and CHN elemental analysis.

After synthesizing the Ŭ-cyanoacyloxyamide prodrugs of **3a**, these compounds were evaluated for their MCT1 inhibition properties using a predominantly MCT1

expressing RBE4 cell line and [^{14}C]-lactate. Gratifyingly, Passerini product **3b** derived from acetaldehyde displayed an IC_{50} value of ~8 ε M compared to CHC which has IC_{50} value >100 ε M. The propionaldehyde Passerini product **3c** also showed similar activity to that of acetaldehyde with an IC_{50} of ~7 ε M. The butyraldehyde product **3d** exhibited a slightly higher IC_{50} value of ~13 ε M. Similarly, the benzaldehyde Passerini product **3e** exhibited IC_{50} value in the 13 ε M range (**Table 3a**).

Table 3a: MCT1 IC_{50}^{*} values of Ŭ-cyanoacyloxyamide prodrugs

Sl. No	**Compound**	**MCT1 IC_{50}**
3b	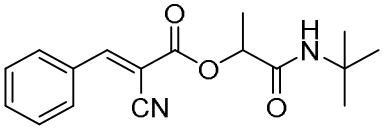	~8 µM
3c	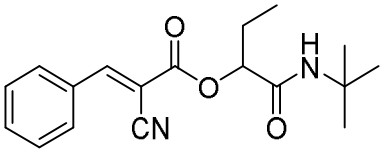	~7 µM
3d	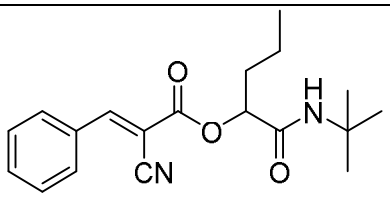	~13 µM
3e	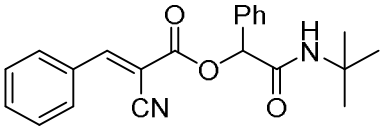	~13 µM

*Experiment conducted in triplicate wells, average±SEM to be determined

Encouraged by the higher inhibitory activity of the Passerini based prodrugs of cyanocinnamic acid **3a**, we then carried out the Passerini reaction on the actual CHC substrate itself. For this purpose we have chosen isopropyl, t-butyl, and benzyl

isocyanides. We did not choose the methyl isocyanide due to its high toxicity and low boiling point. For aldehydes, we have chosen acetaldehyde, and butyraldehyde. The reaction of CHC with isopropyl isocyanide and acetaldehyde was facile and the product **3f** could be obtained in 50% yield after recrystallization of the crude product with ethyl acetate. Similarly, reaction of butyraldehyde with isopropyl isocyanide and CHC gave the corresponding product **3g** in 54% yield (Scheme **3c**). MCT1 inhibition of **3f** and **3g** exhibited IC_{50} values ~10 and 21 ε M, respectively.

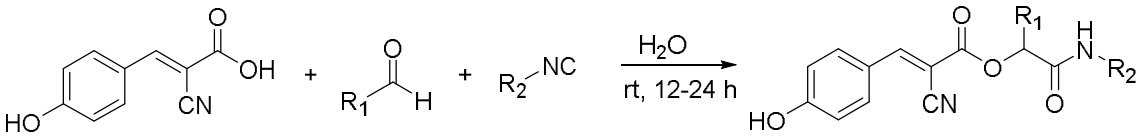

R_2 = isopropyl, R_1 = methyl (**3f**),
R_2 = isopropyl, R_1 = propyl (**3g**),
R_2 = tert-Butyl, R_1 =methyl (**3h**),
R_2 = tert-Butyl, R_1 =ethyl (**3i**),
R_2 = tert-Butyl, R_1 =propyl (**3j,**
R_2 = tert-Butyl, R_1 =phenyl (**3k**),
R_2 = benzyl, R_1 = methyl (**3l**),
R_2 = benzyl, R_1 = ethyl (**3m**),
R_2 =benzyl, R_1 = propyl (**3n**),
R_2 = benzyl, R_1 = phenyl (**3o**)

Scheme 3c: Synthesis of CHC based Ŭ-cyanoacyloxyamides

We then carried out more readily available, less toxic, and inexpensive t-butyl isocyanide, and coupled it with CHC in the presence of acetaldehyde, propionaldehyde, butyraldehyde, and benzaldehyde under Passerini conditions. The corresponding products **3h-3k** were obtained in analytically pure form after recrystallization with ethyl acetate in 47-60% yields. MCT1 inhibition studies of these compounds **3h-3k** using RBE4 cell lines indicated the IC_{50} values ~2-4 ε M range compared to the parent CHC with an IC_{50} of ~150 ε M. Encouraged by this higher potency at lower concentrations, we have also included readily available benzyl isocyanide. In this case also we have included

acetaldehyde, propionaldehyde, butyraldehyde, and benzaldehyde. The Passerini coupling took place smoothly to provide the products **3l-3o** in 46-57% yields. Surprisingly, MCT1 inhibition studies of these compounds showed that the aliphatic Passerini products compounds **3l-3n** did not exhibit activity even at 100 ε M, whereas the benzaldehyde Passerini product **3o** showed ~0.75 ε M inhibition which is ~ 200 times more potent than the parent CHC inhibitor. However, these are preliminary results which have been carried out only once and repetition studies are currently ongoing.

Table 3b: MCT1 IC_{50}* values of CHC based Ŭ-cyanoacyloxyamide derivatives

Sl. No	**Compound**	**MCT1 IC_{50}**
3f	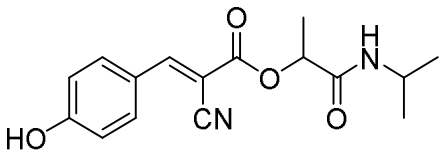	~10 µM
3g	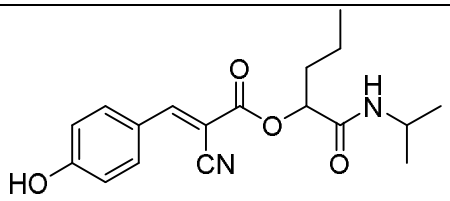	~21 µM
3h	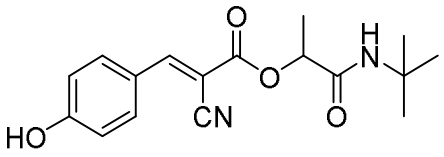	~4 µM
3i	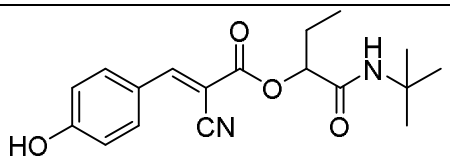	~4 µM

3j	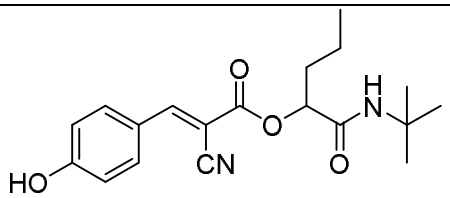	~4 µM
3k	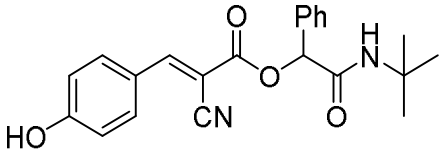	2.4±0.2 µM
3l	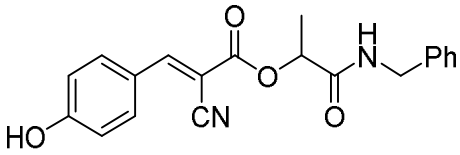	>100 µM
3m	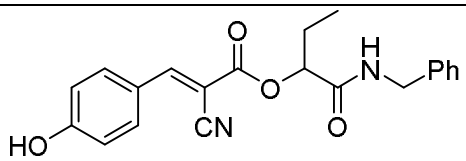	>100 µM
3n	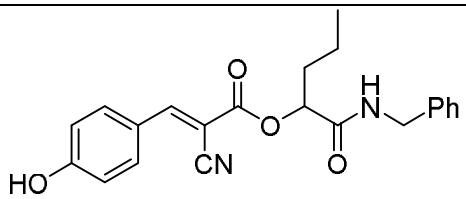	>100 µM
3o	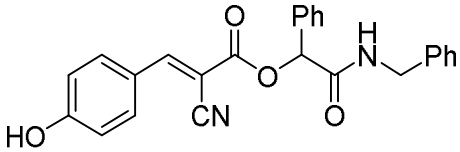	0.75 µM

* *Experiment conducted in triplicate wells, average±SEM to be determined unless specified

We then included methyl, ethyl and phenyl pyruvates as aldehyde surrogates for Passerini coupling with CHC. The keto group in the pyruvate is highly active due to the presence of an electron withdrawing ester group in the Ŭ-position. The Passerini coupling of these pyruvates with CHC and isocyanides was very facile, and the Passerini products

3p-3s were obtained readily in 47-59% yield (**Scheme 3d**). The Passerini product **3p** product gave an IC_{50} value of ~13 ε M. The biological evaluation of other Passerini products **3q-3s** is currently ongoing.

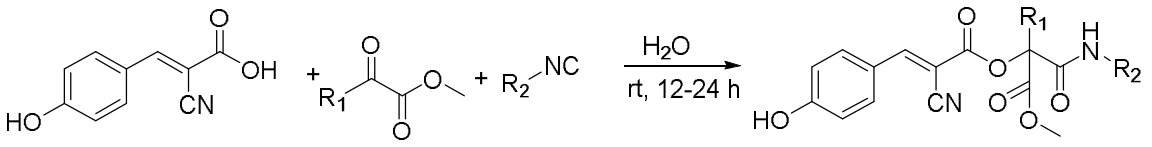

R_2 = tert-Butyl, R_1 = methyl (**3p**),
R_2 = tert-Butyl, R_1 = ethyl (**3q**),
R_2 = isopropyl, R_1 = ethyl (**3r**),
R_2 = isopropyl, R_1 = phenyl (**3s**)

Scheme 3d: Synthesis of pyruvate based Ŭ-cyanoacyloxyamides

Conclusions:

In conclusion, we have designed and synthesized Ŭ-cyanoacyloxyamides from Ŭ-cyanocinnamic acid and 4-hydroxy-Ŭ-cyanocinnamic acid via three component Passerini reaction. The synthesized products were evaluated for their MCT1 inhibition properties using [^{14}C]-lactate and RBE4 cells. These preliminary biological studies indicated that several of Passerini based prodrugs exhibited moderate to good MCT1 inhibition properties at low µM concentration. Importantly, some of these prodrugs showed 100-200 times more potency than the parent CHC molecule. Future studies should involve the calculation of IC_{50} values in triplicate for many of the derivatives that exhibited potency less than 10 µM concentration. These studies should provide a lead candidate compound that should be evaluated for their systemic toxicity, pharmacokinetic/pharmacodynamics properties, BBB penetration concentration, anticancer efficacy studies in a brain tumor model, etc. If brain concentration of the lead compound is not sufficient to induce the tumor growth inhibition, then they can be tested in tumor models that do not involve penetration of BBB.

CHAPTER 4: EXPERIMENTAL AND SPECTRAL CHARACTERIZATION

Materials and Cell Culture Conditions:

Reagent grade hydantoin, 4-hydroxy Ŭ-cyanocinnamic acid, acetaldehyde, propionaldehyde, butyraldehyde, benzaldehyde, methyl pyruvate, methyl 2-ketobutyrate, methyl benzoyl formate, piperidine, and acetonitrile were purchased from Sigma-Aldrich. Tertiary butyl isocyanide, isopropyl isocyanide, and benzyl isocyanide were purchased from Alfa-Aesar. RBE4 cells were obtained from F. Roux* and were cultured in 1:1 Ŭ-MEM (Gibco), F10-HAM (Gibco), 10% heat inactivated FBS (Atlanta Biologicals), 0.3 mg/ml geneticin G418 (Teknova), 1% antibiotic-antimycotic (Gibco).

*Roux, F.; Durieu-Trautmann, O.; Chaverot, N.; Claire, M.; Mailly, P.; Bourre, J. M.; Strosberg, A. D.; Couraud, P. O. *J. Cell Physiol*. **1994**, *159*, 101ï 113.

Representative example of synthesis of benzylideneimidazolidine-2,4-diones:

To a solution of benzaldehyde (5 mmol) in acetic acid (7 mL) was added hydantoin (15 mmol) and ammonium acetate (20 mmol) and the reaction was refluxed for 12 hours. Upon the completion of the reaction (TLC), the reaction mixture was quenched with ice-cold water. The solid was filtered and washed with water and hexanes and purified via recrystallization in ethylacetate to obtain (Z)-5-benzylideneimidazolidine-2,4-dione in 65% yield.

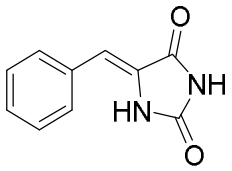

(Z)-5-benzylideneimidazolidine-2,4-dione (**2c**)

Yield: 65%

^{1}H NMR (500 MHz, DMSO-d_6):

ŭ 7.62 (d, *J* = 8.5 Hz, 2H), 7.40 (t, *J* = 7.5 Hz, 2H), 7.33 (t, *J* = 7.0 Hz, 1H), 6.42 (s, 1H)

^{13}C NMR (125 MHz, DMSO-d_6):

ŭ 166.30, 156.45, 133.67, 130.06, 129.46, 129.05, 128.69, 108.98

Anal. Calcd for $C_{10}H_8N_2O_2$ (188.19): C 63.83, H 4.29, N 14.89

Found: C 63.12, H 4.11, N 14.23

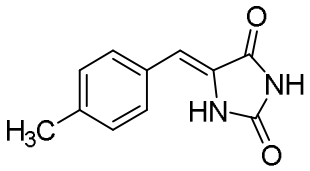

(Z)-5-(4-methylbenzylidene)imidazolidine-2,4-dione (**2d**)

Yield: 69%

^{1}H NMR (500 MHz, DMSO-d_6):

ŭ 7.52 (d, *J* = 8.5 Hz, 2H), 7.21 (d, *J* = 7.5 Hz, 2H), 6.39 (s, 1H), 2.32 (s, 3H)

^{13}C NMR (125 MHz, DMSO-d_6):

ŭ 166.36, 156.43, 138.84, 130.84, 130.10, 130.07, 127.95, 109.2, 21.63

Anal. Calcd for $C_{11}H_{10}N_2O_2$ (202.21): C 65.34, H 4.98, N 13.85

Found: C 65.96, H 5.01, N 14.22

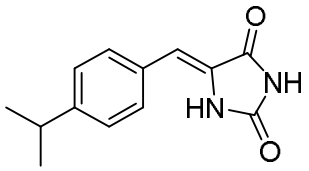

(Z)-5-(4-isopropylbenzylidene)imidazolidine-2,4-dione (**2e**)

Yield: 72%

^{1}H NMR (500 MHz, DMSO-d_6):

ŭ 7.38 (d, *J* = 8.0 Hz, 2H), 7.16 (d, *J* = 8.0 Hz, 2H), 6.37 (s, 1H), 2.85-2.80 (m, 1H), 1.16 (d, *J* = 7.0 Hz, 6H)

^{13}C NMR (125 MHz, DMSO-d_6):

ŭ 166.30, 156.37, 149.66, 131.25, 130.19, 127.99, 127.44, 109.19, 33.99, 24.37

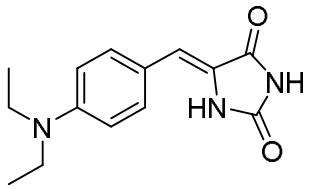

(Z)-5-(4-(diethylamino)benzylidene)imidazolidine-2,4-dione (**2f**)

Yield: 70%

^{1}H NMR (500 MHz, DMSO-d$_6$):

ŭ 11.02 (br s, 1H), 10.21 (br s, 1H), 7.45 (d, *J* = 8.5 Hz, 2H), 6.65 (d, *J* = 8.5 Hz, 2H), 6.33 (s, 1H), 3.41-3.36 (m, 4H), 1.11 (t, *J* = 7.0 Hz, 6H)

^{13}C NMR (125 MHz, DMSO-d$_6$):

ŭ 166.39, 156.20, 148.25, 132.05, 124.17, 120.02, 111.93, 111.20, 44.38, 13.18

Anal. Calcd for $C_{14}H_{17}N_3O_4$ (259.31): C 64.85, H 6.61, N 16.20

Found: C 65.09, H 6.34, N 15.98

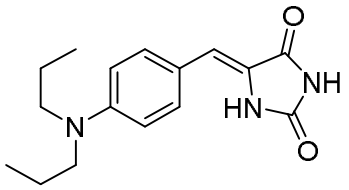

(Z)-5-(4-(dipropylamino)benzylidene)imidazolidine-2,4-dione (**2g**)

Yield: 66%

^{1}H NMR (500 MHz, DMSO-d_6):

ŭ 7.44 (d, *J* = 8.5 Hz, 2H), 6.63 (d, *J* = 8.5 Hz, 2H), 6.33 (s, 1H), 3.29 (t, *J* = 7.5 Hz, 4H), 1.57-1.52 (m, 4H), 0.90 (t, *J* = 7.5 Hz, 6H)

^{13}C NMR (125 MHz, DMSO-d_6):

ŭ 166.38, 156.18, 148.71, 131.96, 124.18, 119.98, 111.98, 111.19, 52.45, 20.76, 11.85

Anal. Calcd for $C_{16}H_{21}N_3O_4$ (287.36): C 66.88, H 7.37, N 14.62

Found: C 66.27, H 7.01, N 14.19

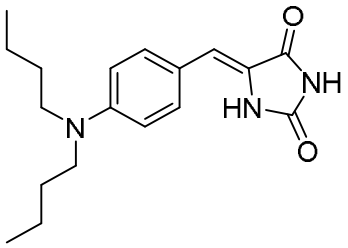

(Z)-5-(4-(dibutylamino)benzylidene)imidazolidine-2,4-dione (**2h**)

Yield: 71%

^{1}H NMR (500 MHz, DMSO-d_6):

ŭ 7.45 (d, *J* = 9.0 Hz, 2H), 6.62 (d, *J* = 9.0 Hz, 2H), 6.33 (s, 1H), 3.33-3.30 (m, 4H), 1.54-1.48 (m, 4H), 1.35-1.31 (m, 4H), 0.93 (t, *J* = 7.5 Hz, 6H)

^{13}C NMR (125 MHz, DMSO-d_6):

ŭ 166.41, 156.21, 148.63, 131.97, 124.21, 119.98, 111.97, 111.15, 50.49, 29.73, 20.36, 14.57

Anal. Calcd for $C_{18}H_{25}N_3O_4$ (315.42): C 68.54, H 7.99, N 13.32

Found: C 68.96, H 8.14, N 13.67

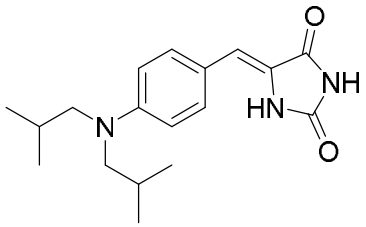

(Z)-5-(4-(diisobutylamino)benzylidene)imidazolidine-2,4-dione (**2i**)

Yield: 68%

^{1}H NMR (500 MHz, DMSO-d_6):

ŭ 10.99 (br s, 1H), 10.18 (br s, 1H), 7.43 (d, *J* = 8.5 Hz, 2H), 6.66 (d, *J* = 9.5 Hz, 2H), 6.33 (s, 1H), 3.22 (d, *J* = 7.0 Hz, 4H), 2.04-1.96 (m, 2H), 0.87 (d, *J* = 6.5 Hz, 12H)

^{13}C NMR (125 MHz, DMSO-d_6):

ŭ 166.37, 156.17, 148.73, 131.77, 124.29, 120.01, 112.72, 111.13, 59.62, 26.81, 20.65

Anal. Calcd for $C_{18}H_{25}N_3O_4$ (315.42): C 68.54, H 7.99, N 13.32

Found: C 68.93, H 7.15, N 12.98

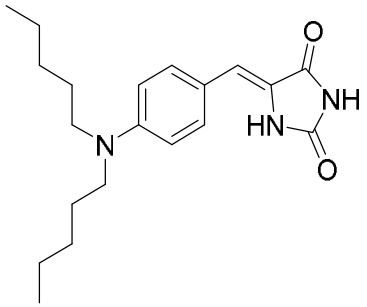

(Z)-5-(4-(dipentylamino)benzylidene)imidazolidine-2,4-dione (**2j**)

Yield: 75%

^{1}H NMR (500 MHz, DMSO-d_6):

ŭ 7.45 (d, *J* = 9.0 Hz, 2H), 6.62 (d, *J* = 9.5 Hz, 2H), 6.33 (s, 1H), 3.33-3.29 (m, 4H), 1.54-1.51 (m, 4H), 1.35-1.27 (m, 8H), 0.89 (t, *J* = 7.0 Hz, 6H)

^{13}C NMR (125 MHz, DMSO-d_6):

ŭ 166.38, 156.17, 148.63, 131.98, 124.17, 119.96, 111.95, 111.16, 50.70, 29.30, 27.22, 22.75, 14.69

Anal. Calcd for $C_{20}H_{29}N_3O_4$ (343.47): C 69.94, H 8.51, N 12.23

Found: C 70.01, H 8.56, N 12.54

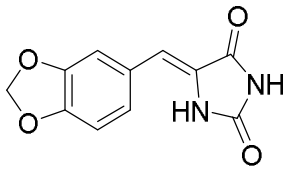

(Z)-5-(benzo[d][1,3]dioxol-5-ylmethylene)imidazolidine-2,4-dione (**2k**)

Yield: 67%

^{1}H NMR (500 MHz, DMSO-d_6):

ŭ 11.18 (s, 1H), 10.45 (s, 1H), 7.21 (s, 1H), 7.13 (d, *J* = 8.0 Hz, 1H), 6.95 (d, *J* = 8.0 Hz, 1H), 6.37 (s, 1H), 6.07 (s, 2H)

^{13}C NMR (125 MHz, DMSO-d_6):

ŭ 166.28, 156.32, 148.51, 148.26, 127.75, 127.02, 125.51, 109.46, 109.43, 102.12, 79.88

Anal. Calcd for $C_{11}H_8N_2O_4$ (232.20): C 56.90, H 3.47, N 12.06

Found: C 56.27, H 3.72, N 12.54

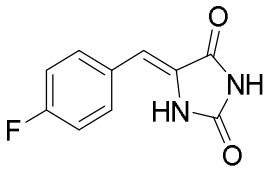

(Z)-5-(4-fluorobenzylidene)imidazolidine-2,4-dione (**2l**)

Yield: 64%

^{1}H NMR (500 MHz, DMSO-d$_6$):

ŭ 11.25 (br s, 1H), 10.56 (br s, 1H), 7.70-7.67 (m, 2H), 7.24 (t, *J* = 8.5 Hz, 2H), 6.43 (s, 1H)

^{13}C NMR (125 MHz, DMSO-d$_6$):

ŭ 166.20, 163.49, 161.53, 156.42, 132.30, 130.29, 128.46, 116.52, 116.35, 107.90

Anal. Calcd for $C_{10}H_7FN_2O_2$ (206.18): C 58.26, H 3.42, N 13.59

Found: C 58.55, H 3.11, N 13.35

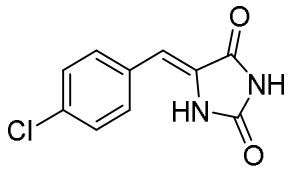

(Z)-5-(4-chlorobenzylidene)imidazolidine-2,4-dione (**2m**)

Yield: 68%

^{1}H NMR (500 MHz, DMSO-d$_6$):

ŭ 10.98 (br s, 2H), 7.64 (d, *J* = 8.5 Hz, 2H), 7.44 (d, *J* = 8.5 Hz, 2H), 6.40 (s, 1H)

^{13}C NMR (125 MHz, DMSO-d$_6$):

ŭ 166.16, 156.42, 133.48, 132.66, 131.71, 129.42, 129.22, 107.48

Anal. Calcd for $C_{10}H_7FN_2O_2$ (206.18): C 58.26, H 3.42, N 13.59

Found: C 57.92, H 3.57, N 13.24

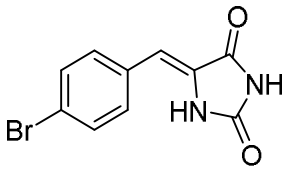

(Z)-5-(4-bromobenzylidene)imidazolidine-2,4-dione (**2n**)

Yield: 75%

^{1}H NMR (500 MHz, DMSO-d_6):

ŭ 10.98 (br s, 2H), 7.56 (m, 4H), 6.38 (s, 1H)

^{13}C NMR (125 MHz, DMSO-d_6):

ŭ 166.15, 156.40, 132.98, 132.32, 131.94, 129.29, 122.19, 107.55

Anal. Calcd for $C_{10}H_7BrN_2O_2$ (267.08): C 44.97, H 2.64, N 10.49

Found: C 44.56, H 2.92, N 10.11

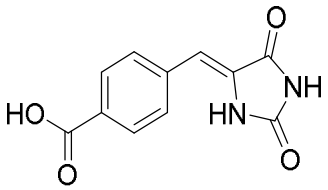

(Z)-4-((2,5-dioxoimidazolidin-4-ylidene)methyl)benzoic acid (**2o**)

Yield: 71%

^{1}H NMR (500 MHz, DMSO-d$_6$):

ŭ 11.35 (br s, 1H), 10.71 (br s, 2H), 7.93 (d, *J* = 8.5 Hz, 2H), 7.72 (d, *J* = 7.0 Hz, 2H), 6.45 (s, 1H)

^{13}C NMR (125 MHz, DMSO-d$_6$):

ŭ 167.61, 166.10, 156.42, 138.00, 130.72, 130.24, 130.21, 129.98, 107.40

Anal. Calcd for $C_{11}H_8N_2O_4$ (232.20): C 56.90, H 3.47, N 12.06

Found: C 56.45, H 3.98, N 12.21

Representative example of synthesis of α-cyanoacyloxyamide derivatives:

To a solution of (*E*)-2-cyano-3-(4-hydroxyphenyl)acrylic acid (1.0 mmol) in water was added acetaldehyde (1.0 mmol) and ter-butyl isocyanide (1.0 mmol) and stirred at room temperature for 12-24 hours. Upon the completion of the reaction (TLC), the solid was filtered and washed with water and hexanes. The crude product was purified via repeated recrystallization in ethylacetate to obtain pure product in 52% yield.

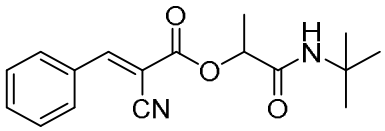

1-(tert-butylamino)-1-oxopropan-2-yl (E)-2-cyano-3-phenylacrylate (**3b**)

Yield: 55%

^{1}H NMR (500 MHz, DMSO-d_6):

ŭ 8.22 (s, 1H), 7.94 (d, *J* = 7.5 Hz, 2H), 7.53-7.45 (m, 3H), 6.21 (br s, 1H), 5.15 (q, *J* = 8.0 Hz, 1H), 1.52 (d, *J* = 6.5 Hz, 3H), 1.34 (s, 9H)

^{13}C NMR (125 MHz, DMSO-d_6):

ŭ 168.75, 160.96, 156.40, 134.15, 131.52, 131.45, 129.70, 115.90, 102.23, 73.40, 51.63, 28.90, 18.32

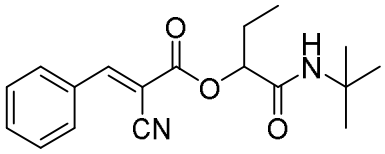

1-(tert-butylamino)-1-oxobutan-2-yl (E)-2-cyano-3-phenylacrylate (**3c**)

Yield: 59%

^{1}H NMR (500 MHz, DMSO-d$_6$):

ŭ 8.25 (s, 1H), 7.96 (d, *J* = 7.0 Hz, 2H), 7.55-7.47 (m, 3H), 6.23 (s, 1H), 5.17 (s, 1H), 2.00-1.97 (m, 2H), 1.368 (s, 9H), 0.94 (t, *J* = 7.5 Hz, 3H)

^{13}C NMR (125 MHz, DMSO-d$_6$):

ŭ 167.93, 161.10, 156.28, 134.06, 131.46, 131.43, 129.63, 115.77, 102.19, 77.70, 51.69, 28.87, 25.26, 8.64

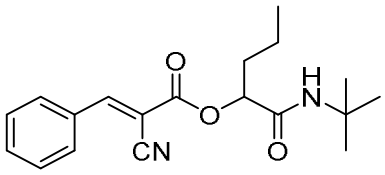

1-(tert-butylamino)-1-oxopentan-2-yl (E)-2-cyano-3-phenylacrylate (**3d**)

Yield: 44%

^{1}H NMR (500 MHz, DMSO-d_6):

ŭ 8.44 (s, 1H), 8.09 (d, *J* = 7.0 Hz, 2H), 7.71-7.61 (m, 4H), 4.98 (t, *J* = 6.0 Hz, 1H), 1.81-1.75 (m, 2H), 1.48-1.38 (m, 2H), 1.28 (s, 9H), 0.94 (t, *J* = 7.0 Hz, 3H)

^{13}C NMR (125 MHz, DMSO-d_6):

ŭ 168.48, 161.97, 156.14, 134.24, 132.06, 131.58, 130.09, 116.19, 103.16, 76.05, 51.06, 34.27, 29.14, 18.59, 14.39

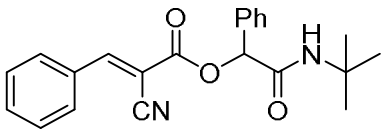

2-(tert-butylamino)-2-oxo-1-phenylethyl (E)-2-cyano-3-phenylacrylate (**3e**)

Yield: 48%

^{1}H NMR (500 MHz, DMSO-d_6):

ŭ 8.45 (s, 1H), 8.07 (d, *J* = 7.0 Hz, 2H), 8.00 (s, 1H), 7.67-7.55 (m, 5H), 7.44-7.37 (m, 3H), 5.99 (s, 1H), 1.21 (s, 9H)

^{13}C NMR (125 MHz, $CDCl_3$):

ŭ 166.71, 160.73, 156.69, 135.59, 134.19, 131.55, 131.44, 129.68, 129.49, 129.14, 127.71, 115.85, 102.06, 52.02, 28.92

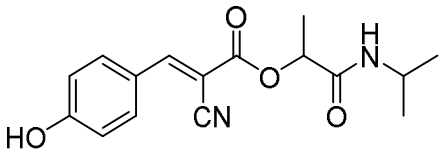

1-(isopropylamino)-1-oxopropan-2-yl (E)-2-cyano-3-(4-hydroxyphenyl)acrylate (**3f**)

Yield: 50%

^{1}H NMR (500 MHz, DMSO-d$_6$):

ŭ 10.87 (br s, 1H), 8.26 (s, 1H), 8.02 (d, *J* = 9.0 Hz, 2H), 7.94 (d, *J* = 7.5 Hz, 1H), 6.97 (d, *J* = 9.0 Hz, 2H), 5.03 (q, *J* = 6.5 Hz, 1H), 3.88-3.84 (m, 1H), 1.43 (d, *J* = 7.0 Hz, 3H), 1.40-1.04 (m, 6H)

^{13}C NMR (125 MHz, DMSO-d$_6$):

ŭ 169.07, 163.75, 162.78, 155.61, 134.77, 123.21, 117.15, 117.11, 97.64, 72.21, 41.21, 22.91, 22.89, 18.25

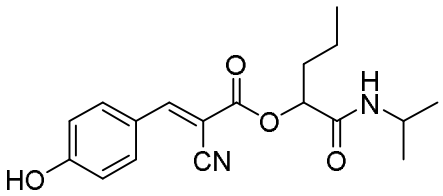

1-(isopropylamino)-1-oxopentan-2-yl (E)-2-cyano-3-(4-hydroxyphenyl)acrylate (**3g**)

Yield: 54%

^{1}H NMR (500 MHz, DMSO-d$_6$):

ŭ 10.87 (s, 1H), 8.25 (s, 1H), 8.02 (d, *J* = 8.5 Hz, 2H), 7.96 (d, *J* = 7.5 Hz, 1H), 6.97 (d, *J* = 8.5 Hz, 2H), 4.93 (dd, *J* = 5.5 Hz, 1H), 3.85 (m, 1H), 1.79-1.74 (m, 2H), 1.43-1.37 (m, 2H), 1.08 (d, *J* = 6.5 Hz, 3H), 1.05 (d, *J* = 6.5 Hz, 3H), 0.92 (t, *J* = 7.5 Hz, 3H)

^{13}C NMR (125 MHz, DMSO-d$_6$):

ŭ 168.36, 163.75, 162.90, 155.63, 134.80, 123.22, 117.16, 117.09, 97.53, 75.59, 41.16, 34.16, 22.95, 22.91, 18.59, 14.32

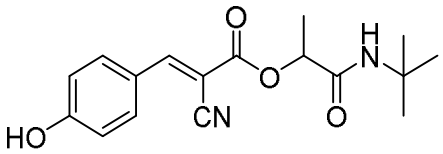

1-(tert-butylamino)-1-oxopropan-2-yl (E)-2-cyano-3-(4-hydroxyphenyl)acrylate (**3h**)

Yield: 52%

^{1}H NMR (500 MHz, DMSO-d_6):

ŭ 10.87 (br s, 1H), 8.27 (s, 1H), 8.03 (d, *J* = 7.0 Hz, 2H), 7.66 (s, 1H), 6.98 (d, *J* = 7.0 Hz, 2H), 5.02 (q, *J* = 6.5 Hz, 1H), 1.42 (d, *J* = 6.5 Hz, 3H), 1.28 (s, 9H)

^{13}C NMR (125 MHz, DMSO-d_6):

ŭ 169.37, 163.78, 152.69, 155.64, 134.79, 123.21, 117.17, 117.14, 97.57, 72.24, 50.96, 29.12, 18.36

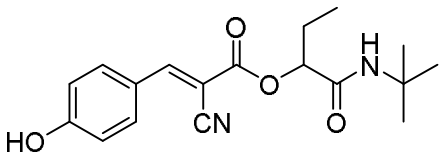

1-(tert-butylamino)-1-oxobutan-2-yl (E)-2-cyano-3-(4-hydroxyphenyl)acrylate (**3i**)

Yield: 60%

^{1}H NMR (500 MHz, DMSO-d_6):

ŭ 8.26 (s, 1H), 8.03 (d, *J* = 8.5 Hz, 2H), 7.65 (s, 1H), 6.97 (d, *J* = 9.0 Hz, 2H), 4.89 (t, *J* = 6.5 Hz, 1H), 1.84-1.78 (m, 2H), 1.27 (s, 9H), 0.95 (t, *J* = 7.5 Hz, 3H)

^{13}C NMR (125 MHz, DMSO-d_6):

ŭ 168.44, 163.74, 162.78, 155.60, 134.78, 123.23, 117.16, 117.09, 97.60, 76.69, 51.02, 29.16, 25.63, 9.92

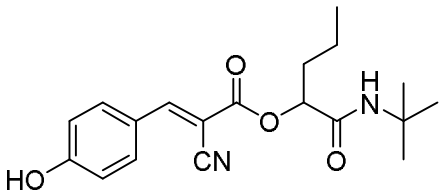

1-(tert-butylamino)-1-oxopentan-2-yl (E)-2-cyano-3-(4-hydroxyphenyl)acrylate (**3j**)

Yield: 49%

^{1}H NMR (500 MHz, DMSO-d$_6$):

ŭ 10.83 (br s, 1H), 8.23 (s, 1H), 8.00 (d, *J* = 9.0 Hz, 2H), 7.65 (s, 1H), 6.95 (d, *J* = 8.5 Hz, 2H), 4.91 (dd, *J* = 5.0 Hz, 1H), 1.76-1.70 (m, 2H), 1.41-1.35 (m, 2H), 1.24 (s, 9H), 0.91 (t, *J* = 7.0 Hz, 3H)

^{13}C NMR (125 MHz, DMSO-d$_6$):

ŭ 168.69, 163.75, 162.79, 155.61, 134.77, 123.22, 117.14, 117.05, 97.57, 75.66, 51.00, 34.30, 29.13, 18.61, 14.37

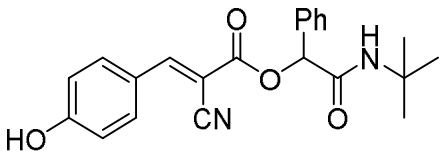

2-(tert-butylamino)-2-oxo-1-phenylethyl (E)-2-cyano-3-(4-hydroxyphenyl)acrylate (**3k**)

Yield: 47%

^{1}H NMR (500 MHz, DMSO-d$_6$):

ŭ 8.29 (s, 1H), 8.03 (d, *J* = 8.5 Hz, 2H), 7.97 (s, 1H), 7.56 (d, *J* = 7.5 Hz, 2H), 7.44-7.36 (m, 3H), 6.98 (d, *J* = 8.5 Hz, 2H), 5.98 (s, 1H), 1.22 (s, 9H)

^{13}C NMR (125 MHz, DMSO-d$_6$):

ŭ 167.30, 163.95, 162.65, 155.96, 136.29, 134.92, 129.28, 129.15, 127.80, 123.17, 117.20, 117.07, 97.19, 77.03, 51.23, 29.05

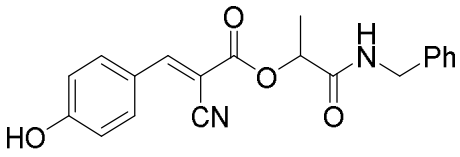

1-(benzylamino)-1-oxopropan-2-yl (E)-2-cyano-3-(4-hydroxyphenyl)acrylate (**3l**)

Yield: 57%

^{1}H NMR (500 MHz, DMSO-d_6):

ŭ 8.66 (t, *J* = 8.0 Hz, 1H), 8.29 (s, 1H), 8.03 (d, *J* = 6.0 Hz, 2H), 7.35-7.24 (m, 5H), 6.98 (d, *J* = 8.5 Hz, 2H), 5.17 (q, *J* = 7.0, 1.0 Hz, 1H), 4.38-4.28 (m, 2H), 1.49 (d, *J* = 6.5 Hz, 3H)

^{13}C NMR (125 MHz, DMSO-d_6):

ŭ 170.23, 163.79, 162.90, 155.72, 139.86, 134.82, 129.03, 127.68, 127.53, 123.22, 117.19, 117.15, 97.65, 72.29, 42.56, 18.32

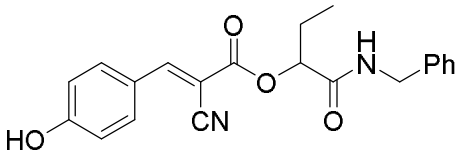

1-(benzylamino)-1-oxobutan-2-yl (E)-2-cyano-3-(4-hydroxyphenyl)acrylate (**3m**)

Yield: 53%

^{1}H NMR (500 MHz, DMSO-d$_6$):

ŭ 10.87 (br s, 1H), 8.66 (s, 1H), 8.28 (s, 1H), 8.03 (d, *J* = 8.0 Hz, 2H), 7.35-7.25 (m, 5H), 6.97 (d, *J* = 8.5 Hz, 2H), 5.03 (t, *J* = 5.5 Hz, 1H), 4.37-4.28 (m, 2H), 1.90-1.85 (m, 2H), 0.97 (t, *J* = 7.0 Hz, 3H)

^{13}C NMR (125 MHz, DMSO-d$_6$):

ŭ 169.37, 163.78, 163.01, 155.63, 139.91, 134.81, 129.00, 127.73, 127.52, 123.22, 117.18, 117.10, 97.66, 76.76, 45.58, 25.55, 9.98

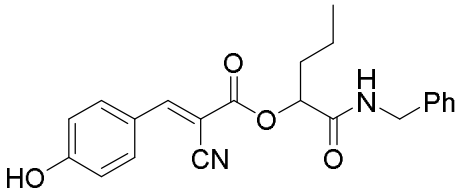

1-(benzylamino)-1-oxopentan-2-yl (E)-2-cyano-3-(4-hydroxyphenyl)acrylate (**3n**)

Yield: 51%

^{1}H NMR (500 MHz, DMSO-d$_6$):

ŭ 10.88 (br s, 1H), 8.68 (t, *J* = 6.0 Hz, 1H), 8.29 (s, 1H), 8.04 (d, *J* = 8.0 Hz, 2H), 7.34-7.26 (m, 5H), 6.99 (d, *J* = 8.0 Hz, 2H), 5.09 (t, *J* = 6.0 Hz 1H), 4.38-4.29 (m, 2H), 1.84 (m, 2H), 1.44 (m, 2H), 0.94 (t, *J* = 7.0 Hz, 3H)

^{13}C NMR (125 MHz, DMSO-d$_6$):

ŭ 169.60, 163.81, 163.05, 155.69, 139.90, 134.83, 129.00, 127.73, 127.52, 123.23, 117.19, 117.09, 97.63, 75.63, 42.61, 34.17, 18.61, 14.29

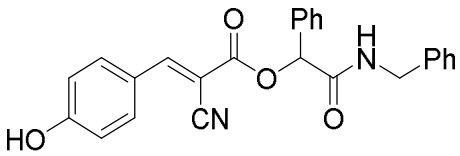

2-(benzylamino)-2-oxo-1-phenylethyl (E)-2-cyano-3-(4-hydroxyphenyl)acrylate (**3o**)

Yield: 46%

^{1}H NMR (500 MHz, DMSO-d_6):

ŭ 8.93 (t, *J* = 8.5 Hz, 1H), 8.34 (s, 1H), 8.05 (d, *J* = 8.5 Hz, 2H), 7.60 (d, *J* = 7.5 Hz, 2H), 7.46-7.40 (m, 3H), 7.29-7.16 (m, 5H), 6.98 (d, *J* = 8.5 Hz, 2H), 6.09 (s, 1H), 4.38-4.24 (m, 2H)

^{13}C NMR (125 MHz, DMSO-d_6):

ŭ 168.31, 163.93, 162.82, 156.06, 139.61, 135.92, 134.95, 129.53, 129.24, 128.96, 127.93, 127.65, 127.54, 123.21, 117.21, 117.04, 97.29, 77.26, 42.66

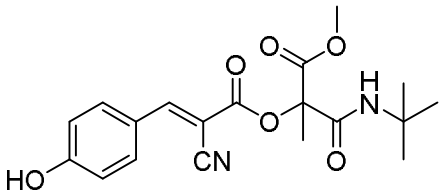

1-(tert-butylamino)-3-methoxy-2-methyl-1,3-dioxopropan-2-yl (E)-2-cyano-3-(4-hydroxy phenyl) acrylate (**3p**)

Yield: 59%

^{1}H NMR (500 MHz, DMSO-d_6):

ŭ 8.32 (s, 1H), 8.04 (d, *J* = 8.5 Hz, 2H), 7.20 (s, 1H), 6.99 (d, *J* = 9.0 Hz, 2H), 3.71 (s, 3H), 1.78 (s, 3H), 1.33 (s, 9H)

^{13}C NMR (125 MHz, DMSO-d_6):

ŭ 168.68, 166.07, 164.38, 161.61, 156.96, 135.21, 123.05, 117.32, 117.20, 96.18, 82.65, 53.71, 51.81, 28.83, 21.25

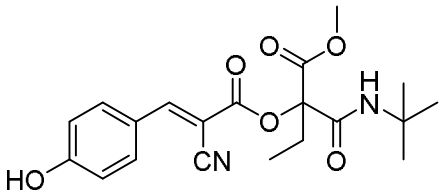

methyl (E)-2-(tert-butylcarbamoyl)-2-((2-cyano-3-(4-hydroxyphenyl)acryloyl)oxy) butanoate (**3q**)

Yield: 47%

^{1}H NMR (500 MHz, DMSO-d_6):

ŭ 8.32 (s, 1H), 8.07 (d, *J* = 8.0 Hz, 2H), 7.23 (s, 1H), 7.01 (d, *J* = 9.0 Hz, 2H), 3.73 (s, 3H), 2.33-2.18 (m, 2H), 1.34 (s, 9H), 0.89 (t, *J* = 7.5 Hz, 3H)

^{13}C NMR (125 MHz, DMSO-d_6):

ŭ 169.01, 164.47, 164.41, 161.54, 157.00, 135.25, 123.07, 117.30, 117.20, 95.97, 85.11, 53.74, 51.94, 28.84, 27.90, 8.05

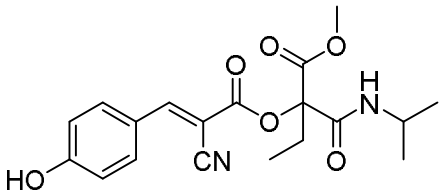

methyl (E)-2-((2-cyano-3-(4-hydroxyphenyl)acryloyl)oxy)-2-(isopropylcarbamoyl) butanoate (**3r**)

Yield: 55%

^{1}H NMR (500 MHz, DMSO-d_6):

ŭ 10.99 (s, 1H), 8.34 (s, 1H), 8.05 (d, *J* = 9.0 Hz, 2H), 7.64 (d, *J* = 8.0 Hz, 1H), 7.00 (d, *J* = 8.5 Hz, 2H), 3.97-3.90 (m, 1H), 3.71 (s, 3H), 2.33-2.14 (m, 2H), 1.15-1.13 (m, 6H), 0.88 (t, *J* = 7.5 Hz, 3H)

^{13}C NMR (125 MHz, $CDCl_3$):

ŭ 171.14, 166.35, 163.57, 162.67, 156.22, 134.73, 123.10, 117.10, 116.13, 95.86, 83.01, 53.73, 42.86, 30.65, 22.58, 22.54, 8.20

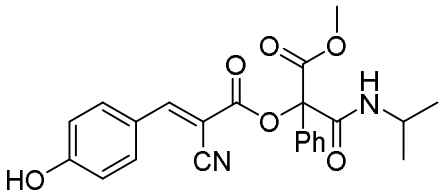

1-(isopropylamino)-3-methoxy-1,3-dioxo-2-phenylpropan-2-yl (E)-2-cyano-3-(4-hydroxy phenyl) acrylate (**3s**)

Yield: 58%

^{1}H NMR (500 MHz, DMSO-d_6):

ŭ 8.44 (s, 1H), 8.12-8.10 (m, 3H), 7.64 (d, *J* = 9.0 Hz, 2H), 7.52-7.44 (m, 3H), 7.02 (d, *J* = 9.0 Hz, 2H), 3.92-3.87 (m, 1H), 3.74 (s, 3H), 1.12 (d, *J* = 6.5 Hz, 3H), 1.09 (d, *J* = 6.5Hz, 3H).

^{13}C NMR (125 MHz, DMSO-d_6):

ŭ 169.06, 164.52, 164.09, 162.51, 157.28, 135.38, 134.76, 129.94, 129.43, 125.98, 123.06, 117.37, 116.96, 95.92, 83.74, 54.31, 42.33, 22.54, 22.39

MCT1 lactate uptake:

RBE4 cells were seeded in 24-well plates at a concentration of $2.5x10^5$cells/well and incubated for 18-24 hours at 37ęC in 5% CO_2 atmosphere. Cells were washed twice with HEPES buffer (pH 7.4) and incubated for ~20 minutes on a 37 ęC hot plate. Synthesized compounds were dissolved in DMSO at various concentrations and 0.8µL of each solution was added into 800µL of HEPES buffer containing 3µM [^{14}C]-L-lactate and 2µM lactate. The buffer from the 24-well plate was removed and 250µL of test compound was added and incubated for further 20 minutes. At the end of 20 minutes, the compound was removed from the wells and 500µL of ice-cold stop buffer (0.1M CHC in HEPES buffer) was added into the wells and the plates are transferred on to ice tray. The wells were washed two more times with ice-cold stop buffer and 250µL of 0.1M NaOH in 5% triton X-100 was added. The wells were placed on a shaker for 40 minutes to obtain cell lysates and 150µL of these lysates were added to 4mL of ecolite (+) scintillation fluid in a 7mL scintillation vial. The radioactive counts in disintegrations per minute (dpm) were obtained using Beckman scintillation counter. DMSO was used as negative control and CHC was used as positive control for each experiment. The dpm values were averaged and normalized with DMSO as 100% to get % lactate uptake.

REFERENCES

1. Cavallo, F.; De Giovanni, C.; Nanni, P.; Forni, G.; Lollini, P. L. ñ2011: The immune hallmarks of cancerò *Cancer. Immunol. Immunother*. **2011**, *60*, 319-26.
2. Hanahan, D.; Weinberg, R. A. ñHallmarks of cancer: The next generationò *Cell* **2011**, *144*, 646ï 74.
3. Ganapathy-Kanniappan, S.; Geschwind, J. F. ñTumor glycolysis as a target for cancer therapy: progress and prospectsò *Mol Cancer* **2013**, *12*, 152.
4. Ganapathy, V.; Thangaraju, M.; Prasad, P. D. ñNutrient transporters in cancer: relevance to Warburg hypothesis and beyondò *Pharmacol Ther* **2009**, *121*, 29ï 40.
5. Sotgia, F.; Whitaker-menezes, D.; Martinez-outschoorn, U. E.; Flomenberg, N.; Birbe, R. C.; Witkiewicz, A. K.; Howell, A.; Philp, N. J.; Pestell, R. G.; Lisanti, M. P. ñMitochondrial metabolism in cancer metastasis: Visualizing tumor cell mitochondria and the ó reverse Warburg effect ô in positive lymph node tissueò *Cell Cycle* **2012**, *11*, 1445ï 54.
6. Pavlides, S.; Whitaker-Menezes, D.; Castello-Cros, R.; Flomenberg, N.; Witkiewicz, A. K.; Frank, P. G.; Casimiro, M. C.; Wang, C.; Fortina, P.; Addya, S.; Pestell, R. G.; Martinez-Outschoorn, U. E.; Sotgia, F.; Lisanti, M. P. ñThe reverse Warburg effect: aerobic glycolysis in cancer associated fibroblasts and the tumor stromaò *Cell Cycle* **2009**, *8*, 3984ï 4001.
7. Pelicano, H.; Martin, D. S.; Xu, R. H.; Huang, P. ñGlycolysis inhibition for anticancer treatmentò *Oncogene* **2006**, *25*, 4633-46.
8. Gatenby, R. A. and Gillies, R. J. ñWhy do cancers have high aerobic glycolysis?ò *Nat Rev Cancer* **2004**, *4*, 891ï 9.
9. Hsu, P. P. and Sabatini, D. M. ñCancer cell metabolism: Warburg and beyond.ò *Cell* **2008**, *134*, 703ï 7.
10. Sonveaux, P.; Végran, F.; Schroeder, T.; Wergin, M. C.; Verrax, J.; Rabbani, Z. N.; De Saedeleer, C. J.; Kennedy, K. M.; Diepart, C.; Jordan, B. F.; Kelley, M. J.; Gallez, B.; Wahl, M. L.; Feron, M.; Dewhirst, M. W. ñTargeting lactate-fueled respiration selectively kills hypoxic tumor cells in miceò *J Clin Invest* **2008**, *118*, 3930ï 42.
12. Peppicelli, S.; Bianchini, F.; Calorini, L. ñDynamic scenario of metabolic pathway adaptation in tumors and therapeutic approachò *Oncoscience* **2015**, *2*, 225ï 32.
13. Ricklin, D.; Hajishengallis, G.; Yang K, Lambris, J. D. ñComplement: a key system for immune surveillance and homeostasisò *Nat Immunol* **2010**, *11*, 785ï 97.
14. Swann, J. B. and Smyth, M. J. ñImmune surveillance of tumorsò *J Clin Invest* **2007**, *117*, 1137ï 46.
15. Felip, E.; Concha, Á.; de Castro, J.; Gómez-Román, J.; Garrido, P.; Ramírez, J.; Isla, D.; Sanz, J.; Paz-Ares, L.; López-Ríos, F. ñBiomarker testing in advanced non-small-cell lung cancer: a National Consensus of the Spanish Society of Pathology and the Spanish Society of Medical Oncologyò *Clin Transl Oncol*. **2015**, *17*, 103-12.
16. Murray, C. M.; Hutchinson, R.; Bantick, J. R.; Belfield, G. P.; Benjamin, A. D.; Brazma, D.; Bundick, R. V.; Cook, I. D.; Craggs, R. I.; Edwards, S.; Evans, L. R.; Harrison, R.; Holness. E.; Jackson, A. P.; Jackson, C. G.; Kingston, L. P.; Perry,

M. W.; Ross, A. R.; Rugman, P. A.; Sidhu, S. S.; Sullivan, M.; Taylor-Fishwick, D. A.; Walker, P. C.; Whitehead, Y. M.; Wilkinson, D. J.; Wright, A.; Donald, D. K. ñMonocarboxylate transporter MCT1 is a target for immunosuppressionò *Nat Chem Biol* **2005**, *1*, 371ï 6.
17. Li, X.; Gu, J.; Zhou, Q. ñReview of aerobic glycolysis and its key enzymes - new targets for lung cancer therapyò *Thorac Cancer* **2015**, *6*, 17ï 24.
18. Zhao, Y. H.; Zhou, M.; Liu, H.; Ding, Y.; Khong, H. T.; Yu, D.; Fodstad, O.; Tan, M. ñUpregulation of lactate dehydrogenase A by ErbB2 through heat shock factor 1 promotes breast cancer cell glycolysis and growthò *Oncogene* **2009**, *28*, 3689ï 701.
19. Zheng, J. ñEnergy metabolism of cancer: Glycolysis versus oxidative phosphorylation (Review)ò *Oncol Lett* **2012**, *4*, 1151ï 7.
20. Wilson, W. R. and Hay, M. P. ñTargeting hypoxia in cancer therapyò *Nat Rev Cancer* **2011**, *11*, 393ï 410.
21. Ciavardelli, D.; Rossi, C.; Barcaroli, D.; Volpe, S.; Consalvo, A.; Zucchelli, M.; De Cola, A.; Scavo, E.; Carollo, R.; D'Agostino, D.; Forlì, F.; D'Aguanno, S.; Todaro, M.; Stassi, G.; Di Ilio, C.; De Laurenzi, V.; Urbani, A. ñBreast cancer stem cells rely on fermentative glycolysis and are sensitive to 2-deoxyglucose treatmentò *Cell Death Dis* **2014**, *5*, e1336.
22. Bobba, A.; Amadoro, G.; La Piana, G.; Calissano, P.; Atlante, A. ñGlycolytic enzyme upregulation and numbness of mitochondrial activity characterize the early phase of apoptosis in cerebellar granule cellsò *Apoptosis* **2015**, *20*, 10ï 28.
23. Wahl, M. L.; Owen, J. A.; Burd, R.; Herlands, R. A.; Nogami, S. S.; Rodeck, U.; Berd, D.; Leeper, D. B.; Owen, C. S. ñRegulation of intracellular pH in human melanoma: potential therapeutic implicationsò *Mol Cancer Ther* **2002**, *1*, 617ï 28.
23. Lucien, F.; Harper, K.; Pelletier, P-P.; Volkov, L.; Dubois, C. M. ñSimultaneous pH measurement in endocytic and cytosolic compartments in living cells using confocal microscopyò *J Vis Exp* **2014**, *86*, e51395
24. Pinheiro, C.; Longatto-Filho, A.; Azevedo-Silva, J.; Casal, M.; Schmitt, F. C.; Baltazar, F. ñRole of monocarboxylate transporters in human cancers: state of the artò *J Bioenerg Biomembr* **2012**, *44*, 127ï 39.
25. Halestrap, A. P. ñThe SLC16 gene family - structure, role and regulation in health and diseaseò *Mol Aspects Med*. **2013**, *34*, 337-49.
26. Halestrap, A. P. and Price, N. T. ñThe proton-linked monocarboxylate transporter (MCT) family: structure, function and regulationò *Biochem J* **1999**, *343 Pt 2*, 281ï 99.
27. Chen, Z.; Lu, W.; Garcia-Prieto, C.; Huang, P. ñThe Warburg effect and its cancer therapeutic implicationsò *J Bioenerg Biomembr* **2007**, *39*, 267ï 74.
28. Warburg, O. ñOn the Origin of Cancer Cellsò *Science.* **1956**, *123*, 309-314.
29. Guile, S. D.; Bantick, J. R.; Cheshire, D. R.; Cooper, M. E.; Davis, A. M.; Donald, D. K.; Evans, R.; Eyssade, C.; Ferguson, D. D.; Hill, S.; Hutchinson, R.; Ingall, A. H.; Kingston, L. P.; Martin, I.; Martin, B. P.; Mohammed, R. T.; Murray, C.; Perry, M. W.; Reynolds, R. H.; Thorne, P. V.; Wilkinson, D. J.; Withnall, J. ñPotent blockers of the monocarboxylate transporter MCT1: Novel immunomodulatory compoundsò *Bioorganic Med Chem Lett* **2006**, *16*, 2260ï 5.

30. Michne, W. F.; Schroeder, J. D.; Guiles, J. W.; Treasurywala, A. M.; Weigelt, C. A.; Stansberry, M. F.; McAvoy, E.; Shah, C. R.; Baine, Y.; Sawutz, D. G. ñNovel inhibitors of the nuclear factor of activated T Cells (NFAT)-mediated transcription of ß-Galactosidase: Potential immunosuppressive and antiinflammatory agentsò *J Med Chem* **1995**, *38*, 2557ï 69.
31. Guile, S. D.; Bantick, J. R.; Cooper, M. E.; Donald, D. K.; Eyssade, C.; Ingall, A. H.; Lewis, R. J.; Martin, B. P.; Mohammed, R. T.; Potter, T. J.; Reynolds, R. H.; St-Gallay, S. A.; Wright, A. D. ñOptimization of monocarboxylate transporter 1 blockers through analysis and modulation of atropisomer interconversion propertiesò *J Med Chem* **2007**, *50*, 254ï 63.
32. Wang, H.; Yang, C.; Doherty, J. R.; Roush, W. R.; Cleveland, J. L.; Bannister, T. D. ñSynthesis and structure-activity relationships of pteridine dione and trione monocarboxylate transporter 1 inhibitorsò *J Med Chem* **2014**, *57*, 7317ï 24.
33. Colen, C.B.; Shen Y.; Ghoddoussi F.; Yu P.; Francis T.B.; Koch B.J.; Monterey M.D.; Galloway M.P.; Sloan A.E.; Mathupala S.P. ñMetabolic targeting of lactate efflux by malignant glioma inhibits invasiveness and induces necrosis: an in vivo studyò. *Neoplasia*. **2011**, *13*, 620-32
34. Gurrapu, S.; Jonnalagadda, S. K.; Alam, M. A.; Nelson, G. L.; Sneve, M. G.; Drewes, L. R.; Mereddy, V. R. ñMonocarboxylate transporter 1 inhibitors as potential anticancer agentsò *ACS Med Chem Lett* **2015**, *6*, 558ï 61.
35. Gurrapu, S.; Jonnalagadda, S. K.; Alam, M. A.; Ronayne, C. T.; Nelson, G. L.; Solano, L. N.; Lueth, E. A.; Drewes, L. R.; Mereddy, V. R. ñCoumarin carboxylic acids as monocarboxylate transporter 1 inhibitors: In vitro and in vivo studies as potential anticancer agentsò *Bioorg Med Chem Lett*. **2016**, *26*, 3282-6.
36. Draoui, N.; Schicke, O.; Fernandes, A.; Drozak, X.; Nahra, F.; Dumont, A.; Douxfils J.; Hermans, E.; Dogné, JM.; Corbau, R.; Marchand, A.; Chaltin, P.; Sonveaux, P.; Feron, O.; Riant, O. ñSynthesis and pharmacological evaluation of carboxycoumarins as a new antitumor treatment targeting lactate transport in cancer cellsò *Bioorganic Med Chem* **2013**, *21*, 7107ï 17.
37. Draoui, N.; Schicke, O.; Seront, E.; Bouzin, C.; Sonveaux, P.; Riant, O.; Feron, O. ñAntitumor activity of 7-aminocarboxycoumarin derivatives, a new class of potent inhibitors of lactate influx but not effluxò *Mol Cancer Ther* **2014**, *13*, 1410ï 8.
38. Ohka, F.; Natsume, A.; Wakabayashi, T. ñCurrent Trends in Targeted Therapies for Glioblastoma Multiformeò *Neurol Res Int*. **2012**, *878425*, 2012.
39. Munson, J.; Bonner, M.; Fried, L.; Hofmekler, J.; Arbiser, J.; Bellamkonda, R. ñIdentifying new small molecule anti-invasive compounds for glioma treatmentò *Cell Cycle* **2013**, *12*, 2200-9.
40. Sravan Kumar, J.; Alam, M. A.; Gurrapu, S.; Nelson, G.; Williams, M.; Corsello, M. A.; Johnson, J. L.; Jonnalagadda, S. C.;Mereddy, V. R. ñSynthesis and biological evaluation of novel benzoxaboroles as potential antimicrobial and anticancer agentsò *J Heterocycl Chem* **2013**, *50*, 814ï 20.
41. Pirrung, M. C. and Das Sarma, K. ñMulticomponent reactions are accelerated in waterò *J Am Chem Soc* **2004**, *126*, 444ï 5.
42. Lengyel, I.; Cesare, V.; Taldone, T. ñA direct link between the Passerini reaction and Ŭ-lactamsò *Tetrahedron* **2004**, *60*, 1107ï 24.

Appendix

NMR Spectrum

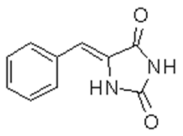
O
NH
HN
O

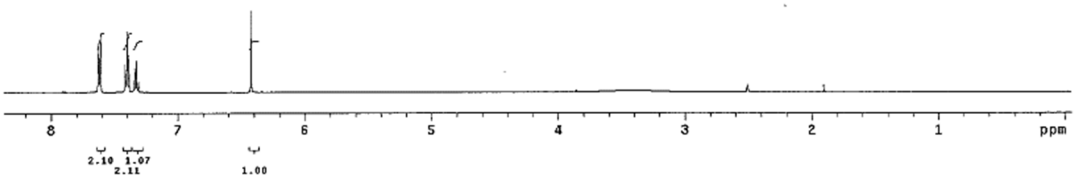
8
7
6
5
4
3
2
1
ppm
2.10
1.07
2.11
1.00

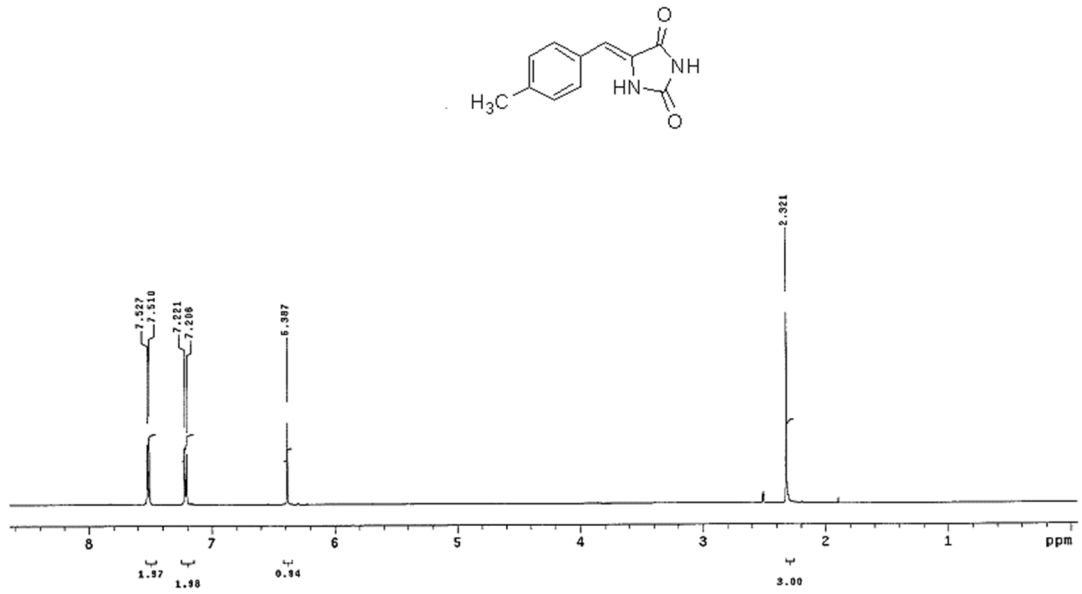
O
NH
HN
O
H3C
7.527
7.510
7.221
7.206
6.387
2.321
8
7
6
5
4
3
2
1
ppm
1.97
1.98
0.84
3.00

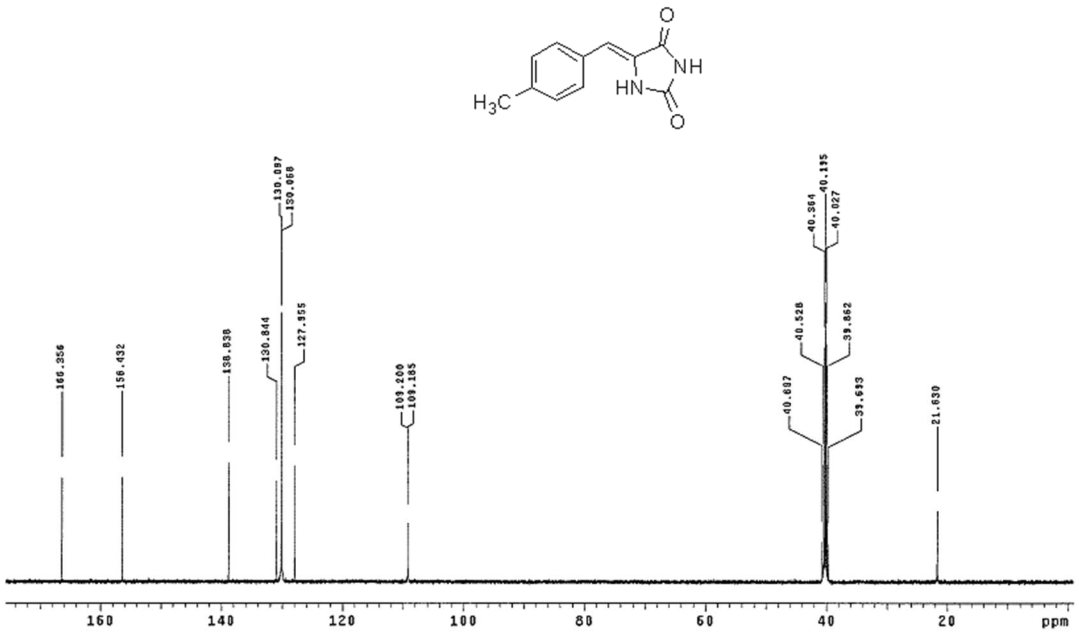
O
NH
HN
O
H3C
166.356
156.432
138.638
130.844
130.087
130.068
127.355
109.200
109.185
40.687
40.528
40.364
40.135
40.027
39.862
39.693
21.630
160
140
120
100
80
60
40
20
ppm

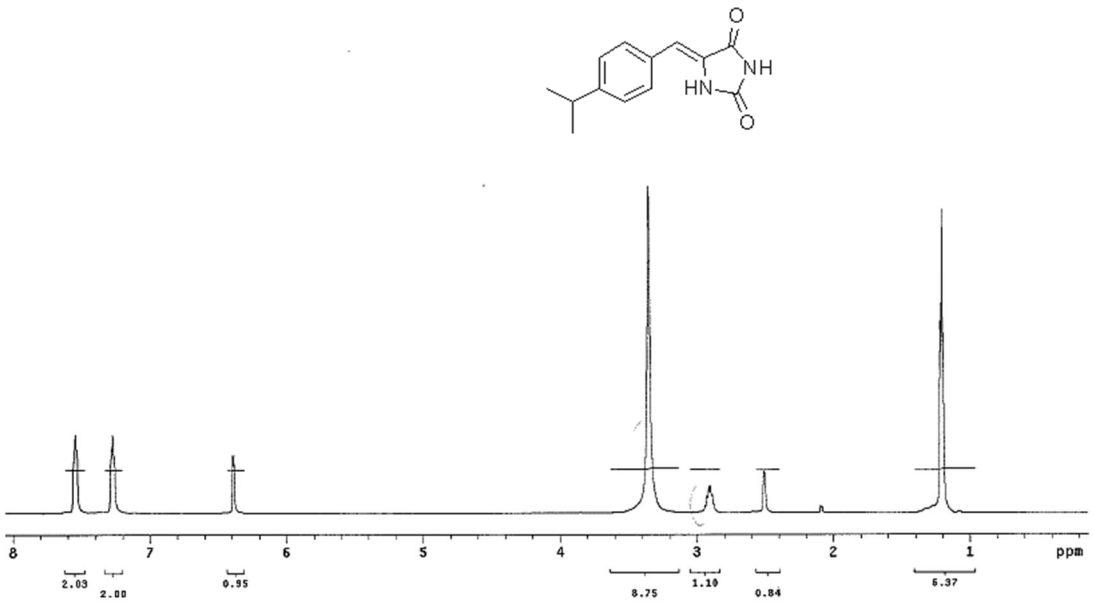
O
NH
HN
O
8
7
6
5
4
3
2
1
ppm
2.03
2.00
0.95
8.75
1.10
0.84
6.37

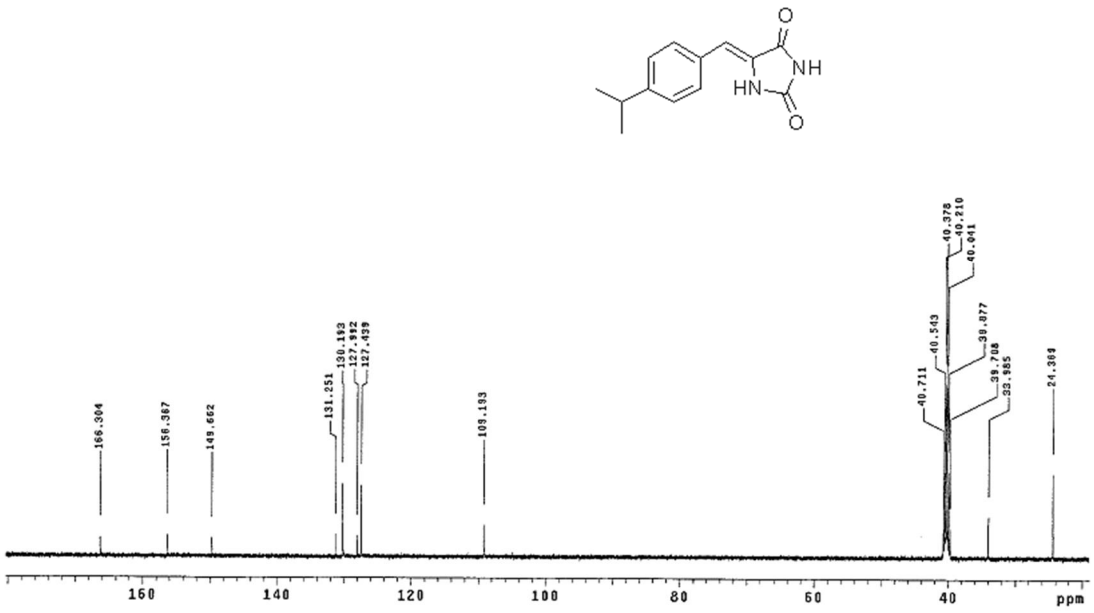
O
NH
HN
O
166.304
156.367
149.662
131.251
130.193
127.932
127.439
109.183
40.711
40.543
40.378
40.210
40.041
39.877
39.708
33.585
24.309
160
140
120
100
80
60
40
ppm

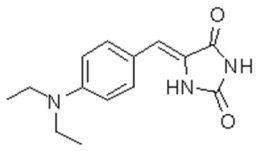
O
NH
HN
O
N

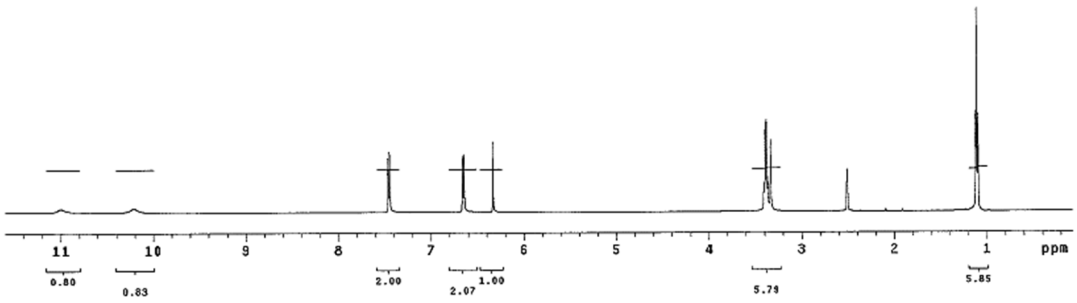
11
10
9
8
7
6
5
4
3
2
1
ppm
0.80
0.83
2.00
2.07
1.00
5.79
5.85

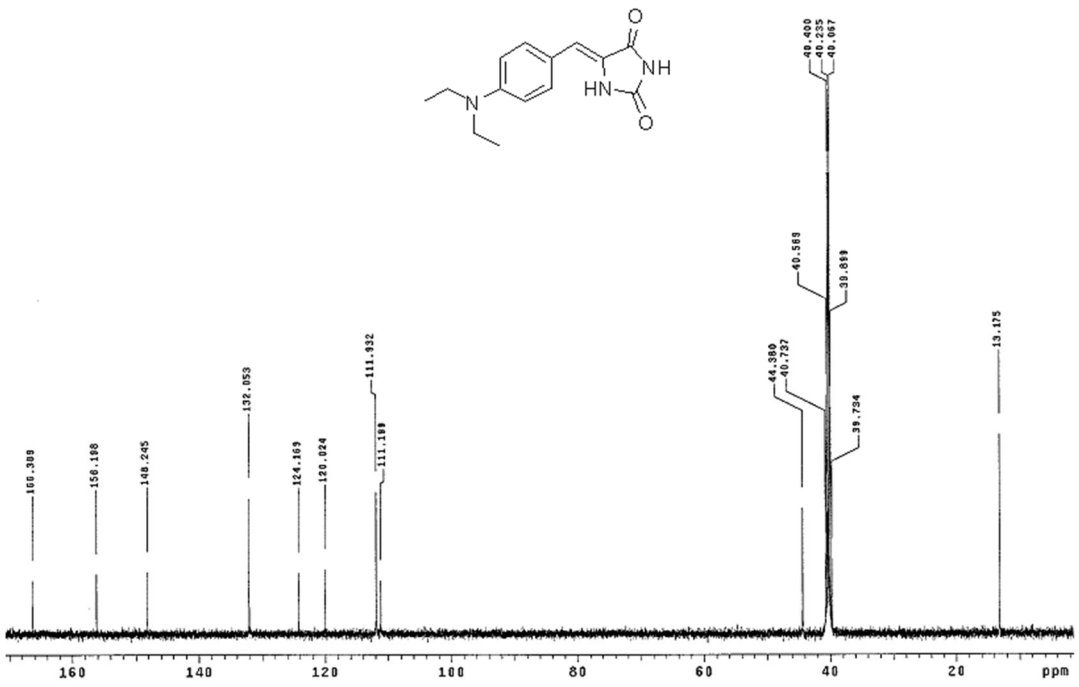
O
NH
HN
O
N
160.389
150.188
148.245
132.053
124.169
120.024
111.932
111.189
44.380
40.737
40.568
40.400
40.235
40.067
39.898
39.734
13.175
160
140
120
100
80
60
40
20
ppm

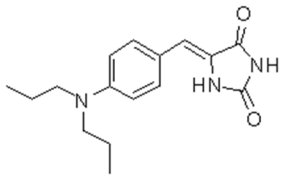
O
NH
HN
O
N

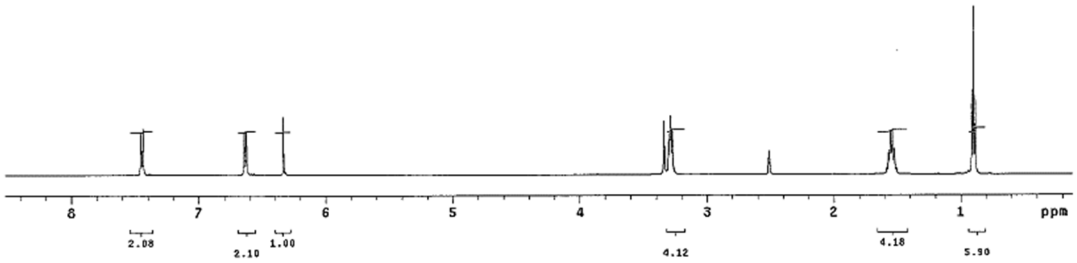
8
7
6
5
4
3
2
1
ppm
2.08
2.10
1.00
4.12
4.18
5.90

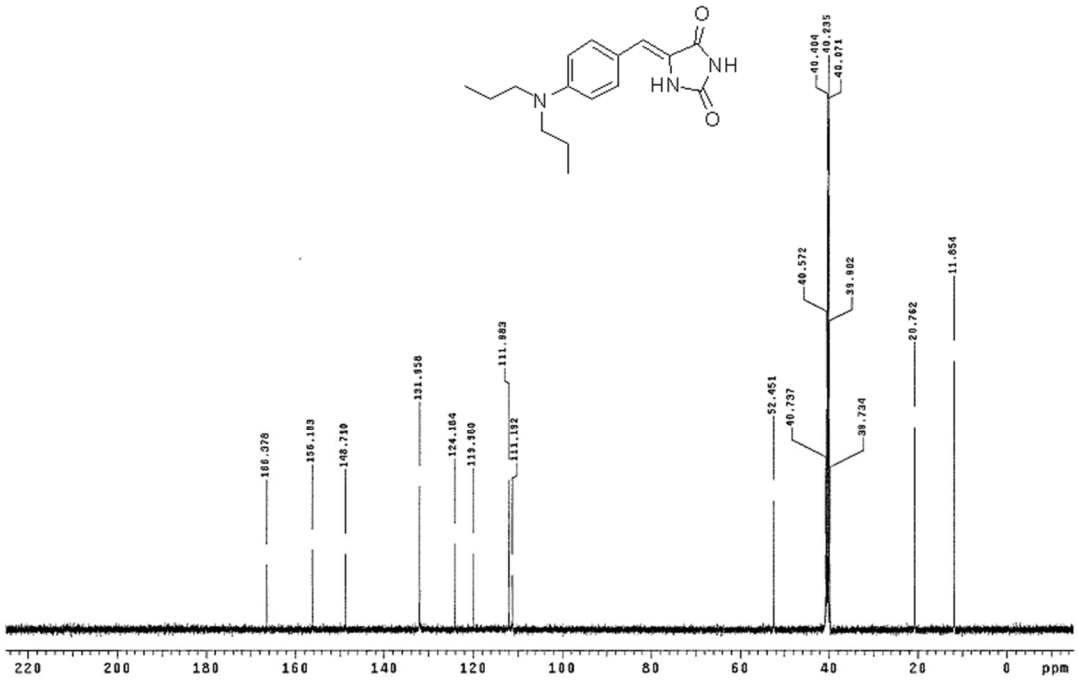
O
NH
HN
O
N
168.378
156.183
148.710
131.458
124.184
119.360
111.983
111.192
52.451
40.737
40.572
40.404
40.235
40.071
39.902
39.734
20.762
11.654
220
200
180
160
140
120
100
80
60
40
20
0
ppm

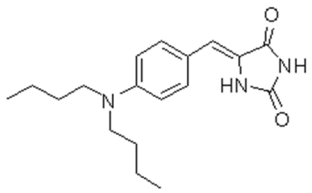
O
NH
HN
O
N

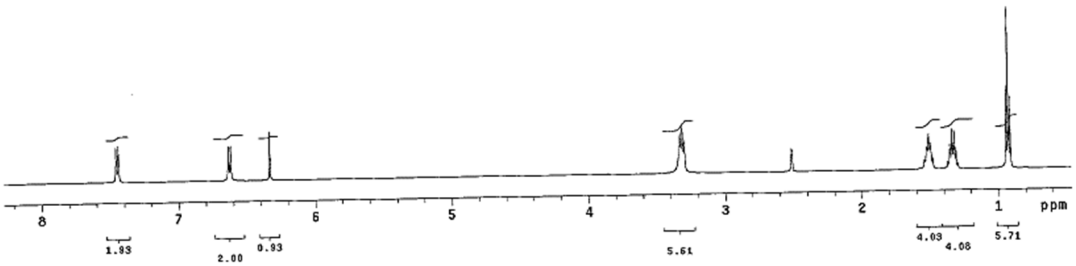
8
7
6
5
4
3
2
1
ppm
1.93
2.00
0.93
5.61
4.03
4.08
5.71

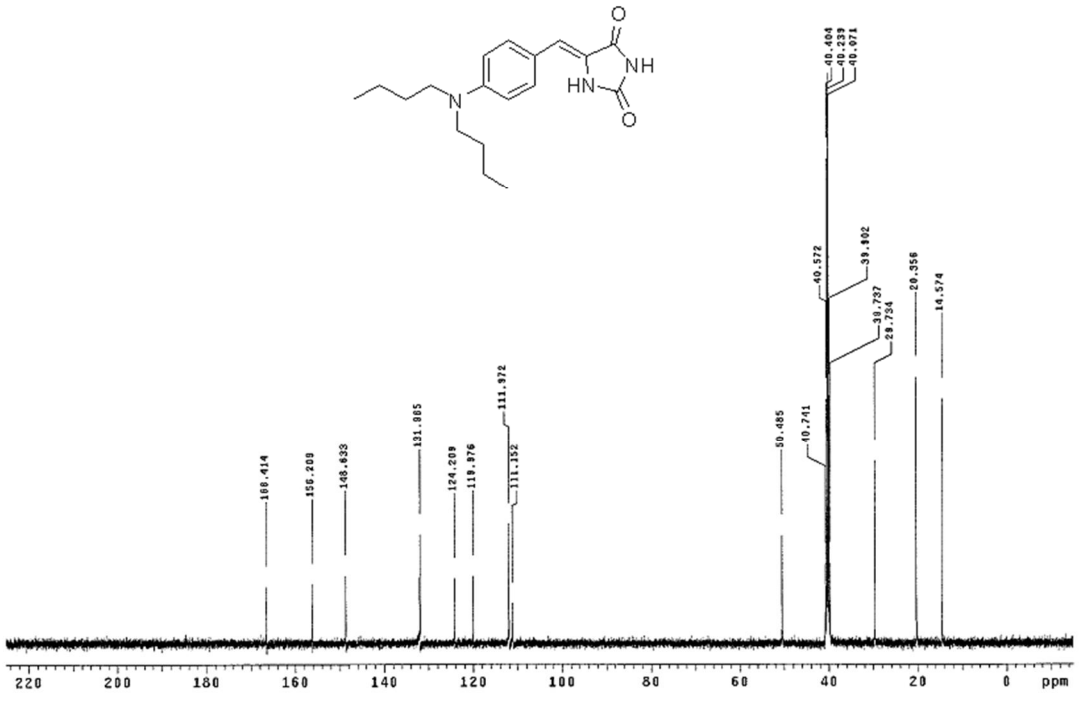
O
NH
HN
O
N
168.414
156.209
148.633
131.985
124.209
119.976
111.372
111.152
50.485
40.741
40.572
40.404
40.239
40.071
39.902
30.737
28.734
20.356
14.574
220
200
180
160
140
120
100
80
60
40
20
0
ppm

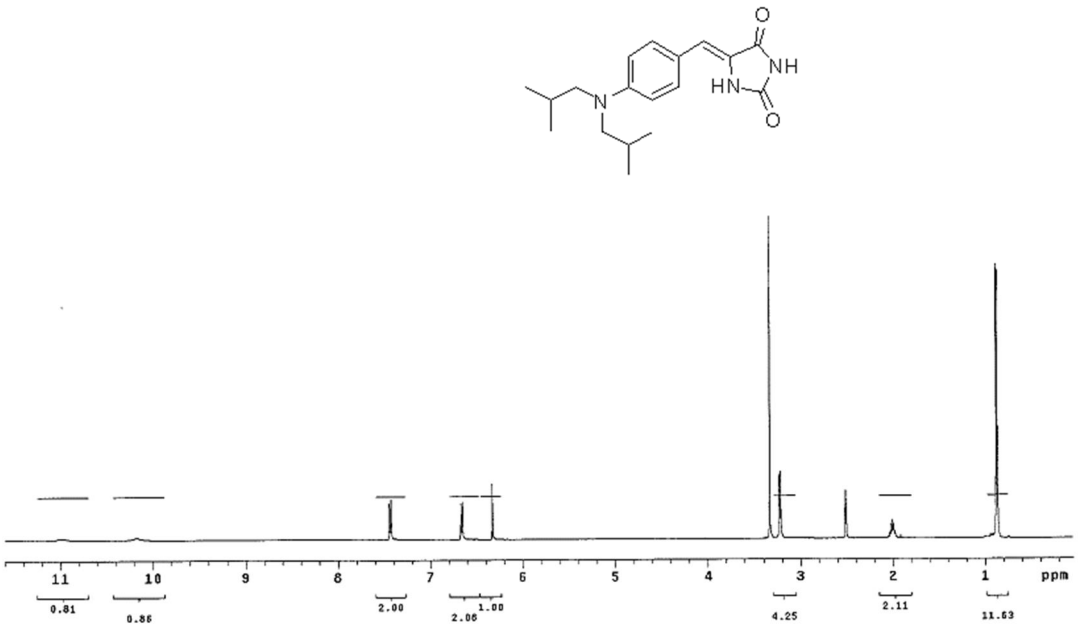
O
NH
HN
O
N
11
10
9
8
7
6
5
4
3
2
1
ppm
0.81
0.86
2.00
2.06
1.00
4.25
2.11
11.63

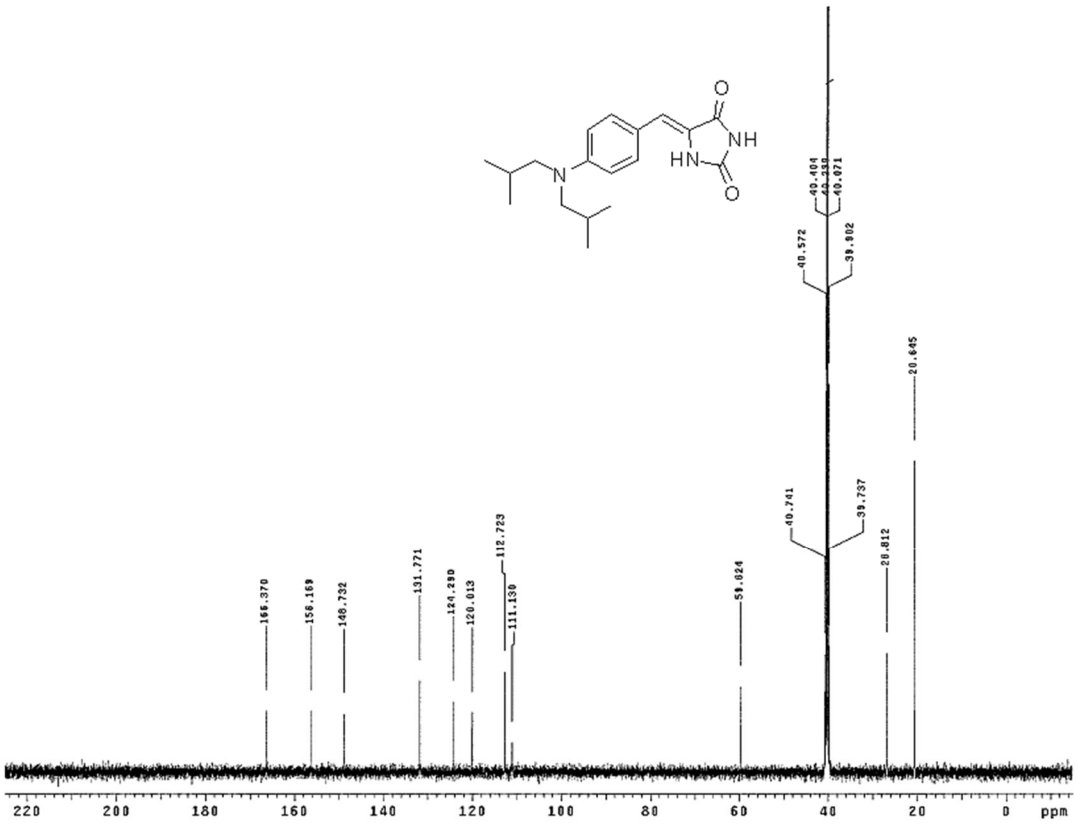
O
NH
HN
O
N
166.370
156.169
140.732
131.771
124.290
120.013
112.723
111.130
51.024
40.741
40.572
40.404
40.338
40.071
39.902
39.737
20.812
20.645
220
200
180
160
140
120
100
80
60
40
20
0
ppm

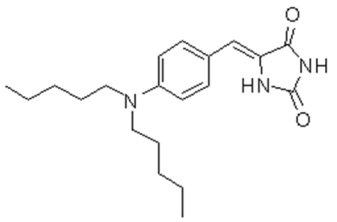
O
NH
HN
O
N

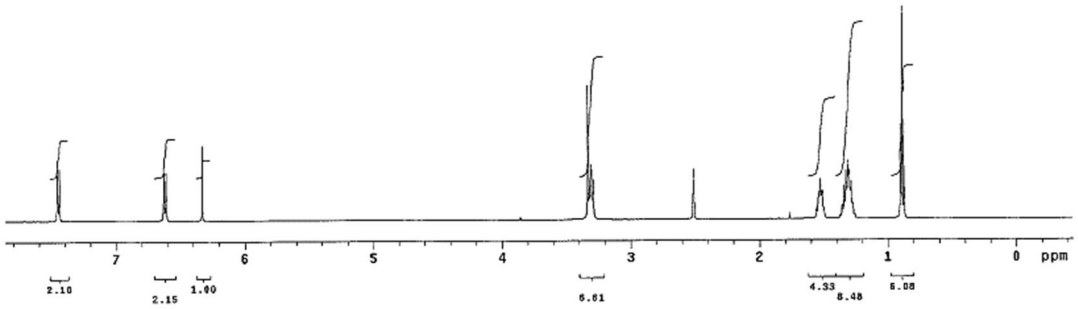
7
6
5
4
3
2
1
0
ppm
2.10
2.15
1.00
6.61
4.33
6.48
6.08

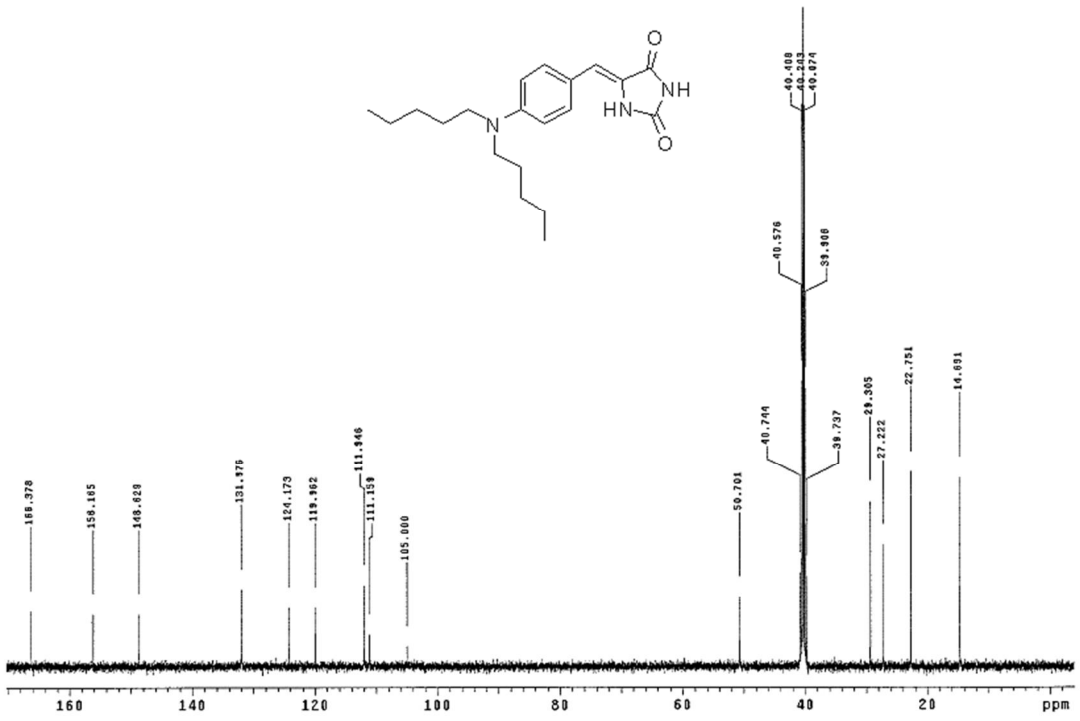
O
NH
HN
O
N
168.378
158.165
148.628
131.476
124.173
119.962
111.446
111.159
105.000
50.701
40.744
40.576
40.408
40.239
40.071
39.737
39.400
29.305
27.222
22.751
14.091
160
140
120
100
80
60
40
20
ppm

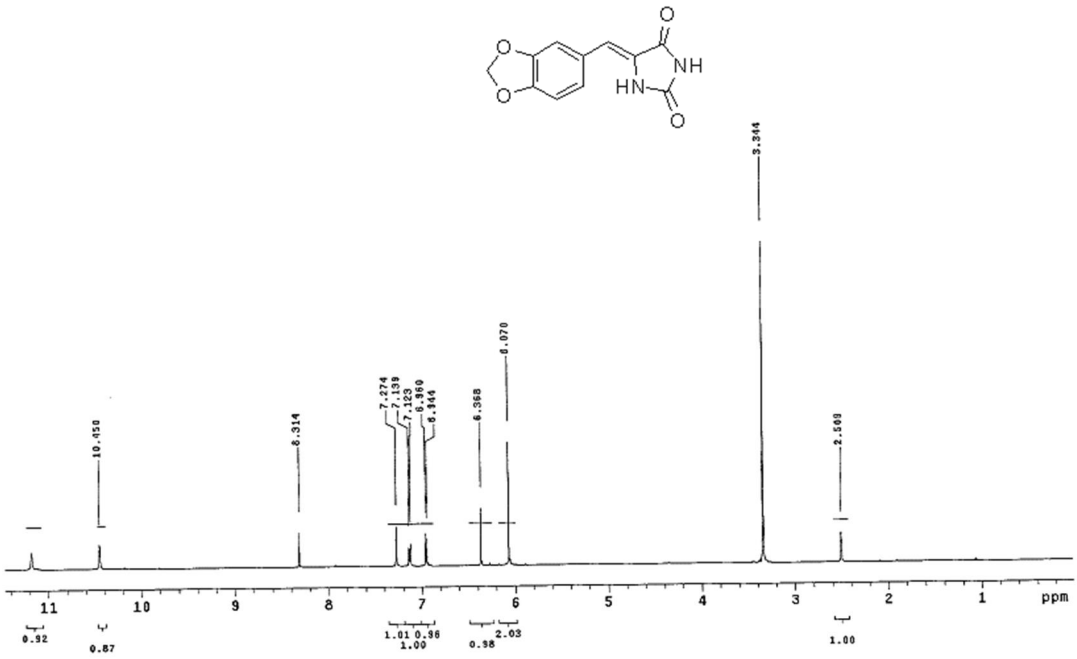
O
O
O
NH
HN
O
10.458
8.314
7.274
7.139
7.123
6.960
6.944
6.368
6.070
3.944
2.568
11
10
9
8
7
6
5
4
3
2
1
ppm
0.92
0.87
1.01
0.36
1.00
0.98
2.03
1.00

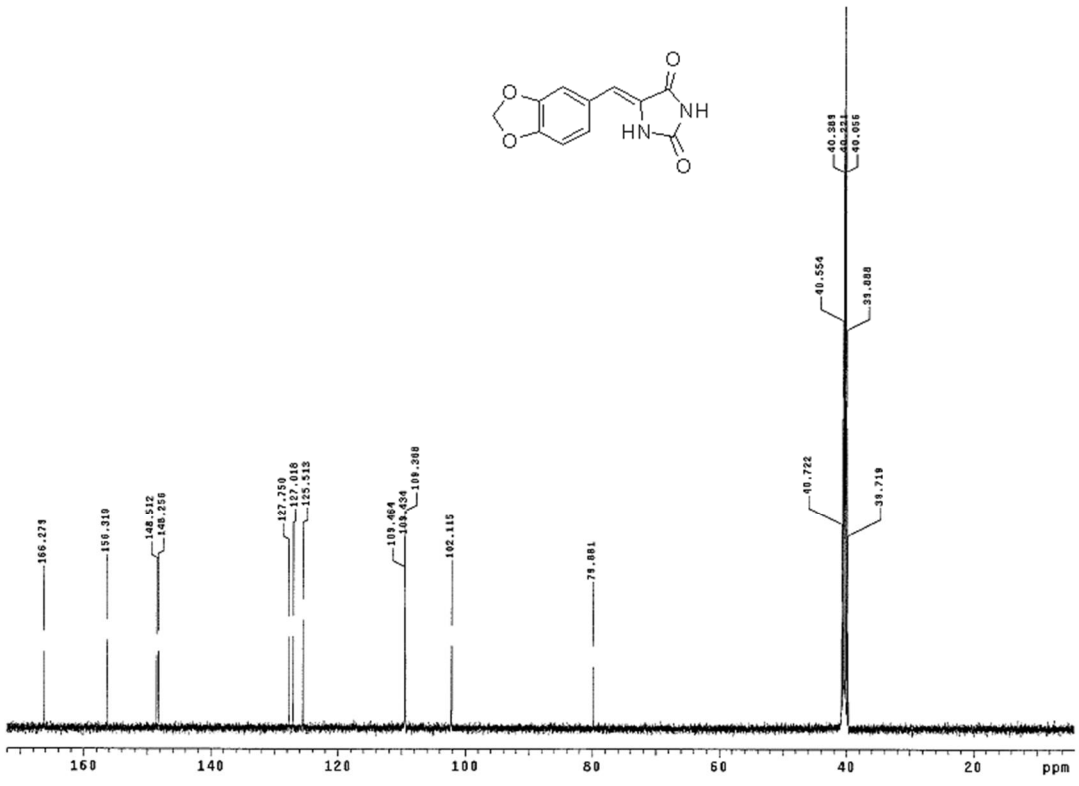
O
O
O
NH
HN
O
166.273
150.319
148.512
148.256
127.750
127.018
125.513
109.464
109.434
109.308
102.115
79.881
40.554
39.888
40.722
39.719
160
140
120
100
80
60
40
20
ppm

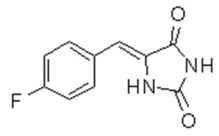
O
NH
HN
O
F

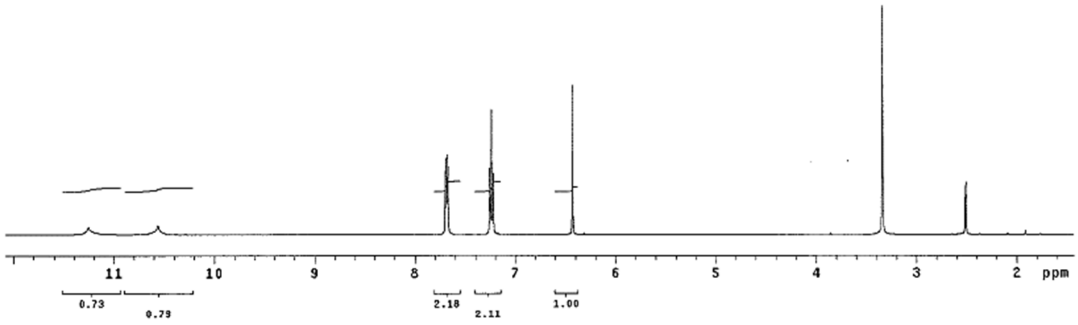
11
10
9
8
7
6
5
4
3
2
ppm
0.73
0.79
2.18
2.11
1.00

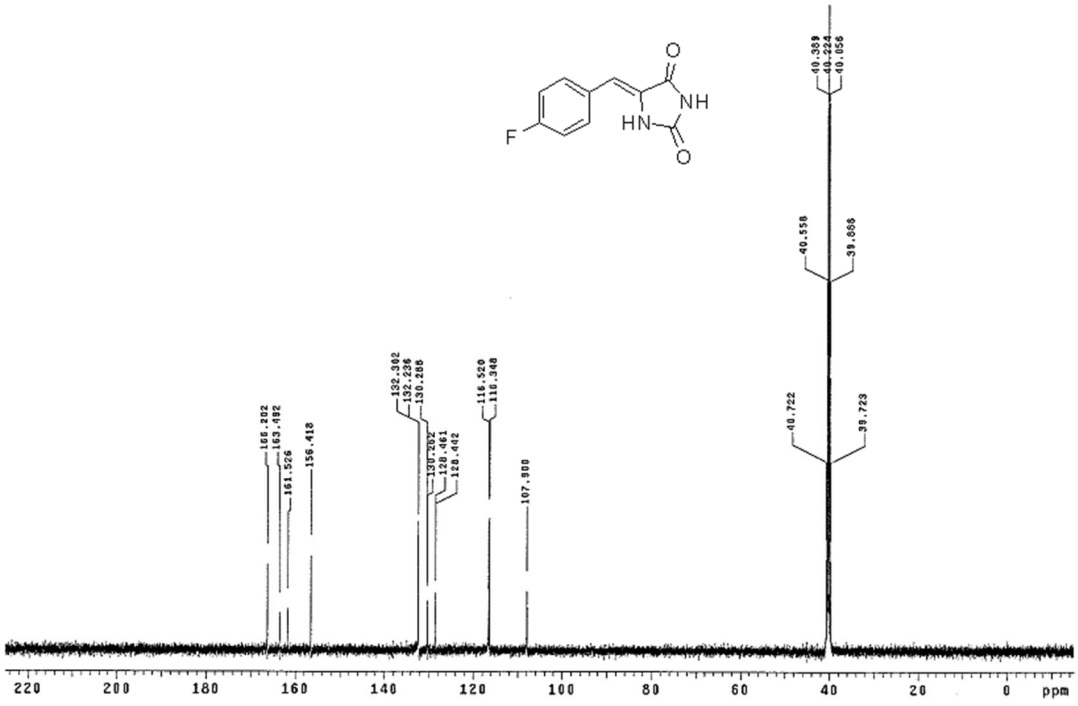
O
NH
HN
O
F
166.202
163.492
161.526
156.418
132.382
132.236
130.286
130.202
128.461
128.442
116.520
116.340
107.988
40.389
40.224
40.056
40.556
39.866
40.722
39.723
220
200
180
160
140
120
100
80
60
40
20
0
ppm

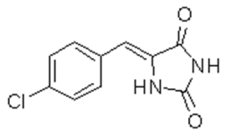
O
NH
HN
O
Cl

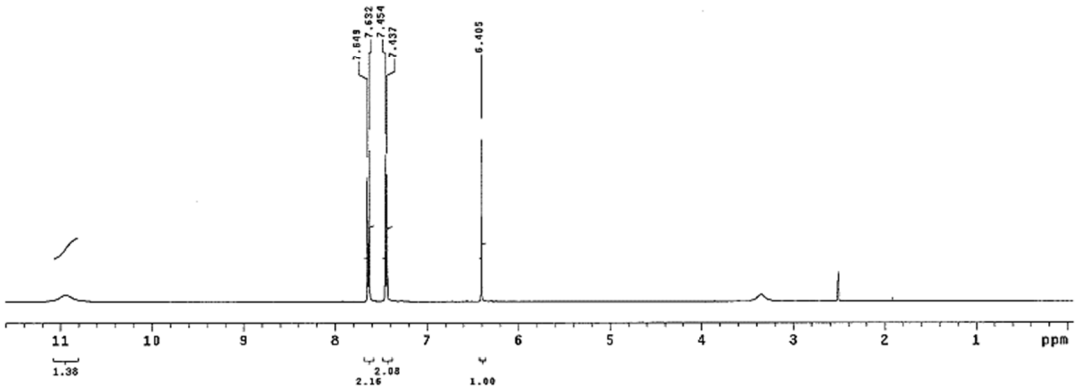
7.649
7.632
7.454
7.437
6.405
11
10
9
8
7
6
5
4
3
2
1
ppm
1.38
2.16
2.08
1.00

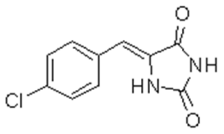
O
NH
HN
O
Cl

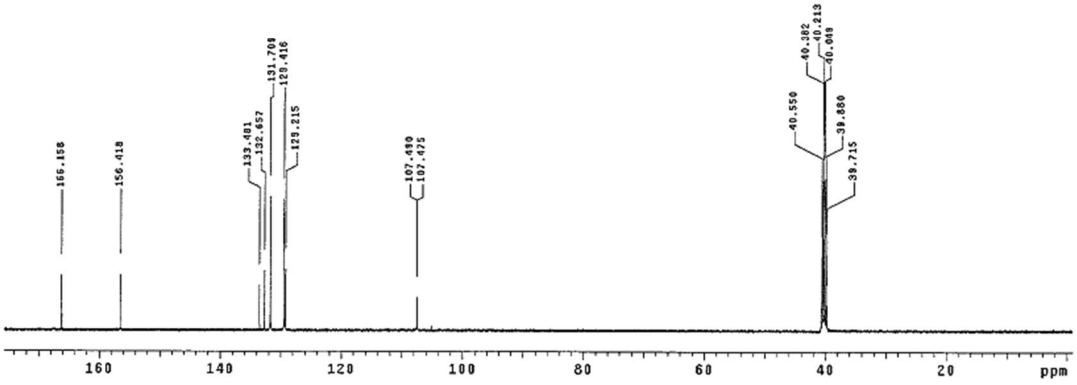
166.158
156.418
133.401
132.957
131.708
129.416
129.215
107.490
107.475
40.550
40.382
40.213
40.046
39.880
39.715
160
140
120
100
80
60
40
20
ppm

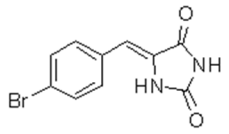
O
NH
HN
O
Br

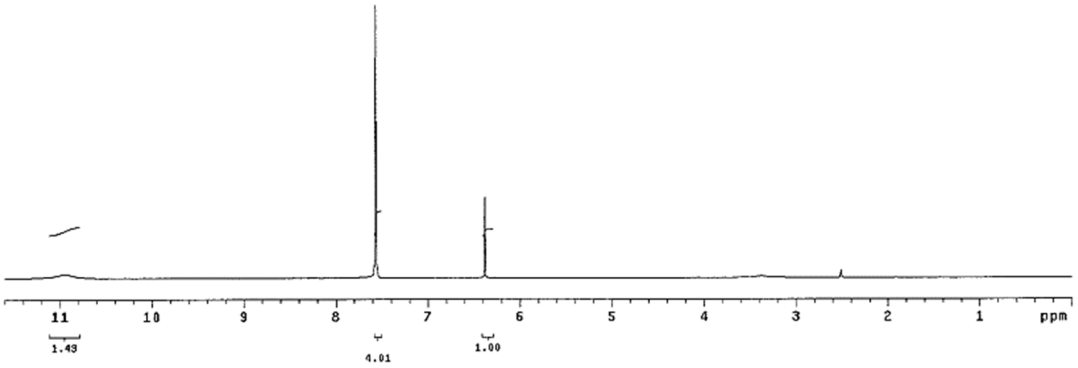
11
10
9
8
7
6
5
4
3
2
1
ppm
1.49
4.01
1.00

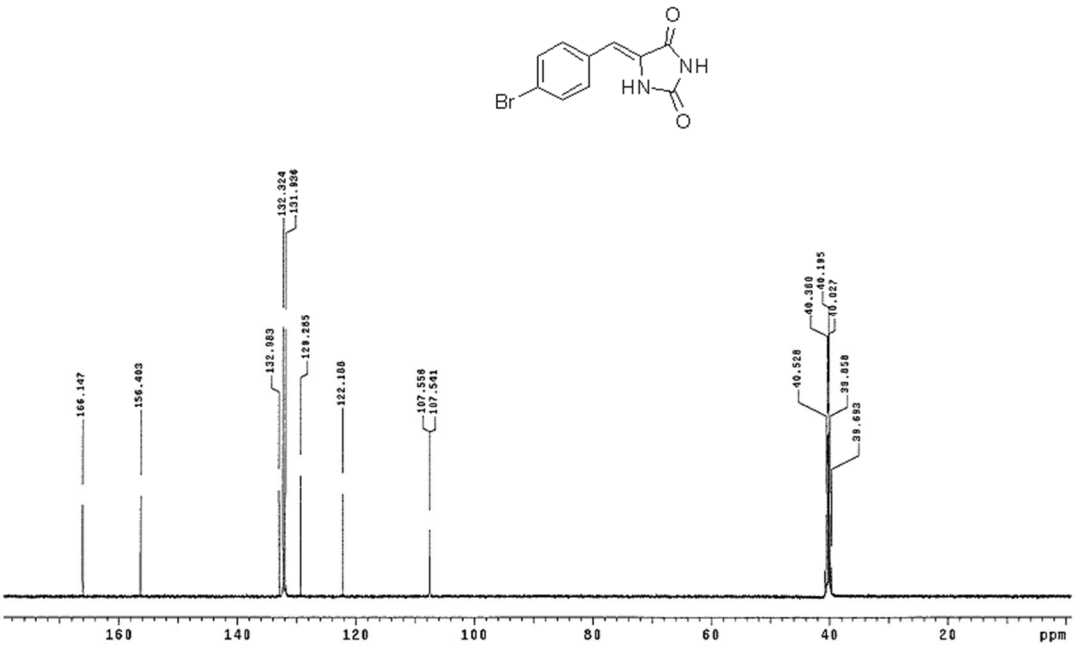
O
NH
HN
O
Br
166.147
156.403
132.983
132.324
131.986
129.285
122.108
107.558
107.541
40.528
40.380
40.195
40.027
39.858
39.693
160
140
120
100
80
60
40
20
ppm

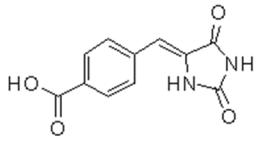
HO
O
O
NH
HN
O

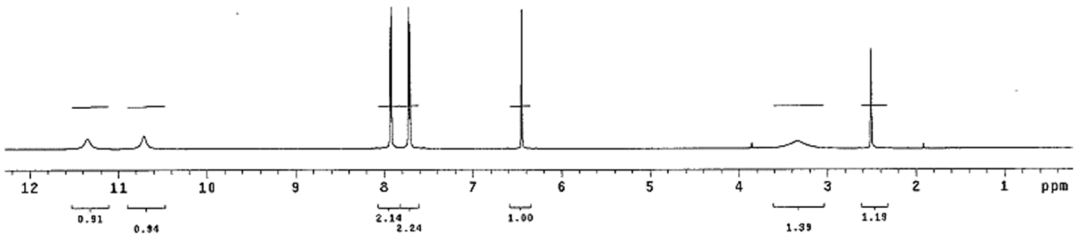
12
11
10
9
8
7
6
5
4
3
2
1
ppm
0.91
0.94
2.14
2.24
1.00
1.39
1.19

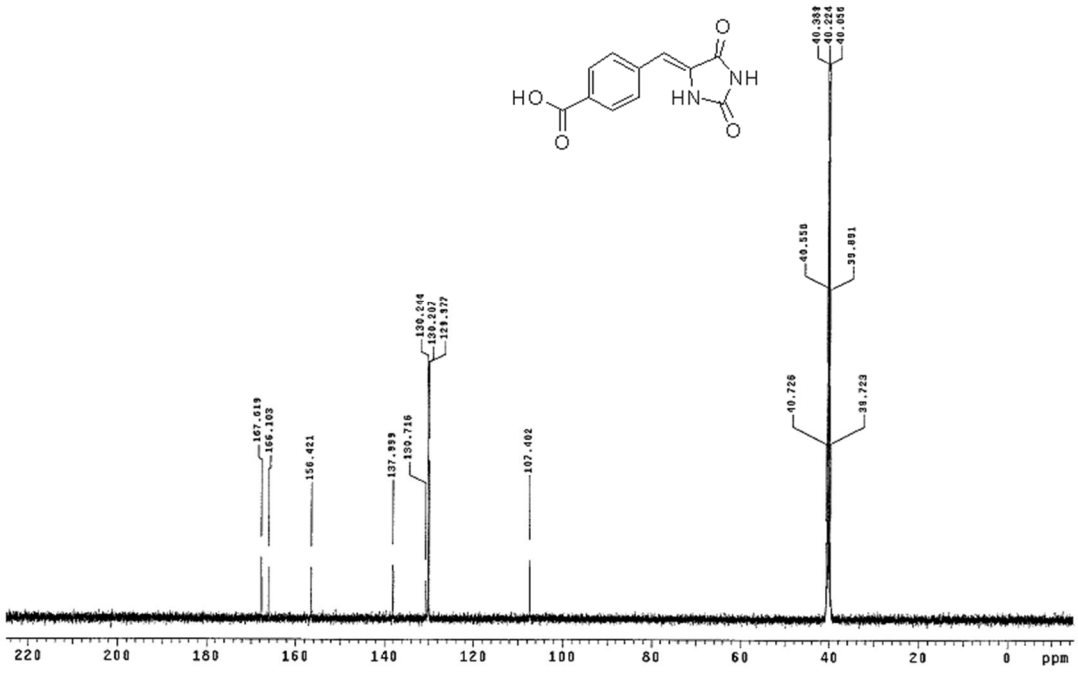
HO
O
O
NH
HN
O
167.619
166.103
156.421
137.959
130.716
130.244
130.207
129.377
107.402
40.388
40.224
40.056
39.891
39.723
ppm

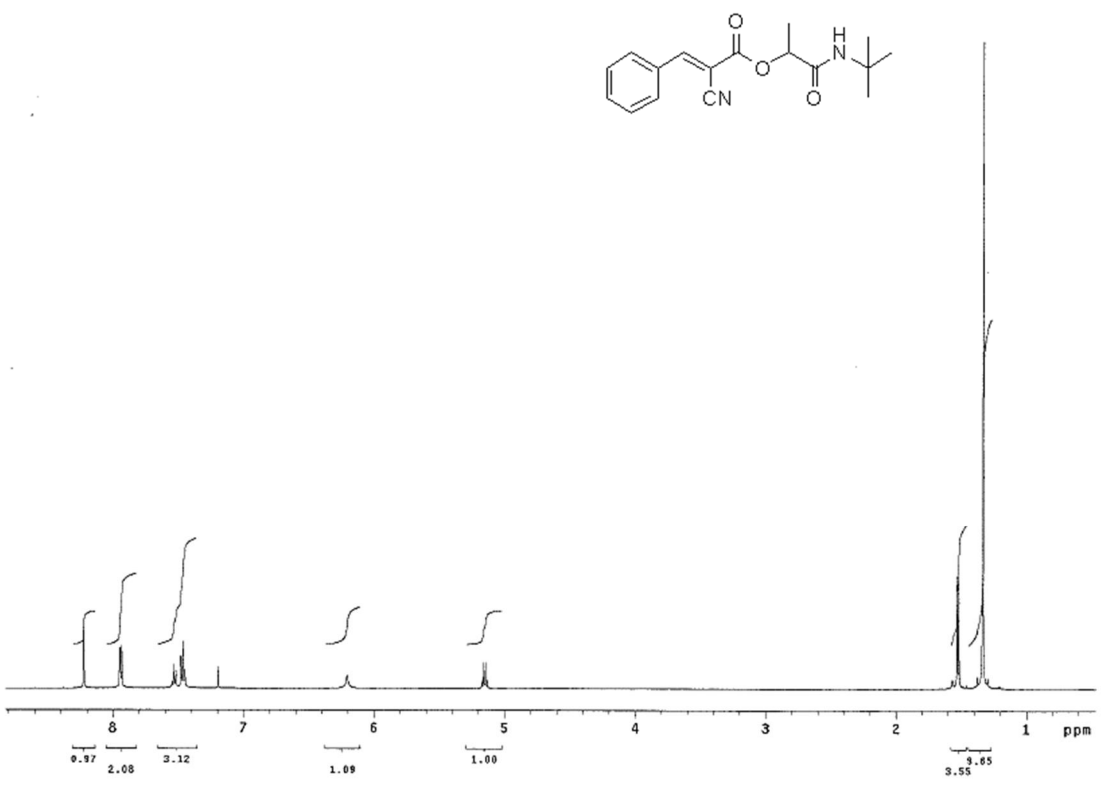
O
O
H
N
CN
O
8
7
6
5
4
3
2
1
ppm
0.97
2.08
3.12
1.09
1.00
9.65
3.55

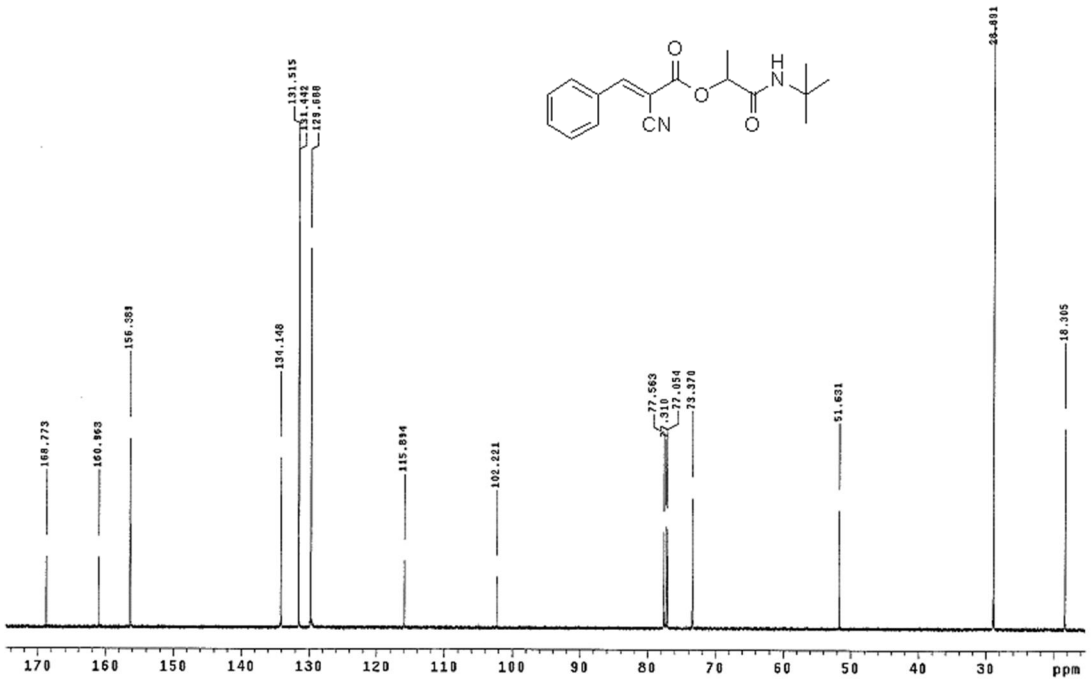
168.773
160.963
156.383
134.140
131.515
131.442
129.088
115.894
102.221
77.563
77.310
77.054
73.370
51.631
28.491
18.305
170
160
150
140
130
120
110
100
90
80
70
60
50
40
30
ppm
O
O
H
N
CN
O

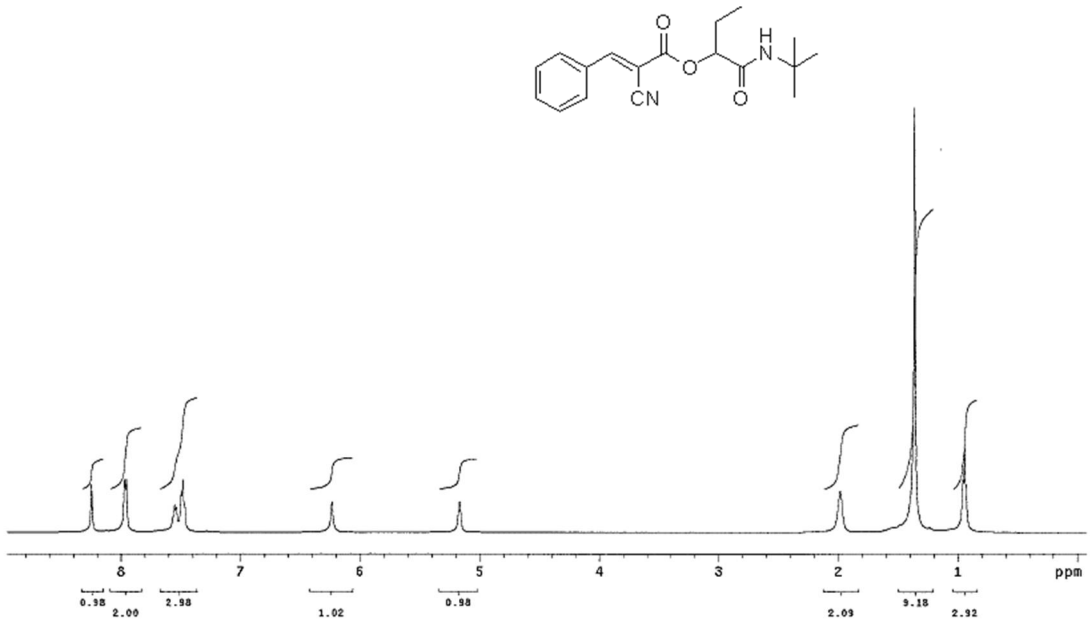
O
H
N
O
CN
O
8
7
6
5
4
3
2
1
ppm
0.98
2.00
2.98
1.02
0.98
2.09
9.18
2.92

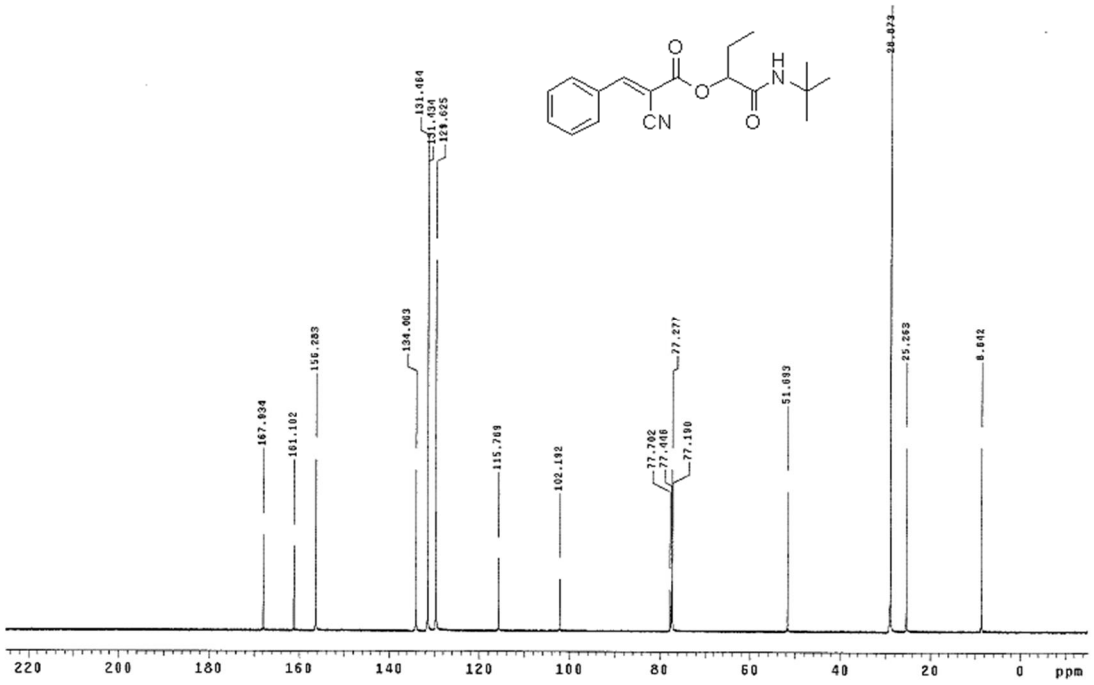
167.034
161.102
156.283
134.003
131.464
131.034
129.625
115.769
102.192
77.702
77.446
77.190
77.277
51.093
28.023
25.263
8.602
220
200
180
160
140
120
100
80
60
40
20
0
ppm
O
O
NH
O
CN

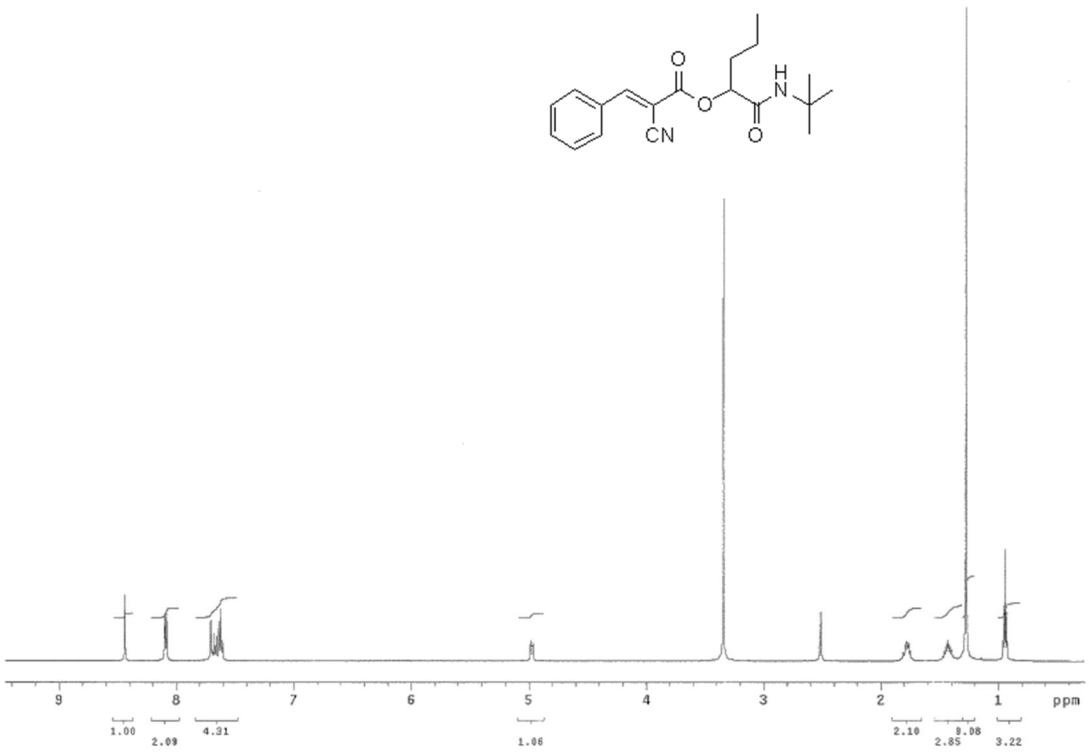
O
O
H
N
CN
O
9
8
7
6
5
4
3
2
1
ppm
1.00
2.09
4.31
1.06
2.10
8.08
2.85
3.22

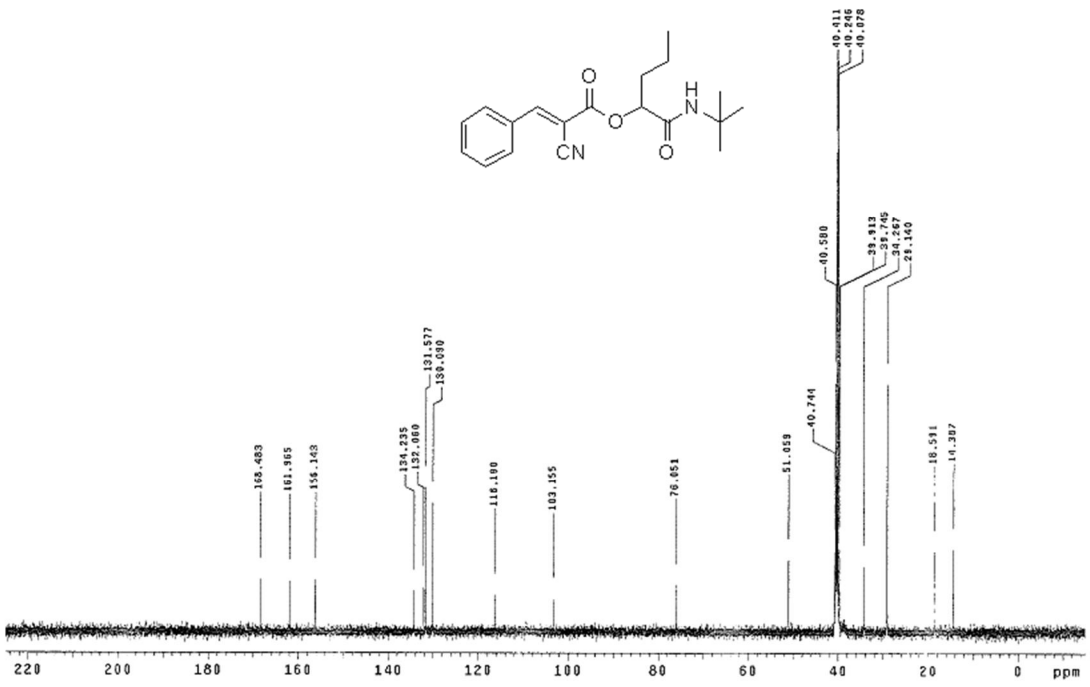
O
O
H
N
O
CN
O
165.483
161.965
156.143
134.235
132.060
131.577
130.090
116.190
103.155
76.651
51.059
40.744
40.580
40.411
40.246
40.078
39.913
39.746
34.267
29.140
18.511
14.307
220
200
180
160
140
120
100
80
60
40
20
0
ppm

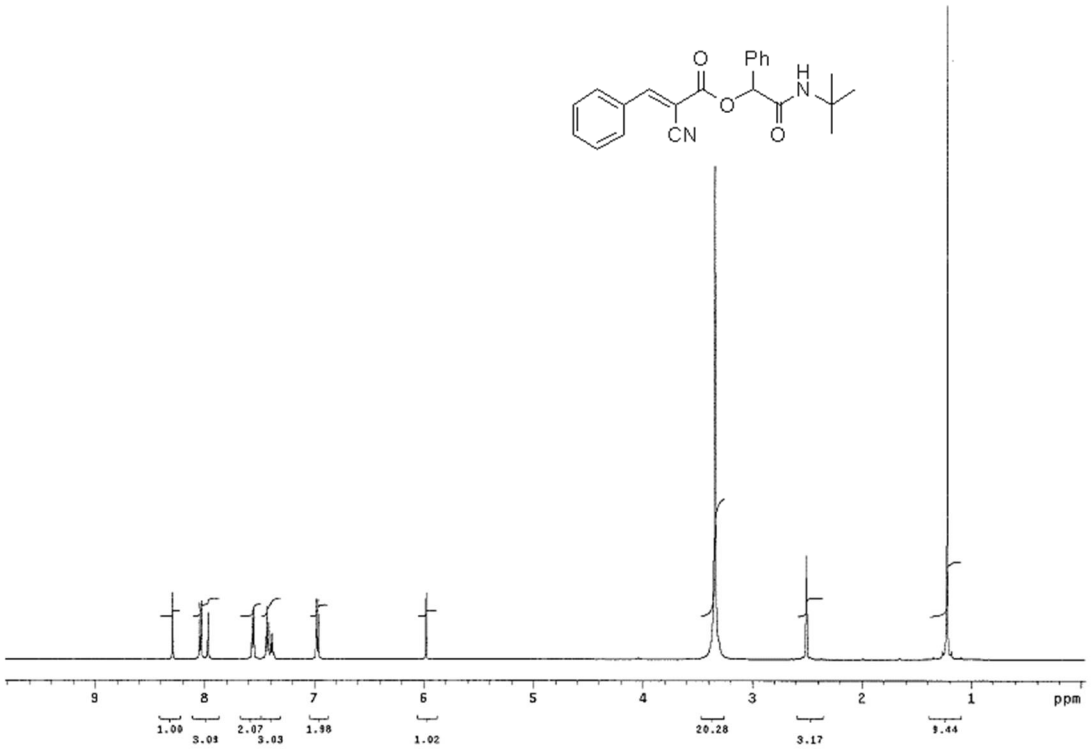
O
Ph
H
N
O
CN
O
9
8
7
6
5
4
3
2
1
ppm
1.00
3.08
2.07
3.03
1.98
1.02
20.28
3.17
9.44

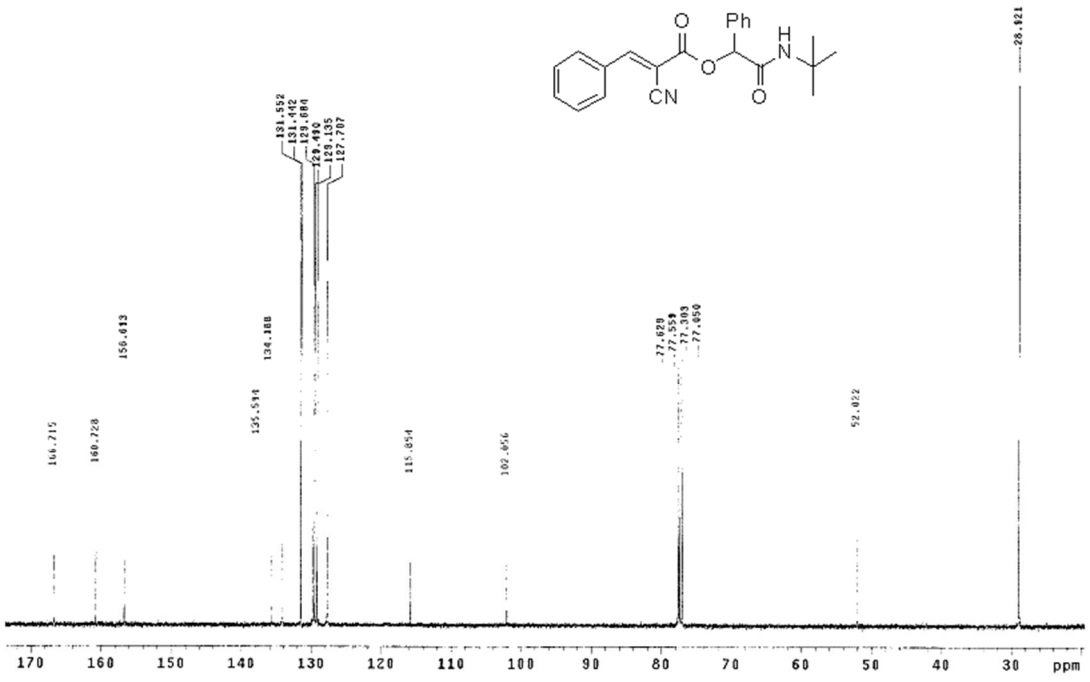
O
Ph
H
N
O
CN
O
166.215
160.728
156.613
155.594
134.188
131.552
131.442
129.684
129.490
129.135
127.707
115.854
102.656
77.629
77.559
77.303
77.050
52.022
28.421
170
160
150
140
130
120
110
100
90
80
70
60
50
40
30
ppm

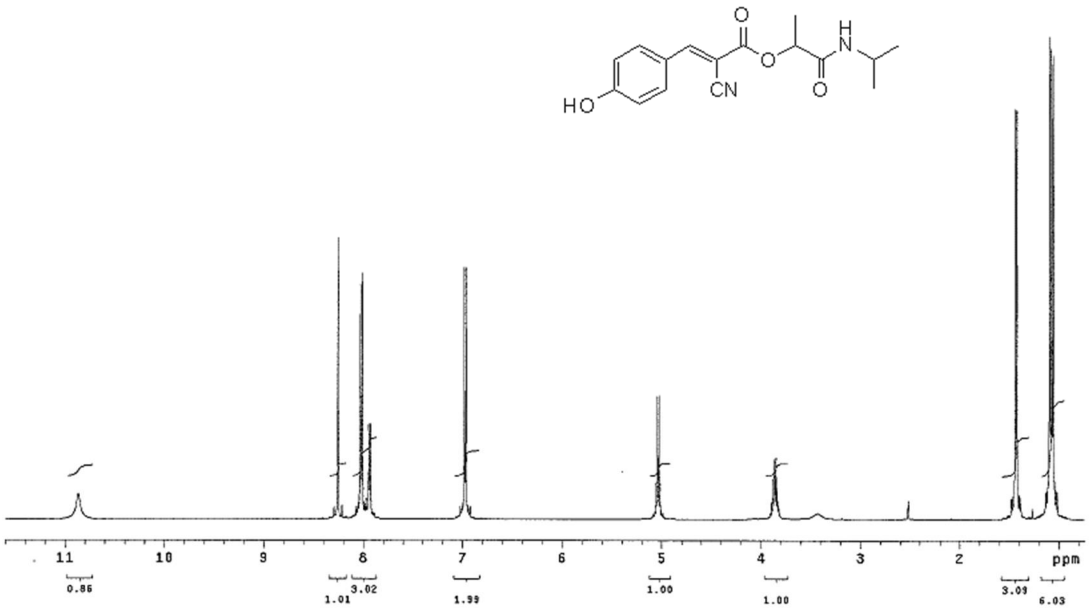
HO
CN
O
O
H
N
O
11
10
9
8
7
6
5
4
3
2
ppm
0.86
1.01
3.02
1.99
1.00
1.00
3.09
6.03

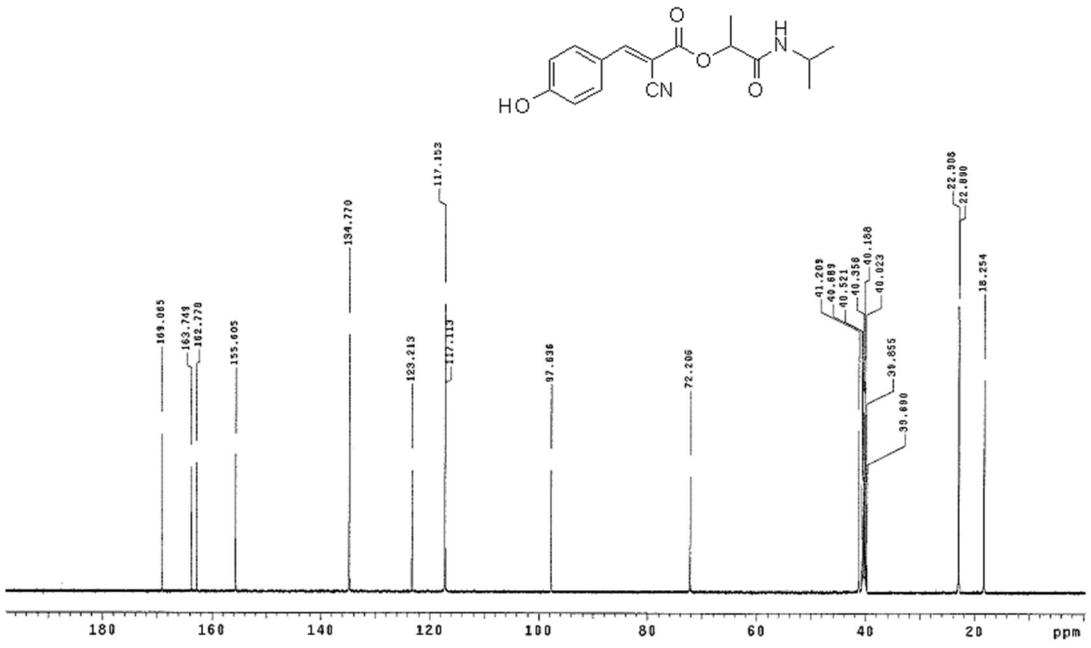
HO
CN
O
O
O
H
N
169.065
163.744
162.770
155.605
134.770
123.213
117.153
117.113
97.636
72.206
41.209
40.689
40.551
40.356
40.188
40.023
39.855
39.690
22.908
22.800
18.254
180
160
140
120
100
80
60
40
20
ppm

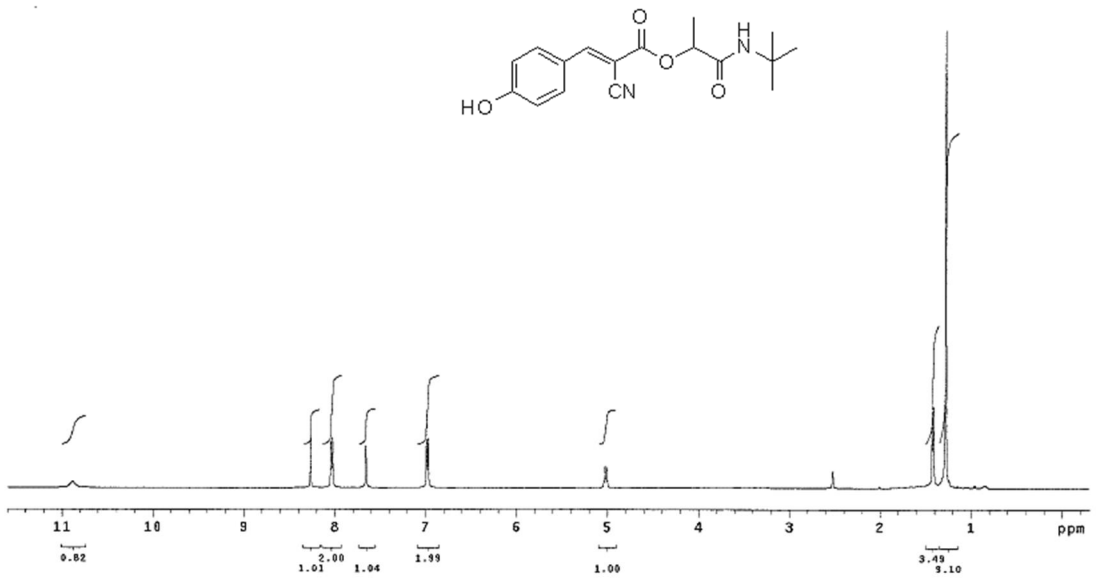
HO
CN
O
O
O
H
N
11
10
9
8
7
6
5
4
3
2
1
ppm
0.82
2.00
1.01
1.04
1.99
1.00
3.49
9.10

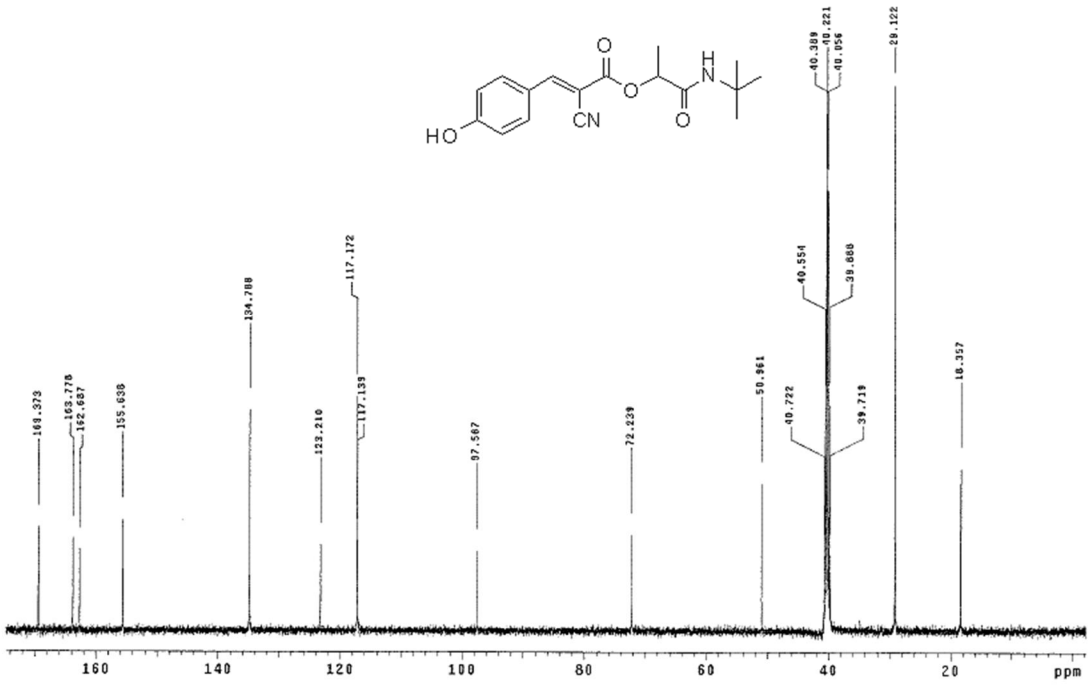
HO
CN
O
O
O
H
N
163.373
163.776
162.687
155.638
134.788
123.210
117.172
117.139
97.567
72.239
50.961
40.722
40.554
40.389
40.221
40.056
39.888
39.719
29.122
18.357
160
140
120
100
80
60
40
20
ppm

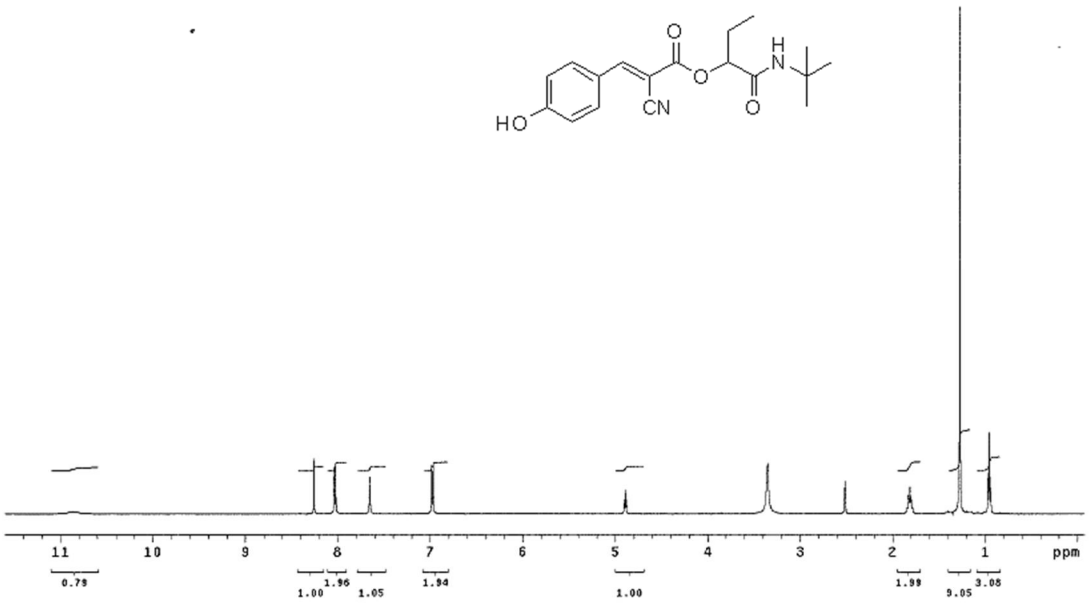
HO
CN
O
O
O
H
N
11
10
9
8
7
6
5
4
3
2
1
ppm
0.79
1.00
1.96
1.05
1.94
1.00
1.99
9.05
3.08

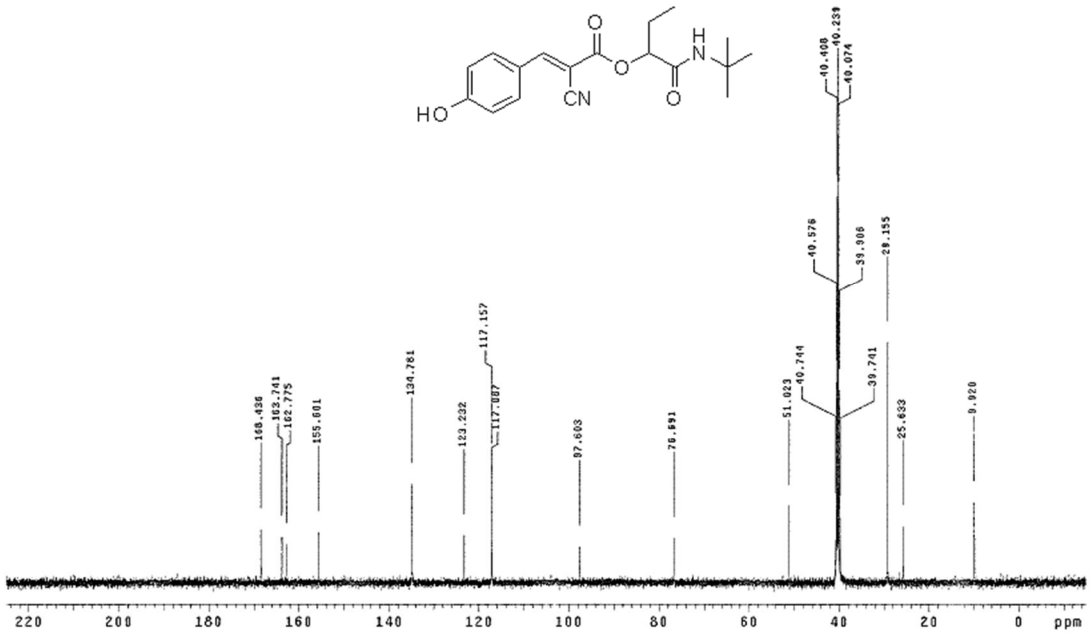
HO
CN
O
O
O
H
N
168.436
163.741
162.775
155.601
134.781
123.232
117.157
117.087
97.603
76.691
51.023
40.744
40.576
40.408
40.239
40.074
39.906
39.741
29.155
25.633
9.920
220
200
180
160
140
120
100
80
60
40
20
0
ppm

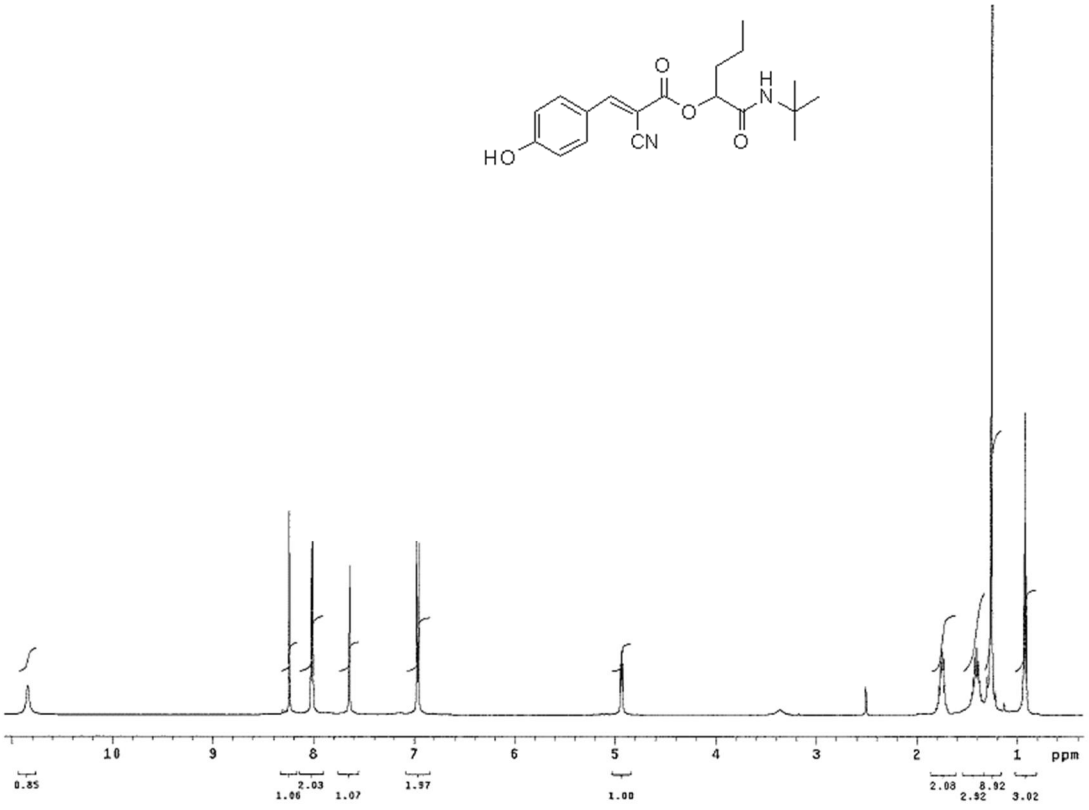
HO
CN
O
O
O
H
N
10
9
8
7
6
5
4
3
2
1
ppm
0.85
1.06
2.03
1.07
1.97
1.00
2.08
2.92
8.92
3.02

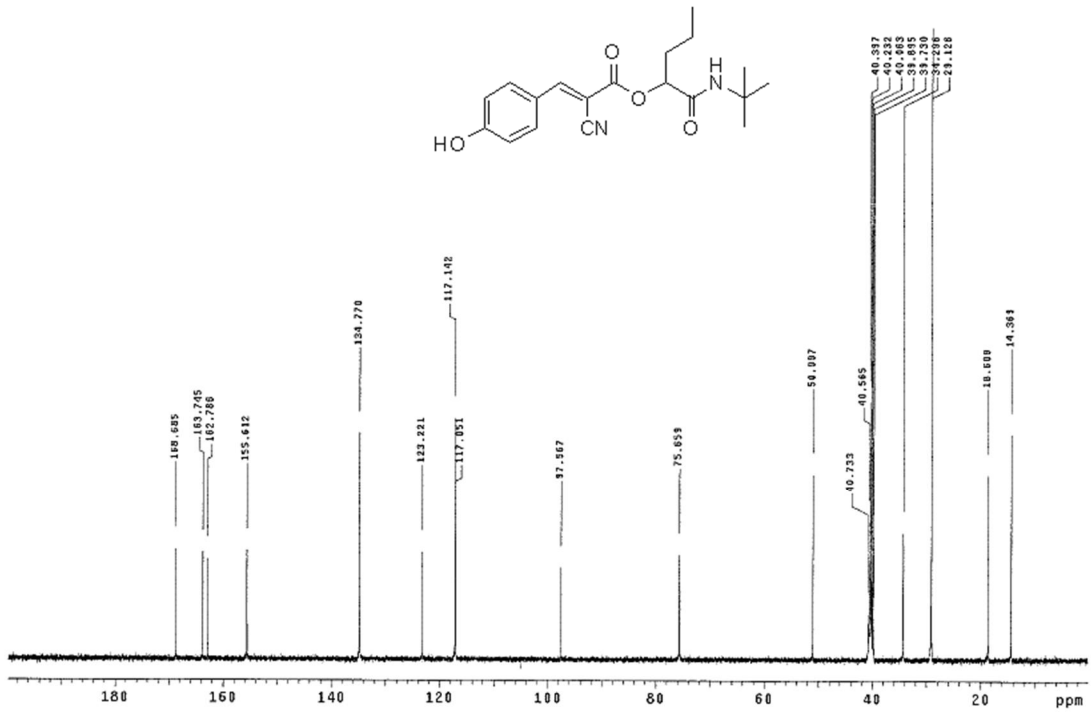
HO
CN
O
O
O
H
N
168.685
163.745
162.788
155.612
134.770
123.221
117.142
117.051
97.567
75.659
50.897
40.733
40.565
40.397
40.232
40.063
39.895
39.730
34.230
23.128
18.600
14.361
180
160
140
120
100
80
60
40
20
ppm

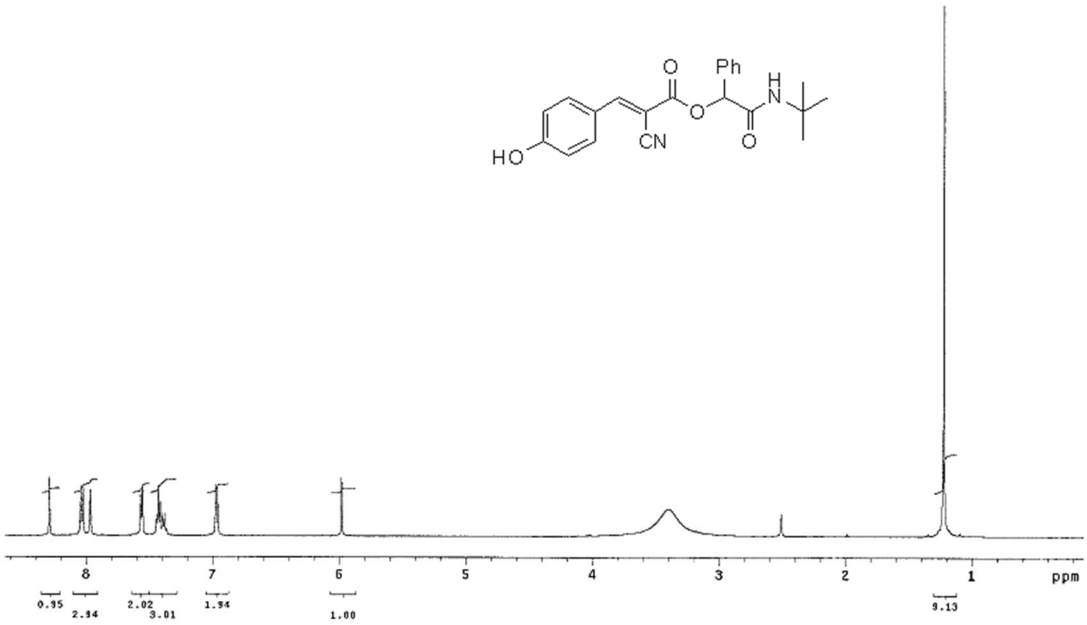
HO
CN
O
O
Ph
O
H
N
8
7
6
5
4
3
2
1
ppm
0.95
2.34
2.02
3.01
1.94
1.00
9.13

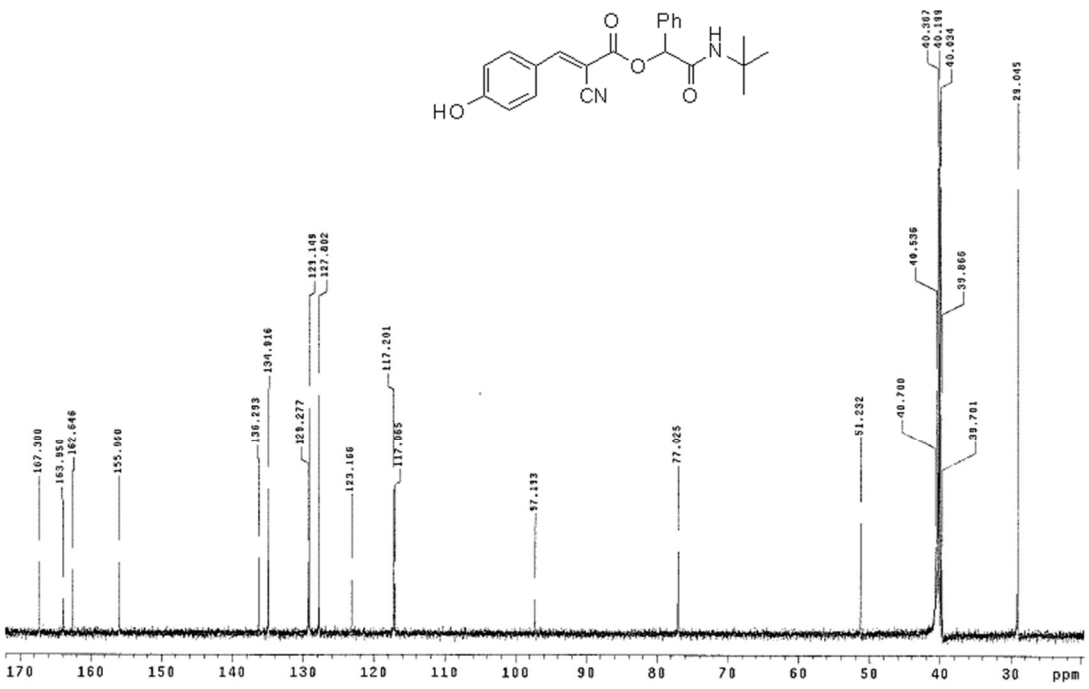
O
Ph
H
N
O
CN
O
HO
167.300
163.950
162.646
155.060
136.293
134.816
129.277
123.149
127.802
123.166
117.201
117.085
57.133
77.025
51.232
40.700
40.536
40.307
40.199
40.034
39.866
39.701
29.045
170
160
150
140
130
120
110
100
90
80
70
60
50
40
30
ppm

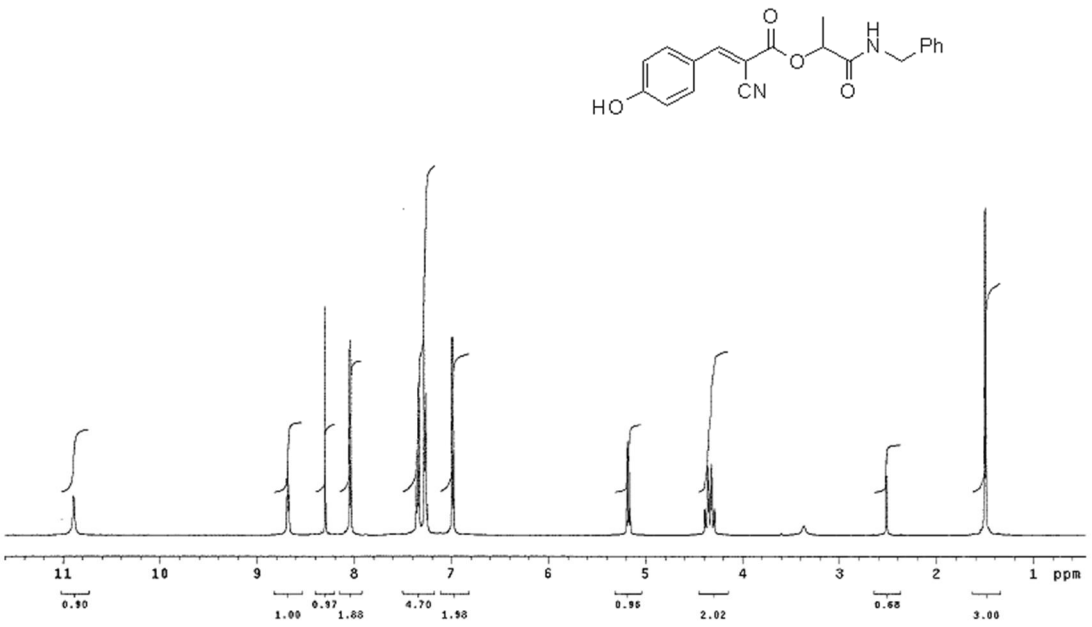
HO
CN
O
O
H
N
Ph
11
10
9
8
7
6
5
4
3
2
1
ppm
0.90
1.00
0.97
1.88
4.70
1.98
0.96
2.02
0.68
3.00

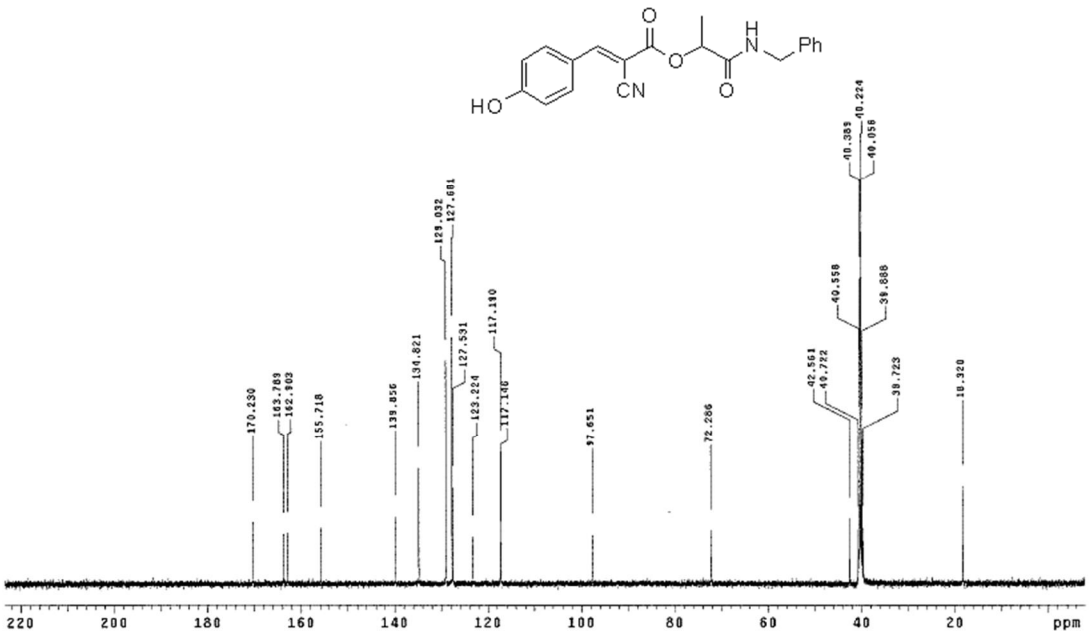
HO
CN
O
O
O
H
N
Ph
170.230
163.789
162.903
155.718
139.856
134.821
129.032
127.601
127.531
123.224
117.190
117.146
97.651
72.286
42.561
40.722
40.558
40.385
40.224
40.056
39.888
39.723
18.328
220
200
180
160
140
120
100
80
60
40
20
ppm

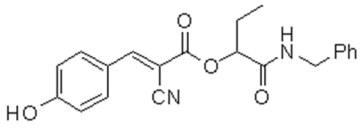
O
H
N
Ph
O
CN
HO

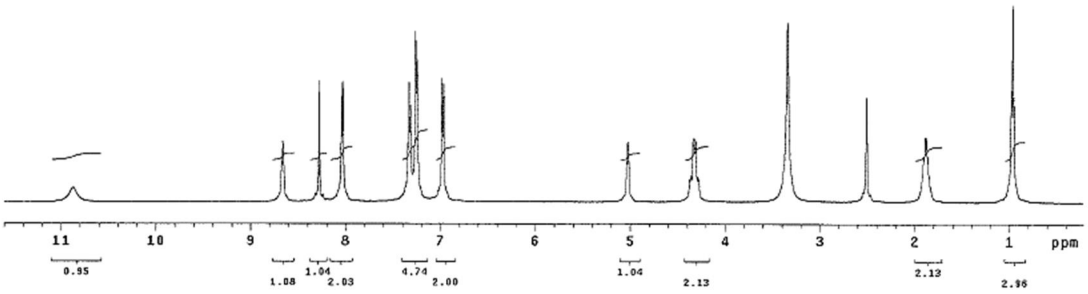
11
10
9
8
7
6
5
4
3
2
1
ppm
0.95
1.08
1.04
2.03
4.74
2.00
1.04
2.13
2.13
2.96

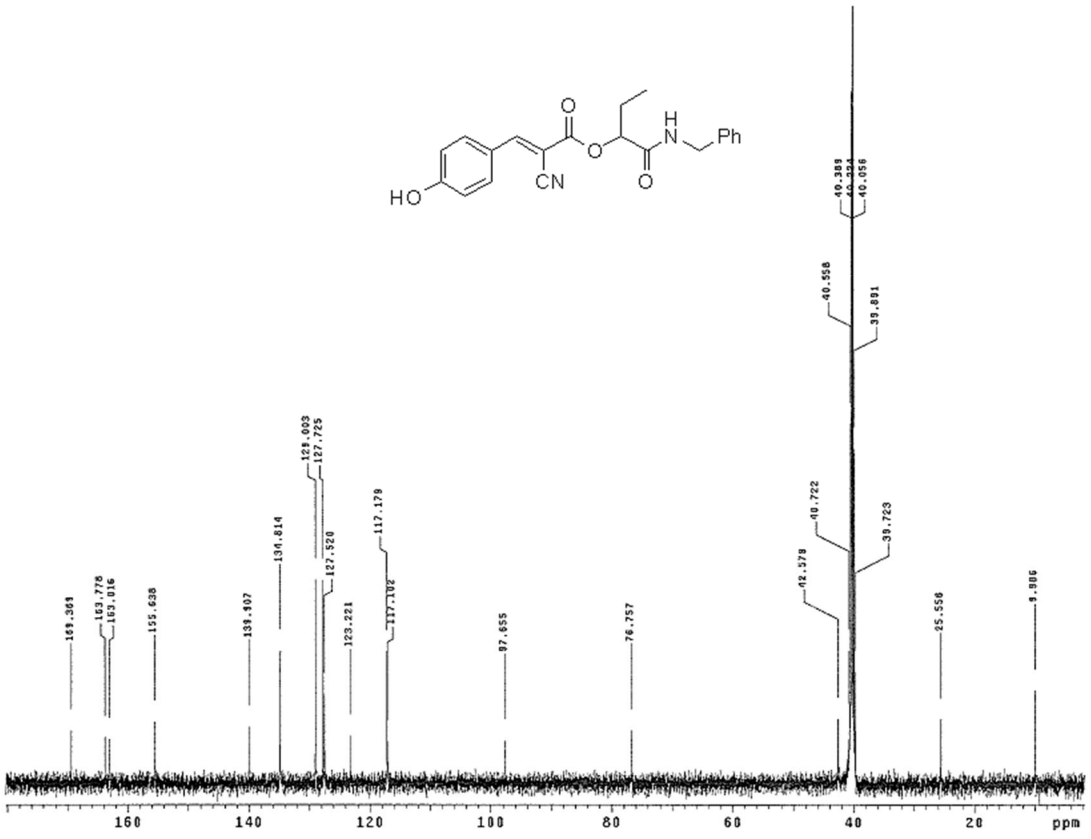
HO
CN
O
O
O
H
N
Ph
169.361
163.778
163.016
155.638
139.407
130.814
128.003
127.725
127.520
123.221
117.179
117.102
97.655
76.757
42.579
40.722
40.556
40.389
40.222
40.056
39.891
39.723
25.550
9.886
160
140
120
100
80
60
40
20
ppm

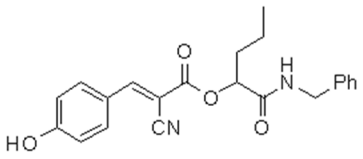
O
H
N
Ph
O
HO
CN
O

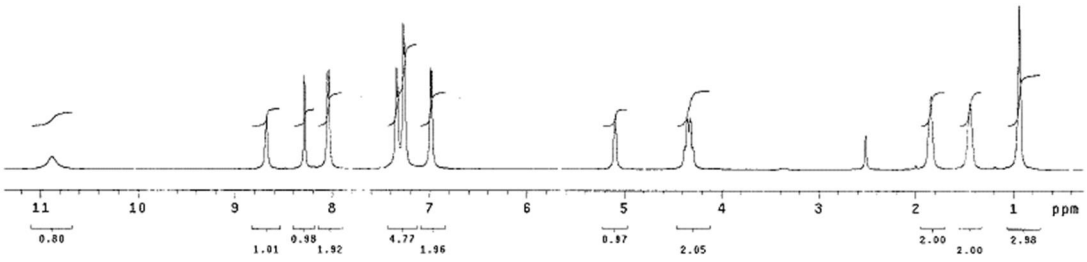
11
10
9
8
7
6
5
4
3
2
1
ppm
0.80
1.01
0.98
1.92
4.77
1.96
0.97
2.05
2.00
2.00
2.98

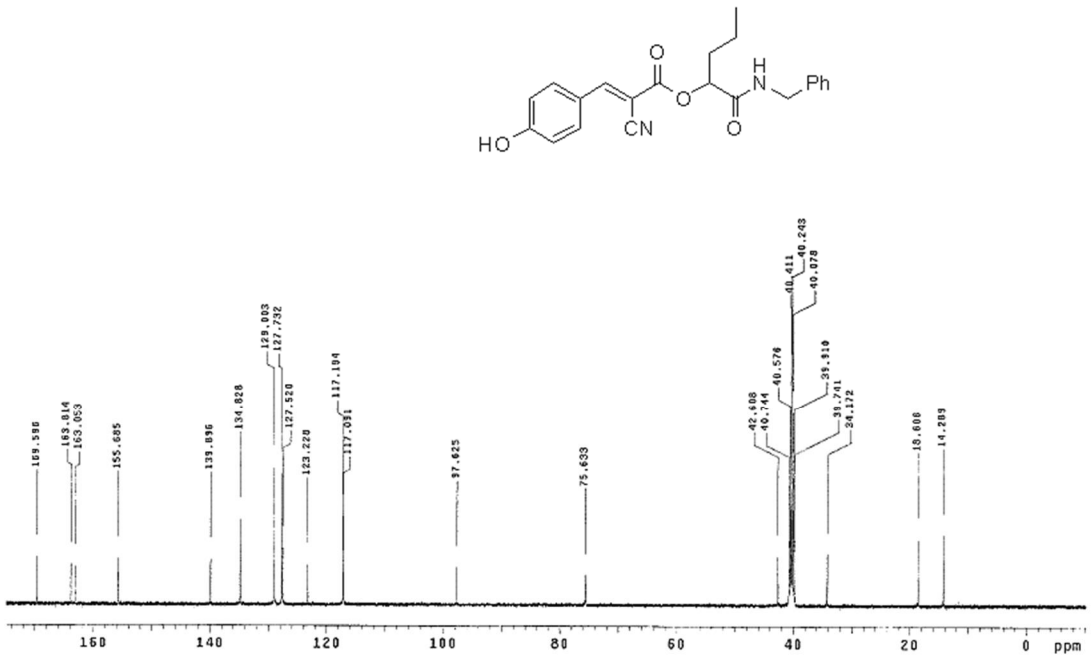
HO
CN
O
O
O
H
N
Ph
169.598
163.814
163.053
155.685
139.836
134.828
129.083
127.732
127.520
123.220
117.194
117.051
97.625
75.633
42.608
40.744
40.576
40.411
40.243
40.078
35.810
31.741
24.172
18.606
14.289
160
140
120
100
80
60
40
20
0
ppm

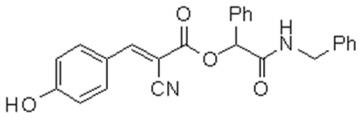
O
Ph
H
N
Ph
O
O
CN
HO

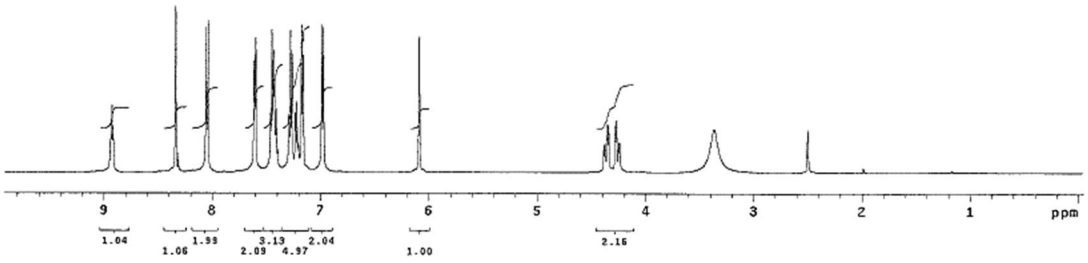
9
8
7
6
5
4
3
2
1
ppm
1.04
1.06
1.93
2.09
3.13
4.97
2.04
1.00
2.16

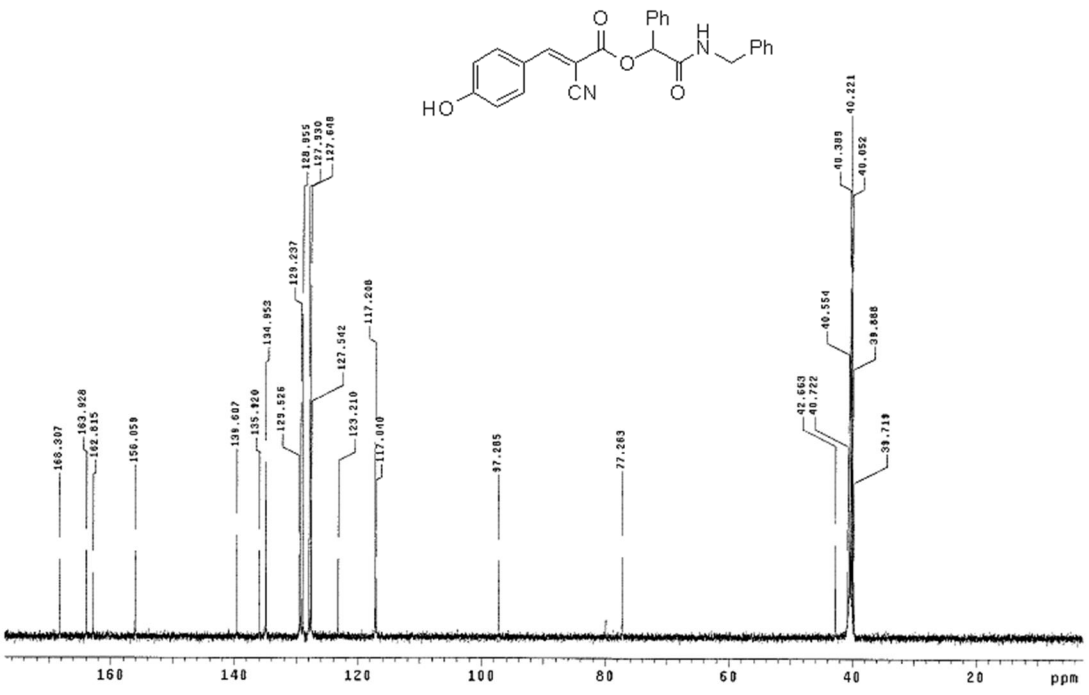
HO
CN
O
O
Ph
H
N
Ph
O
168.307
163.928
162.615
156.059
139.607
135.420
134.952
129.526
129.237
128.955
127.930
127.648
127.542
123.210
117.208
117.040
97.285
77.263
42.663
40.722
40.554
40.389
40.221
40.052
39.888
39.719
160
140
120
100
80
60
40
20
ppm

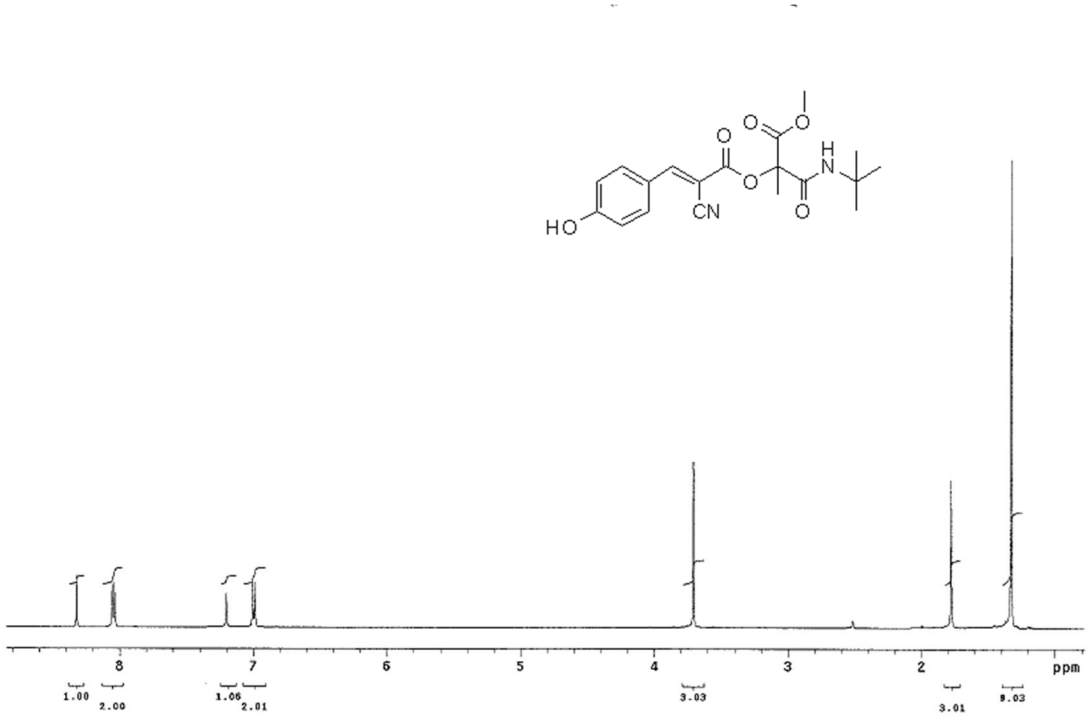
HO
CN
O
O
O
O
O
H
N
8
7
6
5
4
3
2
ppm
1.00
2.00
1.06
2.01
3.03
3.01
9.03

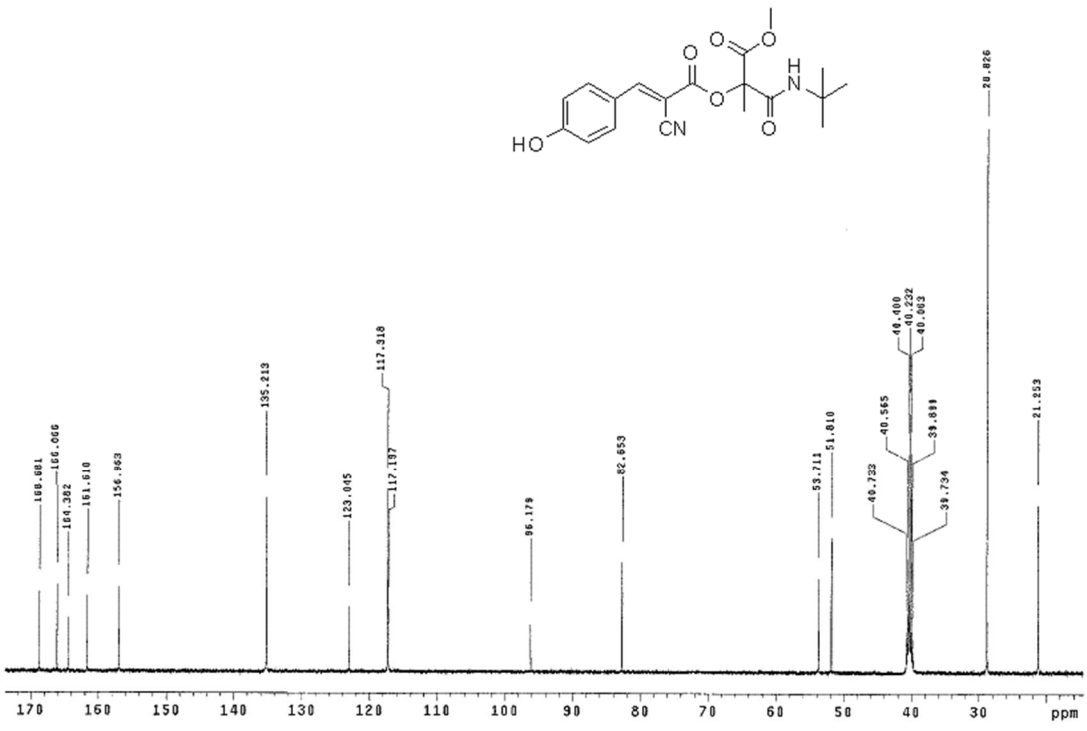
HO
CN
O
O
O
O
H
N
168.681
166.066
164.302
161.610
156.863
135.213
123.045
117.318
117.197
96.179
82.653
53.711
51.810
40.733
40.565
40.400
40.232
40.063
39.894
39.734
28.826
21.253
170
160
150
140
130
120
110
100
90
80
70
60
50
40
30
ppm

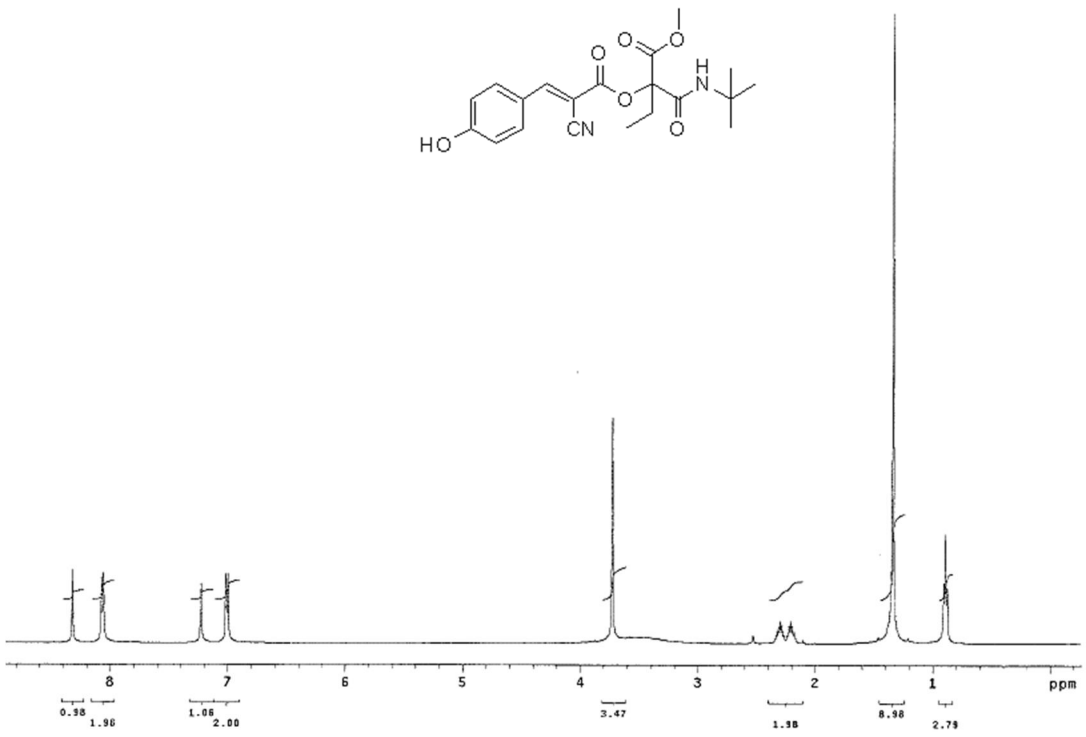
HO
CN
O
O
O
O
H
N
O
8
7
6
5
4
3
2
1
ppm
0.98
1.96
1.06
2.00
3.47
1.98
8.98
2.79

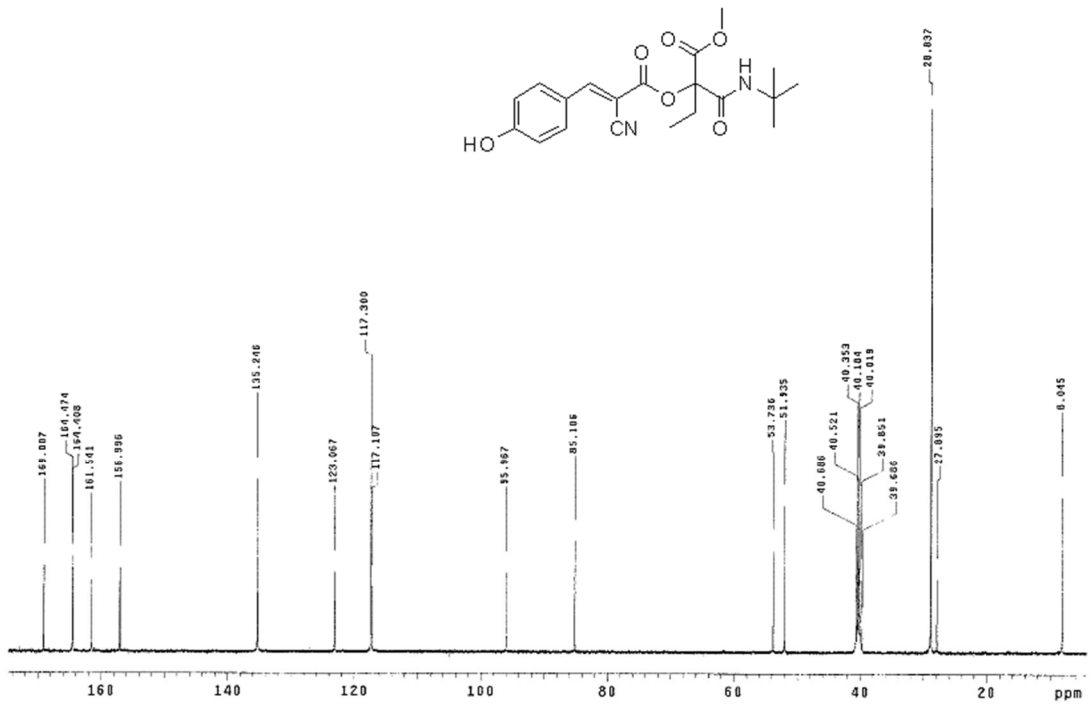
HO
CN
O
O
O
O
O
N
H
165.007
164.474
164.408
161.541
156.996
135.246
123.067
117.300
117.107
95.967
85.106
53.736
51.935
40.680
40.521
40.353
40.186
40.019
39.851
39.686
28.037
27.895
8.045
160
140
120
100
80
60
40
20
ppm

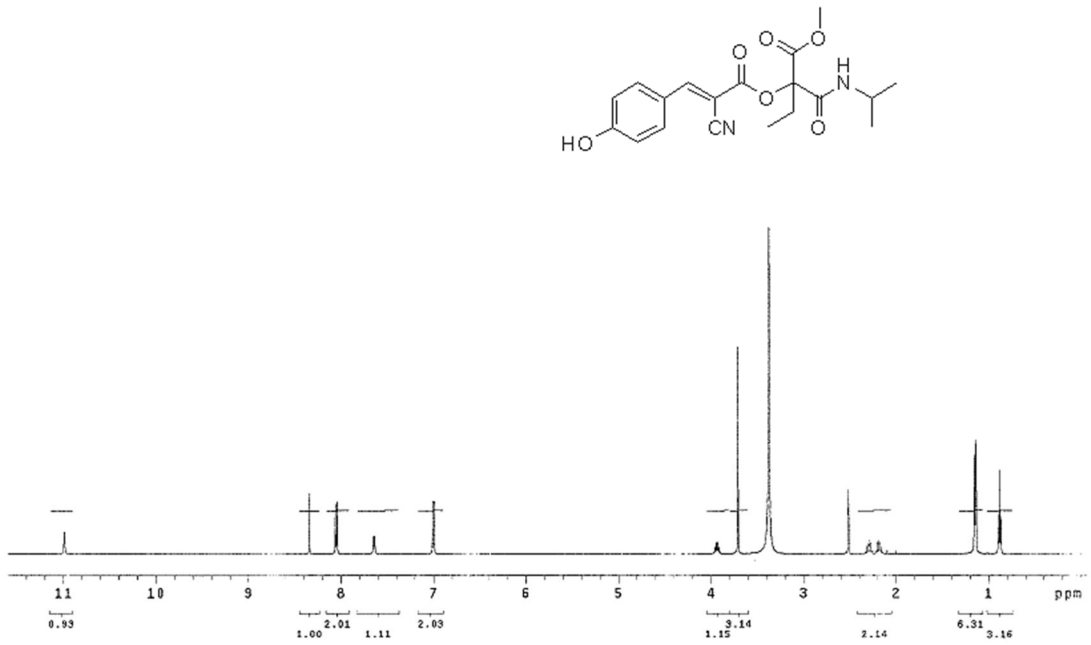
HO
CN
O
O
O
O
H
N
O
11
10
9
8
7
6
5
4
3
2
1
ppm
0.93
1.00
2.01
1.11
2.03
1.15
3.14
2.14
6.31
3.16

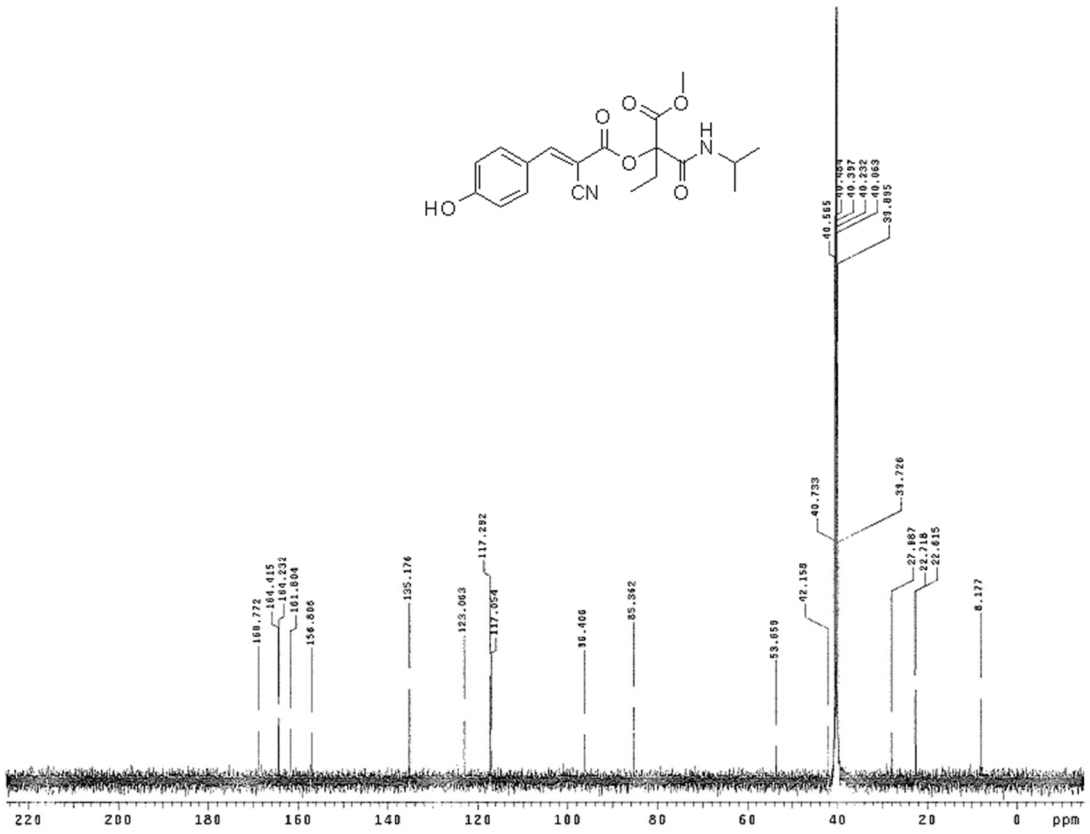
HO
CN
O
O
O
O
N
H
160.772
164.415
164.232
161.804
156.806
135.176
123.063
117.292
117.054
96.406
85.362
53.659
42.158
40.733
34.726
27.887
22.718
22.615
8.177
220
200
180
160
140
120
100
80
60
40
20
0
ppm

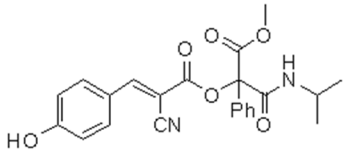
O
O
O
H
N
O
Ph
O
CN
HO

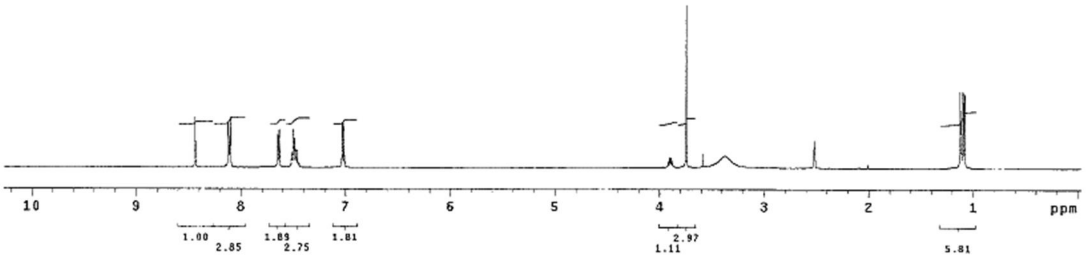
10
9
8
7
6
5
4
3
2
1
ppm
1.00
2.85
1.89
2.75
1.81
2.97
1.11
5.81

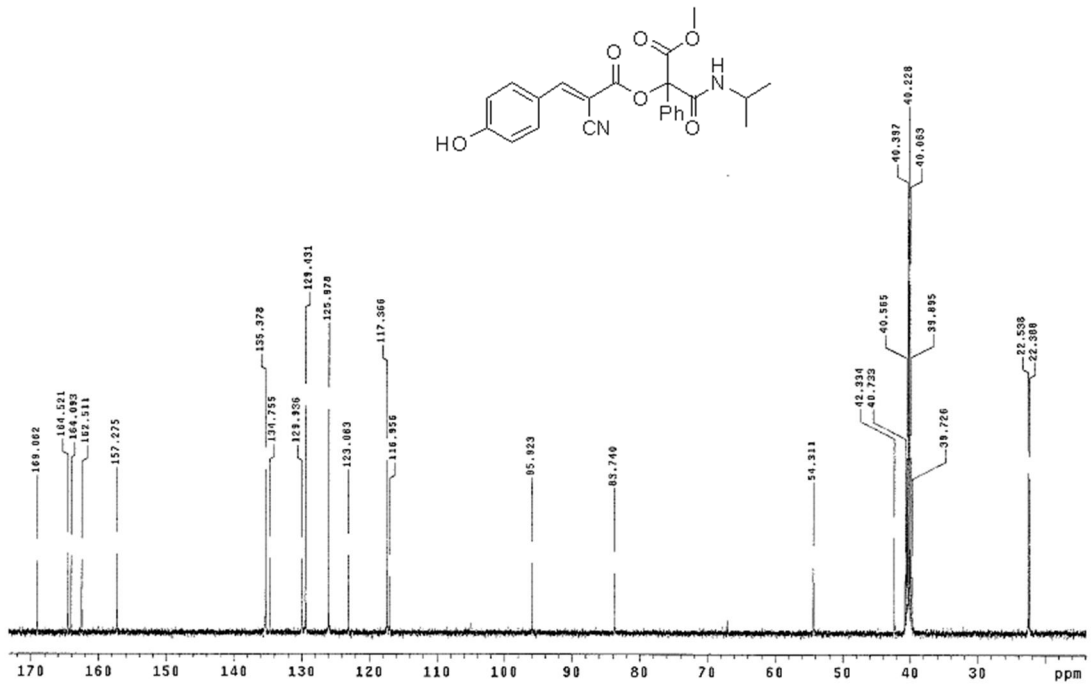
HO
CN
O
O
O
O
Ph
H
N
O
169.062
164.521
164.093
162.511
157.275
135.378
134.755
129.936
129.431
125.978
123.063
117.366
116.956
85.923
83.740
54.311
42.334
40.733
40.565
40.387
40.228
40.063
39.895
39.726
22.538
22.380
170
160
150
140
130
120
110
100
90
80
70
60
50
40
30
ppm